Institut für Ernährungswissenschaften

Justus-Liebig-Universität Gießen

Effects of highly purified olive polyphenols on mitochondrial function in a cellular model of Alzheimer's disease

Dissertation

zur Erlangung des akademischen Grades

Doctor rerum naturalium (Dr. rer. nat.)

Vorgelegt von

Rekha Grewal

2020

This thesis was accepted as a doctoral dissertation in fulfilment of the requirements for the degree of *doctor rerum naturalium* by the Faculty of Agricultural Sciences, Nutritional Sciences and Environmental Management, Justus-Liebig-University Giessen.

Gutachter: 1. Prof. Dr. Gunter P. Eckert

2. Prof. Dr. Thomas Linn

Day of Disputation: 14.12.2021

Balraj S. Grewal

Table of content

List of Abbreviations

3D	three-dimensional
ACTB	Beta-actin
AD	Alzheimer´s Disease
ADP	adenosine diphosphate
AMPK	adenosine monophosphate-activated protein kinase
ANT	ATP-ADP translocase
ApoE	apolipoprotein E
APP	amyloid precursor protein
APS	ammonium persulfate
ATP	adenosine triphosphate
Aβ	amyloid-β
BBB	Blood brain barrier
BCA	bicinchoninic acid
BDNF	brain derived neurotrophic factor
BMI	body mass index
cAMP	cyclic adenosine monophosphate
CAT	catalase
COX	cytochrome c oxidase
CREB	cAMP response element binding protein
CS	citrate synthase

CSF	cerebrospinal fluid
CT	computed tomography
ctrl	control
Da	Dalton
DMEM	Dulbecco´s Modified Eagle Medium
DMSO	dimethyl sulfoxide
DNA	deoxyribonucleic acid
Drp1	dynamin-related protein 1
DTNB	5,5´-dithiobis-(2-nitrobenzoic acid)
ERR	estrogen-related receptor
EtOH	ethanol
ETS	electron transport system
EVVO	extra virgin olive oil
FAD	Flavin adenine dinucleotide
FCCP	carbonyl cyanide-4-(trifluormethoxy)phenylhdrazon
FCPC	fast centrifugal partition chromatography
FCS	fetal calf serum
FIS	fission
GAPDH	glyceraldehyde 3-phosphate dehydrogenase
GPx	glutathione peroxidase
HBSS	Hank´s Balanced Salt Solution

HEK	human embryonic kidney
HEPES	4-(2-hydroxyethyl)-1-piperazineethanesulfonic acid
IGF	insulin like growth factor
iPSC	induced pluripotent stem cells
IU	international units
LDL	low density lipoprotein
LRP	lipoprotein receptor related protein
max	maximum
MedDiet	Mediterranean diet
Mfn	mitofusin
mio	million
MMP	mitochondrial membrane potential
MRT	magnetic resonance imaging
mtDNA	mitochondrial DNA
MTG	mitotracker green
NAD	nicotinamide adenine dinucleotide
NFT	neurofibrillary tangles
NMDA	*N*-methyl-D-aspartate
NRF	nuclear respiratory factor
OPA	optic atrophy protein
OXPHOS	oxidative phosphorylation

PBS	phosphate buffered saline
PCR	polymerase chain reaction
PET	positron emission tomography
PGC-1α	peroxisome proliferator-activated receptor gamma coactivator 1- α
PGK	phosphoglycerate kinase
PI	protease inhibitor
PKA	protein kinase A
PMSF	phenylmethylsulfonyl fluorid
PPARγ	peroxisome proliferator-activator receptor γ
ppm	parts per million
PSEN	presenilin
RCR	respiratory control ratio
Rh123	Rhodamine-123
RNS	reactive nitrogen species
ROS	reactive oxygen species
rRNA	ribosomal ribonucleic acid
SDS	sodium dodecyl sulfate
SIRT	sirtuin
SOD	superoxide dismutase
TEMED	tetramethylethylendiamine
Tfam	mitochondrial transcription factor A

TH	tyrosine hydroxylase
TIMM	translocase of the inner mitochondrial membrane
TOMM	translocase of the outer mitochondrial membrane
Tris	tris(hydroxymethyl)aminomethane
UCP	uncoupling protein
VDAC	voltage dependent anion channel

List of Figures

List of Tables

1 Introduction

1.1 Alzheimer´s disease

Changes in behaviour or loss of memory are the first outward signs of Alzheimer´s disease (AD), with 60% to 80% estimated cases, the most common form of dementia (Alzheimer´s Association, 2020). Declines in cognition, disruption of language and accumulation of behavioural alterations are underpinned by structural and microscopic changes in the brain. To date, nearly 50 million people worldwide are suffering from dementia, whereas only 10% of all AD cases arise before the age of 65, known as familial or early-onset AD and over 90% represent the sporadic form or late-onset AD. Due to the increase in population and ageing, the global number of patients is expected to triple by 2050 (Gaudreault and Mousseau, 2019). Despite extensive research into the pathology, AD cannot be cured yet. More than 25 years the accumulation of the peptide amyloid-β (Aβ) dominates the research of AD (amyloid cascade hypothesis). Concerning the amyloid cascade hypothesis, clumps of Aβ, known as plaques that form outside cells and neurofibrillary tangles (NFTs) consisting of hyperphosphorylated tau, that form inside cells are proposed to be the initiating step and trigger neurodegenerative processes that lead to the loss of memory and cognitive ability (Hardy and Higgins, 1992). In 1907, Alois Alzheimer firstly described these two cellular hallmarks of AD (Alois Alzheimer, 1906). In 1984, the isolation of Aβ revealed the process how the peptide is produced (Glenner and Wong, 1984). Aβ derives from the much larger amyloid precursor protein (APP), which sits in and crosses the cell membrane. Even though APP´s primary function is not known, it has been implicated to play an important role in brain development, memory and synaptic plasticity. There are three major splice isoforms of APP (APP_{695}, APP_{751}, APP_{770}), whereas APP_{695} is the predominant neuronal form, and the other two forms are mainly expressed in peripheral cells and platelets (Nalivaeva and Turner, 2013; Chen et al., 2017). APP can be processed by two pathways: non-amyloidogenic and amyloidogenic. In the non-amyloidogenic pathway, APP is first cleaved by the enzyme α-secretase, releasing soluble APP (sAPPα), and additionally an 83-amino-acid C-terminal fragment (C83) of APP is generated which remains inserted in the membrane. In the next step γ-secretase cuts C83 which liberates the C-terminal fragment P3. In the amyloidogenic pathway the outermost portion of APP is first cleaved off by the β-secretase 1 and 2 (BACE1 and BACE2), whereas γ-secretase then cuts the remaining membrane-bound portion of APP (C99), freeing Aβ (Takagi-Niidome et al., 2015) (see Figure 1.1). The length of

Aβ varies because γ-secretase can cut APP at a number of sites. The most common isoforms are $A\beta_{40}$ and $A\beta_{42}$ (Olsson et al., 2014). Post-translational modifications of Aβ show a variety of modifications like oxidation, phosphorylation, nitration, racemization, isomerization and glycosylation which can all alter the oligomerization, and formation of fibrils (Polanco et al., 2018). Oligomers can then either be precursors of amyloid fibrils or not produce fibrils, although they may still be cytotoxic (Iadanza et al., 2018). Fibrils deposit in amyloid plaques, which can be formed extracellular, and inside cells, while the specific process of plaque formation is not fully understood yet (Polanco et al., 2018).

Mutations in APP have been reported to either increase the production of Aβ or influence the ratio of $A\beta_{42}/A\beta_{40}$ resulting in increased self-aggregation (Weggen and Beher, 2012). AD causing mutations also occur in genes encoding for γ-secretase proteins presenilin 1 (PSEN1) and presenilin 2 (PSEN2) affecting the location where γ-secretase cuts APP (Sun et al., 2017). Generally, genes play a strong role, especially in early-onset AD showing heritability over 90% and in late-onset AD showing 58-79% (Freudenberg-Hua et al., 2018). The major susceptibility gene for sporadic AD is apolipoprotein E (APOE) with its three major allelic variants APOE2, 3, and 4, and is found both, in the periphery and the central nervous system (Mahley, 1988). As we carry two copies of almost all genes, people carry two copies of APOE, which can be either of same or of different variants. Compared to the most common form APOE3/3 genotype, APOE4 allele is associated with a high risk of AD and a younger onset of the disease, while APOE2 is associated with a low risk to develop AD (Reiman et al., 2020). The increased risk of developing AD is up to 4-fold with people carrying one copy of APOE4 and 15-fold in people who have two copies (Yamazaki et al., 2019).

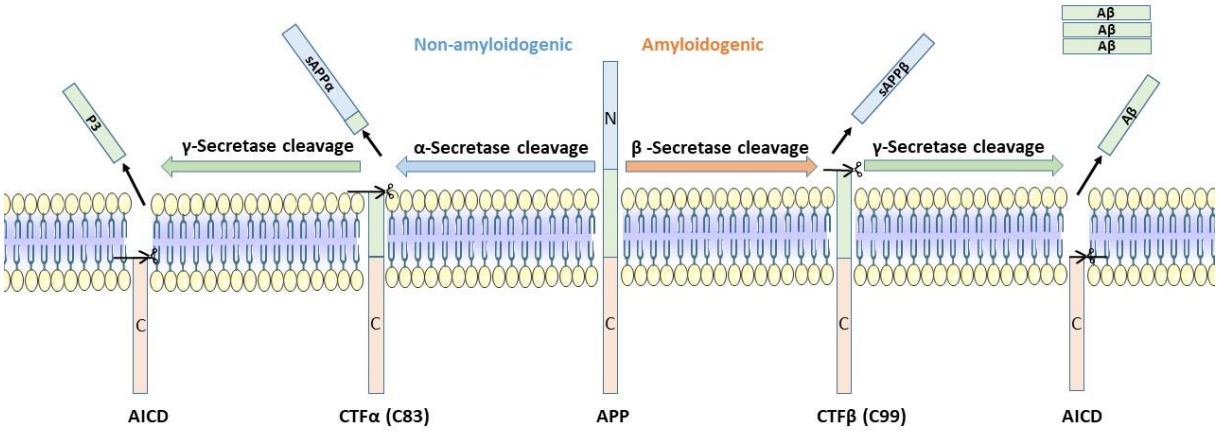

Figure 1.1 APP proteolysis in the non-amyloidogenic pathway and amyloidogenic pathway (adapted from (Chen et al., 2017)). The non-amyloidogenic pathway is initiated by the α-secretase, which cleaves APP to generate CTFα or rather C83 and the soluble N-terminal fragment sAPPα, whereas the release of Aβ is prevented. Amyloidogenic APP processing starts with the β-secretase releasing C-terminal fragment CTFβ or C99 and the N-terminal sAPPβ. C99 is subsequently cleaved by γ-secretase into Aβ and an APP intracellular domain (AICD). AICD can migrate to the nucleus where it regulates gene expression involving the induction of apoptotic genes.

While the genetic evidence strongly supports the relevance of amyloid plaques in inducing AD pathology, the amyloid cascade hypothesis is controversially discussed and has never been universally accepted. Especially, plaque formation does not correlate with the severity of cognitive decline in patients with AD (Nelson et al., 2012). Additionally, plaques are found in the brains of many elderly people with normal cognition (Price, 1994). Amyloid plaques might occur in a pre-symptomatic stage of the disease (Murphy and LeVine, 2010). Obviously, Aβ is necessary but not sufficient in the AD cascade and there are other factors playing a crucial role. Another counter argument to the amyloid hypothesis is the disappointing outcome of clinical phase 3 trials in targeting Aβ, mostly explained by drugs being given at the wrong point of the progression of AD, assuming that the pathology accumulates 15-20 years prior to the onset of clinical symptoms (Vermunt et al., 2019).

Besides the amyloid hypothesis, tau aggregation is another hypothesis. The tau hypothesis targets the microtubule-binding phosphoprotein tau - the main constituent of neurofibrillary tangles (NFTs) which is also a neuropathological hallmark of AD. NFTs contain hyperphosphorylated and aggregated tau. An abnormal phosphorylation of tau, in particular 3

to 4-fold higher, leads to an inhibition of microtubule assembly activity and even disrupts microtubule (Ksiezak-Reding et al., 1992; Ivanov et al., 2020). Microtubules are the main structural component of the cytoskeleton of neurons and are involved in axonal transport (Lasser et al., 2018). It has been demonstrated that dephosphorylation of hyperphosphorylated tau removes NFTs in AD brain samples and restores its biological activity (Iqbal et al., 2010). Both, Aβ plaques and NFTs lead to dysfunction, degeneration and loss of neurons and synapses, what might be of synergistic cause (Masters et al., 2015).

A large body of evidence demonstrates an impaired energy metabolism, in particular a significantly reduced glucose utilization, occurring decades before the onset of the disease (Kapogiannis and Mattson, 2011; Crane et al., 2013; Croteau et al., 2018). Glucose hypometabolism may play a primary role, especially in the sporadic form of AD. It has been shown, that young ApoE4 carriers with no Aβ deposition revealed an impaired glucose metabolism (Jagust and Landau, 2012). On the other hand, other cases suggest that glucose hypometabolsim could be a secondary event after Aβ deposition, as a continuous Aβ increase in autosomal dominant AD patients is only followed by an impaired glucose metabolism (Gordon et al., 2018; McDade et al., 2018). However, abnormalities in glucose metabolism also involve insulin resistance characterized by diminished capacity of cells to respond to physiological levels of insulin, and impaired mitochondria together with the linked processes of oxidative stress or rather mitochondrial dysfunction (discussed in chapter 1.2). Insulin and insulin like growth factors (IGFs) are responsible for neuronal survival, energy metabolism, and neuronal plasticity as well as having a key role in learning and memory (D'Ercole et al., 1996). In the brain of AD patients, insulin resistance is increased which implements a decrease in glucose uptake associated with the disturbance in nervous functions (Talbot et al., 2012). The development of insulin resistance might occur through an excess of reactive oxygen species (ROS) and therefore due to mitochondrial dysfunction (Kim et al., 2008). On the other hand, research indicates that an impaired fatty acid oxidation causes insulin resistance and further impairs mitochondrial function through reduced ATP synthesis (Turner and Heilbronn, 2008). It is still not clear which of the two scenarios arise first.

As mentioned before, another early and primary event in the pathology of AD is contributed to the dysfunction of mitochondria, underlying the mitochondrial cascade hypothesis (Swerdlow et al., 2010). The mitochondrial cascade hypothesis was firstly introduced by Swerdlow and Khan in 2004 (Swerdlow and Khan, 2004). According to the hypothesis mitochondrial

dysfunction is considered to be an early event and a primary event in the pathophysiological cascade of AD (Swerdlow et al., 2010). The hypothesis maintains three major parts. First, the mitochondrial cascade hypothesis postulates that a genetic individual decline in mitochondrial function is a significant risk factor for developing late-onset AD. Second, age-associated mitochondrial changes are depended on inherited and environmental factors. Third, AD chronology is determined by the rate of change of mitochondrial function through individual genetic and environmental factors. The dysfunction increases over decades until a threshold is reached and histologic changes associated with AD start (Swerdlow et al., 2014) (see Figure 1.2). The hypothesis assumes to split autosomal dominant AD, with an excessive Aβ accumulation leading to impaired mitochondrial function, from sporadic AD, with an age related occurrence of mitochondrial dysfunction.

Besides the hypothesis discussed, there are modifiable risk factors for AD like diabetes, mid-life obesity, mid-life hypertension, high cholesterol, and smoking (Baumgart et al., 2015).

By the time AD is diagnosed, substantial neuronal loss and neuropathological lesions might already damaged brain regions. Therefore, an early diagnosis is essential. Current diagnosis of AD include psychometrical tests, brain imaging and cerebrospinal fluid (CSF) collections. There are several psychometrical tests to assess cognitive performance. Various forms of brain imaging such as computed tomography (CT), magnetic resonance imaging (MRI) and electron emission tomography (PET) provide visualisation of Aβ fibrils as well as structural and functional details of the brain. The fluid biomarker CSF detects soluble Aβ monomers, total tau and phosphorylated tau (Anoop et al., 2010). These imaging techniques are of high accuracy and are able to detect the presence of AD-associated pathophysiological and neuropathological changes. However, these assays are expensive, lack of accessibility or are invasive. Therefore, cost-effective, accurate and standardized early diagnostics are indispensable. The use of blood-based biomarkers is one of those possibilities, what would reflect the full spectrum of molecular mechanisms underlying the multifactorial pathology of AD (Hampel et al., 2018; Schindler et al., 2019).

In Germany, there are currently four medications for symptomatic AD approved for the use in mild-to-moderate AD, including three cholinesterase inhibitors (donepezil, rivastigmine, and galantamine) and an uncompetitive *N*-methyl-D-aspartate (NMDA) receptor modulator (memantine) for moderate-to-severe AD. Additionally, German guidelines recommend, the

standardized ginkgo biloba extract, EGb761 for the treatment of AD (Deutschl and Maier, 2016).

Until now, over 20 compounds failed in phase three trials at various stages of AD, showing no improvement of cognitive performance and global functioning (Long and Holtzman, 2019). To date, there are 132 agents in clinical trials with 28 agents in phase 3 trials. Over half of the phase three ongoing trials (61%) are disease modifying and focus on amyloid as either small molecules, monoclonal antibodies or biological therapies. Other mechanisms include tau pathogenicity, neuroprotection, anti-inflammation, and metabolic interventions. 39% are symptomatic agents addressing cognitive enhancement or behavioural and neuropsychiatric symptoms (Cummings et al., 2019). The clinical trial design should include and focus more widely on combination therapies and on lifestyle and metabolic interventions to prevent AD. Since mitochondrial dysfunction is increasingly recognized as one of the early events in the progression of AD, it may be essential to focus on preventive strategies to slow down the progression of AD.

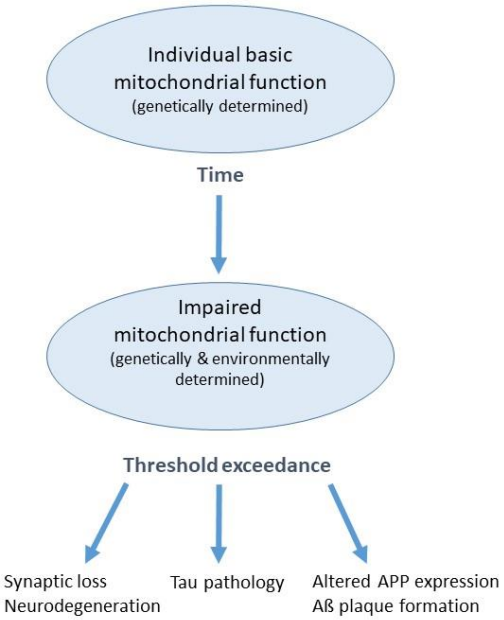

Figure 1.2 The mitochondrial cascade hypothesis (adapted and modified from (Müller, 2016)). The mitochondrial cascade hypothesis postulates that an individual impairment of mitochondrial function is a major risk factor for late-onset AD. Furthermore, genetic and environmental factors influence the increase of mitochondrial dysfunction over decades

1.2 Mitochondria as a therapeutic target for AD

1.2.1 Mitochondria form and function

Around two billion years ago, mitochondria might have been evolved by endosymbiosis of an α-proteobacterium by a precursor of the eukaryotic cell, assumed as in the classical endosymbiont hypothesis. According to their ancestors, mitochondria comprise a double-membrane, the core of energy production in form of adenosine triphosphate (ATP) and the circular genome, mitochondrial DNA (mtDNA). The form and composition of the network forming organelle has altered drastically and acquired new additional functions during evolution (Gray, 2012). mtDNA which inheritance exclusively maternal, has been reduced during evolution and lost to the nucleus, leaving the organelle to encode only for 13 of 1500 mitochondrial proteins, the reason why mitochondria depend on the nucleus for most of their proteins and lipids. Besides their most notably function being the main energy producer via oxidative phosphorylation (OXPHOS), mitochondria perform many other key roles in the cell. They are responsible in iron and calcium homeostasis, central carbon metabolism, metabolism of dietary substrates, fats, and proteins, produce precursors of lipids, proteins, and DNA, and also generate metabolic by-products like ROS and ammonia (Nunnari and Suomalainen, 2012; Haas, 2019). Recent research has uncovered how mitochondria play active roles in cellular communication through signalling pathways with other organelles and it is now clear that mitochondria are part of nearly all aspects of cell function, affecting processes such as neurodegeneration, cancer, inflammation, metabolic signalling and cell death (Spinelli and Haigis, 2018).

Mitochondria range in the size from 0.75 to 3 μm^2 in diameter and vary considerably in size and structure depending on the cell type or physiological state (Miyazono et al., 2018). They contain of an inner and outer mitochondrial membrane, which separate two compartments, the intermembrane space and the innermost matrix compartments (see Figure 1.3). In the mitochondrial matrix, oxidation of fatty acid, glucose and amino acid metabolism takes place via the beta-oxidation and citric acid cycle. The outer membrane isolates the mitochondrion from the cytosol, contains proteins including porins allowing molecules up to 5000 Da to shuttle via passive diffusion, and is permeable to salts, sugars, and coenzymes, while the inner mitochondrial membrane permeability is limited to oxygen, carbon dioxide and water. Both

membranes harbour translocases to import nuclear encoded proteins into the mitochondrion, through the translocase of the outer membrane (TOM) and the translocase of the inner membrane (TIM), shuttling proteins into the matrix (Pfanner and Meijer, 1997; Pfanner and Wiedemann, 2002). The inner membrane is highly structured with invaginations the so-called cristae, providing a large amount of surface and housing the protein complexes of the electron transport system (ETS). The cristae is also presumed to increase the charge density and local pH to enhance ATP production through OXPHOS (Strauss et al., 2008).

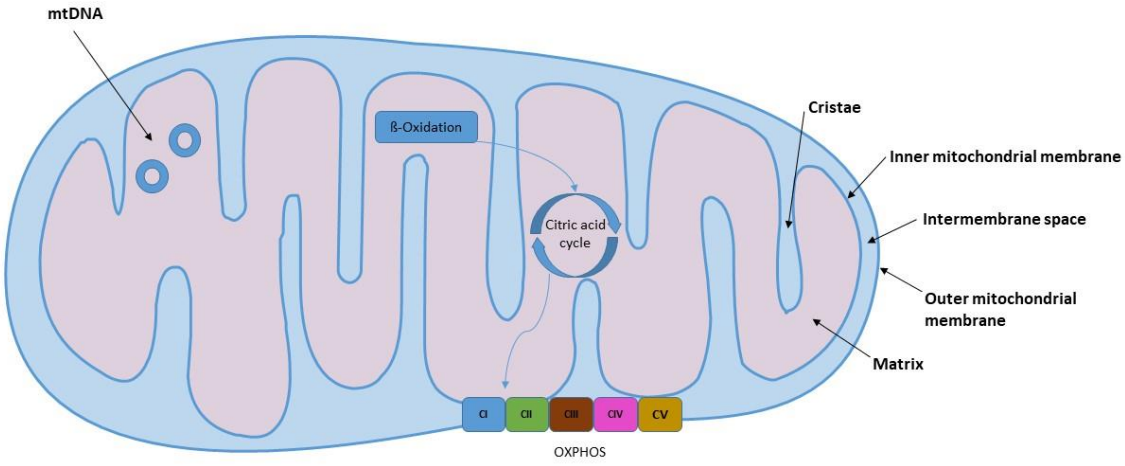

Figure 1.3 Schematic view of a mitochondrion. Mitochondria consist of an inner and an outer mitochondrial membrane, in between the intermembrane space. The outer mitochondrial membrane acts as a diffusion barrier and isolates the mitochondrion from the cytosol, in which it has a higher permeability than the inner one. The inner mitochondrial membrane forms invaginations the so-called cristae, enlarging the surface and harbouring respiratory chain complexes (CI-CV). The matrix harbours the citric acid cycle, which generates electrons through the β-oxidation and supplies them for OXPHOS (own figure).

The mitochondrial respiratory chain and OXPHOS system

The OXPHOS system harbours five multimeric complexes embed in the inner mitochondrial membrane. Complexes I-IV comprise the respiratory chain, which transfer electrons from reducing equivalents to water, creating a proton gradient across the inner mitochondrial

membrane, which is utilized to power complex V, the ATP synthase to produce ATP from ADP and inorganic phosphate.

Nicotinamide adenine dinucleotide in its oxidised form (NADH) and flavin adenine dinucleotide in its hydroquinone form ($FADH_2$), which are derived from the citric acid cycle and β-oxidation, transfer electrons to complex I (ubiquinone oxidoreductase) and complex II (succinate dehydrogenase). Complex I oxidizes NADH to NAD^+ and H^+ and transfers two electrons to ubiquinone (coenzyme Q) resulting in the reduced form ubiquinol. Complex II, which links the citric acid cycle to OXOHOS catalyses the oxidation from succinate to fumarate, while also oxidizing $FADH_2$ to FAD^+ and H^+ producing ubiqinol. In the next step, electrons are transported from ubiquinol to complex III (cytochrome c oxidoreductase). Transfer of electrons to cytochrome c facilitates complex III to oxidize ubiquinol. In turn, cytochrome c reduces complex IV (cytochrome c oxidase, COX). Eventually, electrons are donated to molecular oxygen, and water is formed. Simultaneously, a proton motive force across the inner mitochondrial membrane is built up by complex I, III and IV, which is used to generate ATP through complex V. Summarized, complex I, III and IV pump protons out of the matrix into the inter membrane space creating a negative charge in the inner side of the membrane and a positive charge on the outer side what generates the mitochondrial membrane potential (MMP). Figure 1.4 gives an overview of the respiratory chain.

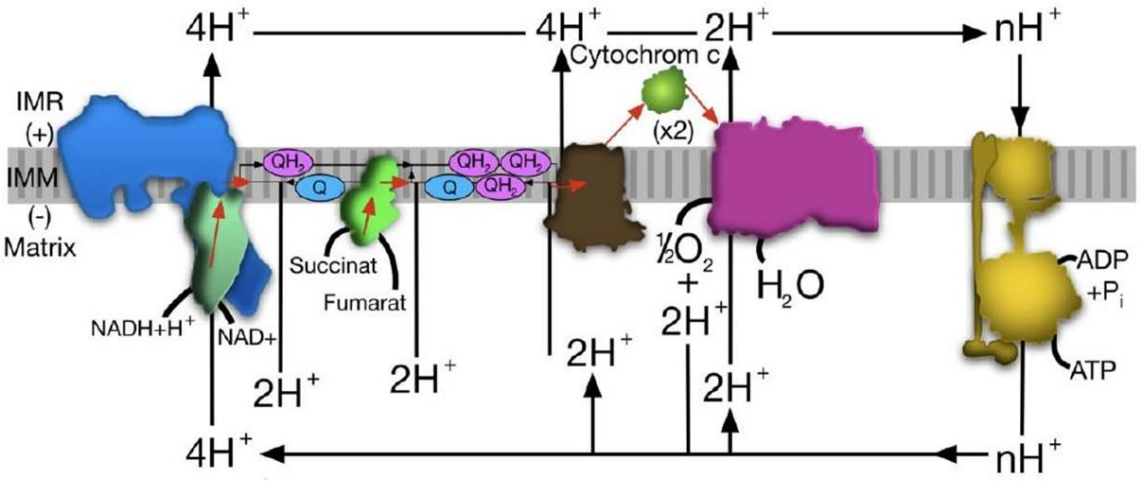

Figure 1.4 Overview of the respiratory chain and the ATP synthase (modified from (Rich and Maréchal, 2010)). The red arrows show the transfer of two electrons from oxidation of NADH or succinate of complex I or complex II. These electrons are then transferred to complex IV via cytochrome c oxidase, which catalyzes the electron transfer to the final electron acceptor oxygen. Simultaneously, a proton motive force is generated by complex I, III and IV resulting in a negative charge in the inner side of the membrane and a positive charge on the outer side, which generates the mitochondrial membrane potential. IMR = intermembrane space, IMM = inner mitochondrial membrane.

Mitochondrial biogenesis

Mitochondria are of highly dynamic nature – they undergo continuous cycles of balanced fusion and fission processes to maintain their architecture, function and quantity. Fission, which is characterized by the division of one mitochondrion into two mitochondria, is needed to increase the number of mitochondria before biogenesis and to isolate defect mitochondria for autophagy, whereas mitochondrial fusion is the union of two mitochondria resulting in one mitochondrion. Fusion is required for organelle distribution to and from distal locations of demand (Youle and Narendra, 2011; Friedman and Nunnari, 2014). The cytosolic dynamin related protein 1 (Drp1) is associated with fission and is recruited to the outer mitochondrial membrane by the mitochondrial fission 1 protein (FIS1). Fusion of the outer mitochondrial membrane is ensured by the two large mitofusin proteins 1 and 2 (Mfn1/2), followed by fusion of the inner mitochondrial membrane, mediated by the optic atrophy protein 1 (OPA1) (Tilokani et al., 2018). Mitochondrial biogenesis is tightly controlled and occurs through the action of the

PPARγ-1α (PGC-1α) family co-activators, which respond to changes in nutrient status and the metabolic state of the cell, as well as environmental signals (Wai and Langer, 2016). Peroxisome proliferator-activated receptor gamma coactivator 1-alpha (PGC-1α) is the master regulator of mitochondrial biogenesis, including activation of genes of the respiratory chain and β-oxidation, elevation in mitochondrial number, replication of mtDNA, and augmentation of mitochondrial respiratory capacity. These effects exert through direct interaction with coactivators such as the nuclear respiratory factors 1 and 2 (NRF1 and 2) among other transcription factors to regulate nuclear gene expression (Finck and Kelly, 2006). NRF1 and 2 are positive transcription regulators by acting on many genes, including genes of respiratory subunits and additionally activating the mitochondrial transcription factor A (Tfam). Tfam is a key activator of mitochondrial transcription and participates in mitochondrial genome replication with its major factor in regulating mtDNA copy number (Shi et al., 2012). As mentioned before, PGC-1α responds to changes in nutrient status, for example ratios of NAD^+/NADH and AMP/ATP which are sensed through sirtuin 1 (SIRT1) and adenosine monophosphate-activated protein kinase (AMPK). PGC-1α is directly regulated by deacetylation from SIRT1 and phosphorylation through AMPK. There are seven mammalian sirtuins (SIRT1-7) functioning as gene regulators by deacetylating transcription factors, and as regulators of activities of metabolic enzymes in response to calorie restriction or other stresses. AMPK plays a key role in cellular energy homeostasis. The kinase responds to low ATP levels or rather high AMP, which in turn activates PGC-1α and triggers a wide range of catabolic pathways directed to increase cellular levels of ATP (Wang et al., 2019). cAMP response element–binding protein (CREB) is another activator of PGC-1α transcription. CREB integrates multiple signalling pathways in various cell types, but mainly required for cAMP response (Herzig et al., 2001).

1.2.2 Mitochondrial dysfunction

Mitochondria are involved in a huge number of cellular processes and are present in all eukaryotic cells relying on aerobic metabolism (B. Alberts, 2015). Mitochondria are the powerhouse of the cell by metabolizing nutrients and producing ATP through OXPHOS to maintain the normal homeostasis and function of the cell. Furthermore, mitochondria have key roles in several intracellular pathways, including lipid biosynthesis, regulation of calcium concentration and cell apoptosis. Due to their involvement in these essential functions of the

cell, it is not surprising that disturbance of mitochondrial function are largely associated with many common chronical diseases, including neurodegenerative diseases (Nicolson, 2014; Bhatti et al., 2017). As mitochondrial function becomes impaired with age, it is believed and shown in several studies to be a major and early event to the ageing process, and therefore also in neurodegenerative diseases such as AD (Grimm et al., 2016; Chakravorty et al., 2019; Reddy and Oliver, 2019). A large body of evidence has shown mitochondrial abnormalities in the brain of AD patients (Swerdlow, 2018).

An impaired electron transport chain and thus a reduction in the synthesis of ATP as well as the loss of the potential of the inner mitochondrial membrane are main hallmarks of mitochondrial dysfunction. It is well known, that mitochondrial respiratory enzymes as well as numerous other mitochondrial enzymes are altered in AD brain (Bubber et al., 2005; Yao et al., 2009). In particular, defects in complex IV are considered to be central in AD (Parker et al., 1990; Rapoport, 1991; Mutisya et al., 1994) and are mainly linked to changes in mtDNA (Krishnan et al., 2012; Weidling and Swerdlow, 2019). A result of the electron transport process is the production of reactive oxygen species (ROS) and related reactive nitrogen species (RNS), at moderate levels acting as second messengers within the cells (Di Meo et al., 2016). However, in case of an impaired respiratory system the production of these highly reactive free radicals is increased. Dismutase enzymes and antioxidants counter the effects of oxidative damage induced by ROS/RNS, whereas various antioxidative enzymes such as glutathione peroxidase (GPx), superoxide dismutase (SOD), and catalase (CAT) are impaired in AD (Ansari and Scheff, 2010). The excessive generation of ROS/RNS occurs as a result of an imbalance between the levels of antioxidants and oxidants in favour of oxidants and furthermore of the impaired OXPHOS. This oxidative environment triggers the damage of cellular lipids, proteins, and DNA. Additionally, the damage to mitochondrial membrane lipids can result in increased proton and ion leak back across the inner mitochondrial membrane into the mitochondrial matrix, resulting in a partial loss of the electrochemical gradient (Nicolson, 2014), which in turn again impairs the mitochondrial respiratory chain. Consistent with bioenergetics deficits in AD, genes encoding for mitochondrial ETC subunits and associated metabolic pathways, are as well significantly downregulated (Brooks et al., 2007).

Furthermore, there are studies demonstrating changes in mitochondrial structure, disrupted cristae and decreased mitochondrial surface area in AD brain (Baloyannis et al., 2004). Defected mitochondria can cause as well mitochondrial bioenergetics deficits through enhanced

ROS/RNS generation or an improper respiratory complex assembly. Additionally, it causes a depletion of mtDNA due to a reduced exchange of mitochondrial content (Mishra and Chan, 2014). This underscores the importance of a balance between fission and fusion events for maintaining a healthy pool of mitochondria with proper distribution. Moreover, mitochondrial quality control is regulated by the processes of mitochondrial biogenesis and mitochondrial autophagy, known as mitophagy. Mitophagy involves the degradation of damaged or dysfunctional mitochondria (Hales, 2004; Youle and van der Bliek, 2012). A most recent study found significantly impaired mitophagy in the brain of AD patients (Fang et al., 2019).

Additionally, it has been reported that Aβ peptide is able to translocate into mitochondria (Stewart et al., 2000). The accumulation of Aβ in mitochondria causes inhibition of complexes II and IV of the respiratory chain resulting in reduced OXPHOS and increased production of ROS (Rhein et al., 2009b). Furthermore, Aβ inhibits protein import inside the mitochondria leading to damages and mutations of mtDNA (Lakatos et al., 2010). Moreover, the accumulation of Aβ leads to impaired mitochondrial dynamics featured by abnormal fusion and fission processes, untypical morphology and degradation, causing reduced clearance of impaired mitochondria which further enhances mitochondrial dysfunction (Manczak et al., 2011).

The strong evidence that mitochondrial deficits could lead to AD related hallmarks suggest mitochondrial dysfunction to play a primary role in the progression of AD, especially in the sporadic form. On the other hand, in case of patients with early-onset AD or rather with autosomal dominant mutations, Aβ accumulation plays the primary role, where mitochondrial dysfunction seems to be of secondary event in amplifying neuronal impairment in AD. Nevertheless, whether mitochondrial dysfunction is either a primary or secondary event, impaired mitochondrial bioenergetics, increased oxidative stress and disturbed mitochondrial genome are consistent features of mitochondrial abnormalities in AD. Any of these abnormalities interact with each other to mediate or amplify neurodegeneration. Figure 1.5 summarizes mechanisms of mitochondrial dysfunction.

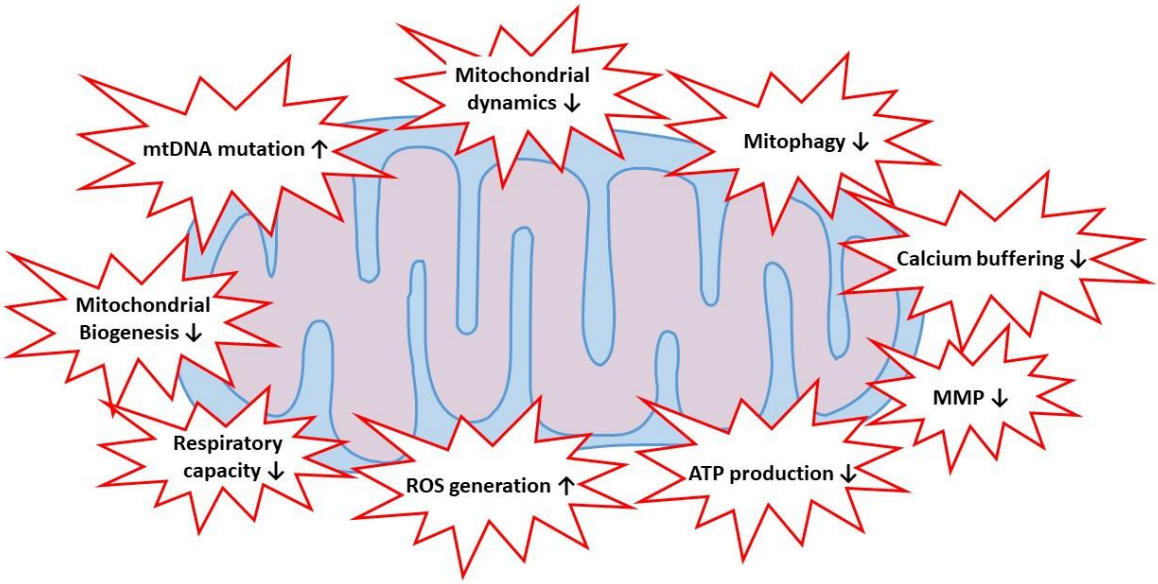

Figure 1.5 Mitochondrial dysfunction. Mitochondrial dysfunction is accompanied by altered mitochondrial dynamics, decreased mitophagy, impaired calcium homeostasis, low MMP, decreased ATP level, increase in ROS production, downregulation of respiratory capacity, impaired mitochondrial biogenesis and excess of mtDNA mutations (own figure).

1.3 Prevention of AD

AD negatively affects quality of life, global functioning and physical health. Among others, it is the leading cause of disability worldwide and a significant health concern. Despite of intensive efforts into the causes of AD, there is no effective therapy up to now. Anyhow, the onset of AD might be modifiable by the management of potential risk factors. Therefore, the importance of prevention as a therapeutic goal has gained focus in the current field of AD research. Strategies to prevent AD through non-pharmacological treatments are lifestyle interventions such as physical activity, cognitive activity, socialization and a healthy diet (Norton et al., 2014). Diet and exercise have yielded promising results in modulating brain morphology and function and are known to act at the mitochondrial level (Maliszewska-Cyna et al., 2017; Cenini and Voos, 2019).

1.3.1 Nutrition in the prevention of AD

The preclinical stage of AD, only detectable by brain imaging or cerebrospinal fluid measurements accompanied with no measurable cognitive deficits, describe the first stage of AD. At this stage lifestyle changes may stabilize or reverse the progression of the disease (Carrillo et al., 2013). Today, it is accepted and evident, that environmental factors and lifestyle play a crucial role in the onset and progression of AD. This also reflects the multifactorial complexity of AD (Bertram and Tanzi, 2008). Notably, the late-onset form is with over 50% chiefly attributed to modifiable risk factors (Barnes and Yaffe, 2011). Balanced and healthy dietary habits throughout the entire life contribute to healthy ageing. Healthy eating seems to have a high potential in preventing the development of AD, also because of reducing risk factors such as cardiovascular diseases or diabetes (Tuomilehto et al., 2001; Rees et al., 2012). The influence of dietary patterns were shown in AD and ageing animal models (Hagl et al., 2016b; Hagl et al., 2016a; Reutzel et al., 2018; Grewal et al., 2020).

Modifiable risk factors such as obesity, diabetes and hypertension are all related to dietary patterns. There are three main dietary styles including the Mediterranean diet (MedDiet), which will be described in the next section, the dietary to stop hypertension (DASH) and a combination of both, called the MIND diet. All play a significant role in the prevention or delay of cognitive decline. As high blood pressure is one of the risk factors for developing AD, the DASH diet gained attention on its impact on AD. The Dash diet is characterized by a high intake of fruits, vegetables, nuts, low-fat dairy products and low amounts of animal products. A small number of cohort studies have shown an improvement of the DASH diet on cognitive function and a reduced risk of AD (Wengreen et al., 2013; Tangney et al., 2014). On the other hand, a more recent study showed no improvement after a 4-year intervention with the DASH diet (Berendsen et al., 2017). Smith et al. has shown that the DASH diet should be primarily addressed to patients with hypertension and overweight as the diet seems to be most beneficial in these cases (Smith et al., 2010). The MIND diet incorporates a high intake of plant foods, olive oil, fatty fish and a low intake of saturated and trans-fats. In a prospective study, the MIND diet was able to slow the rate of cognitive decline (Morris et al., 2015a) and reduce the risk of AD by 35% in a study over 4 years (Morris et al., 2015b).

Nevertheless, it seems obvious that the most effective strategy to prevent AD is a general healthy lifestyle including activity, physical exercise and a balanced nutrition. Due to the multifactorial etiology of AD, interventions that address multiple risk factors and disease

mechanisms simultaneously may be more effective in preventing AD or dementia than unimodal approaches. In several European countries, randomized controlled trials have already been conducted to investigate the effects of multimodal interventions in elderly people living independently.

In 2015 a randomised controlled two year multi-domain study with an intervention of diet, exercise, cognitive training, and vascular risk monitoring in elderly people with an increased risk for AD, called the FINGER (Finnish Geriatric Intervention Study to Prevent Cognitive Impairment and Disability)-study was carried out. Eating habits, physical activity, BMI and overall cognition were significantly improved (Ngandu et al., 2015). Even if some effects of the multi-domain lifestyle-based intervention were small, they may imply large effects. Since a third of all AD cases are attributed to low education, obesity, physical inactivity, diabetes, smoking and depression, the prevalence could be reduced by 10% per decade in the prevalence of the mentioned factors (Norton et al., 2014). The observed beneficial effects on cognition could lead to a moderate delay in the onset of AD in the long term and thus contribute to an improvement in the individual and social situation. To evaluate long-term effects of the FINGER-study a 7-year follow-up is planned.

Another multimodal intervention study, the Multi-domain Alzheimer Preventive Trial (MAPT)-study investigated the effects of omega 3 polyunsaturated fatty acid supplementation and a multi-domain intervention including physical activity, cognitive training, and nutritional advice, alone or in combination in elderly people (≥70) with memory complaints. The study was carried out with 1680 participants over a period of three years. Both intervention strategies, either alone or in combination, had no significant effects on cognitive decline in elderly subjects with cognitive abnormalities (Andrieu et al., 2017). The lack of success could be amongst others attributed to the fact that polyunsaturated fatty acids must be ingested at an early age and over several years to help reduce the risk of AD (Yassine et al., 2017). Another problem was a low compliance and the high number of participants with a high education. The intervention in mentally active people will most likely do not do much, as their cognitive performance remains at high level for a long time.

The results show that early interventions before first symptoms occur are essential in order to achieve an improvement. Lifestyle-related risk factors have a very long–term effect and can hardly be represented in their full effectiveness even in study periods of 2-4 years. Another limitation relies in the clinical instruments with which mental deterioration is measured. Small

improvements might not be detected due to the low sensitivity and inaccuracy of the used instruments. Furthermore, these studies only investigated the effects on metabolic and cognitive parameters but not on possible mechanisms contributing to an improvement to cognitive function. On the other hand, several studies have examined the influence of the Mediterranean diet and physical activity at the molecular biological level. Animal studies have already shown that dietary factors have positive effects on mitochondrial function which might slow down the progression of AD (Hagl et al., 2016b; Hagl et al., 2016a; Reutzel et al., 2018; Grewal et al., 2020). Therefore, multimodal interventions should also consider molecular parameters, to investigate potential mechanisms of action of these preventive strategies.

1.3.2 Mediterranean diet

The Mediterranean diet (MedDiet) is mainly composed of vegetables, fruits, fish and olive oil. In Mediterranean regions the prevalence of AD is low compared to those of other countries (Solfrizzi et al., 2003; Panza et al., 2004; Scarmeas et al., 2009a). Systematic reviews and meta-analysis have elaborated that the MedDiet lowers the incidence of AD (Singh et al., 2014; Aridi et al., 2017; Hill et al., 2019). Cao et al. reported that adherence to the MedDiet leads to a reduction of developing AD to 31% (Cao et al., 2016). A randomized multicenter study compared in participants bearing a high risk of vascular disease, cognitive performance after a nutritional intervention of the MedDiet with EVOO and nuts compared to a low-fat control diet. After 6.5 years of intervention, the MedDiet group significantly improved their cognitive function compared to the control group (Martínez-Lapiscina et al., 2013).

The integral component of the MedDiet is the high intake of olive phenols present in extra virgin olive oil (EVOO) (Visioli et al., 2018). EVOO has been recently proposed as promising tool for the prevention of late-onset AD (Román et al., 2019).

Polyphenols have been shown to improve mitochondrial bioenergetics and biogenesis *in vitro* and *in vivo* (Schaffer et al., 2006; Schaffer et al., 2012; Wood Dos Santos et al., 2018; Dilberger et al., 2019). Moreover, several clinical studies have shown to improve cognitive performance and slow down the progression of memory impairment (Scarmeas et al., 2006b; Scarmeas et al., 2006a; Scarmeas et al., 2009b; Valls-Pedret et al., 2015).

1.3.3 Olive polyphenols

Olive oil consists with 98% mainly of triacylglycerols. The remaining 2% comprise nearly 250 minor compounds, including aliphatic and triterpenic alcohols, sterols, hydrocarbons and phenolic compounds. The phenolic fraction of olive oil contains different groups, including phenolic acids such as vanillic acid, caffeic acid and p-hydroxycinnamat, phenylethyl alcohols like tyrosol and hydroxytyrosol, flavones, lignans and secoiridoids like oleuropein and ligstroside derivatives (Alonso-Salces et al., 2010; Ouni et al., 2011).

Mechanism of action

The most essential properties of plant phenols are their ability to form complexes with other biomolecules and of course to scavenge free radicals, which are both the basis for many of the functions that polyphenols have as secondary plant metabolites in the chemical defense mechanism. The basic structure of the phenol function is a phenyl ring with a hydroxy group (PhOH) and therefore being of amphiphilic nature. The combination of the hydrophobic character of its planar aromatic ring with its hydrophilic polar hydroxy substituent makes it function either as a hydrogen-bond donor or as an acceptor. The hydrogen bond as well as the hydrophobic π–stacking (van der Waals interaction) are responsible for many properties of the plant polyphenols to interact physically with other biomolecules, in particular proteins (Daayf and Lattanzio, 2009) (see Figure 1.6). In case of at least two adjacent hydroxy groups, polyphenols are also able to chelate metals (Andjelkovic et al., 2006). The otherwise almost inert phenyl ring changes its reactivity even through the substitution with only one single hydroxy group. Phenol in its stabilized enolic form has a soft nucleophilic character, whereas in biological environments a deprotonation to phenolat anion changes the phenol into a harder nucleophile and therefore acting in many ionic reactions as a carbon- or oxygen-based nucleophile (Clayden, 2009) (see Figure 1.7). Additionally, phenols are very sensitive to oxidation processes. Dehydrogenation leads to the production of phenoxy radicals (PHO·), furthermore phenolat anions can be oxidized in a one-electron process. The resulting generation of delocalized-stabilized radicals are claimed to be part of the conversion of simple plant phenolics into more complex oligo or polymeric polyphenols. The capacity of the phenol functional group to donate a hydrogen atom and as second mechanism the single-electron transfer of PhOH to a free radical R· with formation of a stable radical cation $PHR^{\cdot+}$, are both

fundamental processes that underlie the health benefiting antioxidant properties of plant phenols (Wright et al., 2001b) (see Figure 1.8).

Not surprisingly, beneficial health effects of EVOO are mainly attributed to olive phenols. Recent studies confirm that specific olive phenols of EVOO - in particular secoiridoid derivatives are responsible for the health-promoting effects such as antihypertensive, anti-inflammatory and antimicrobial effects (Gavahian et al., 2019; Schwingshackl et al., 2019).

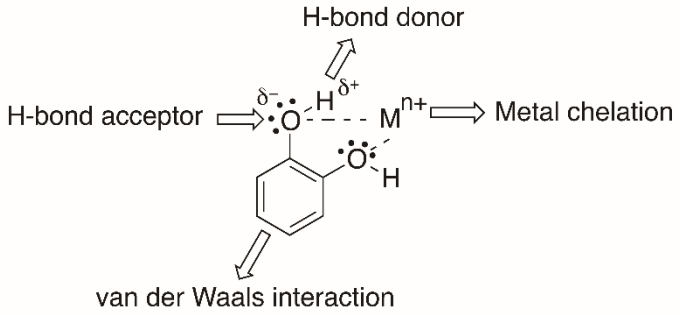

Figure 1.6 Complementary effects of the phenol functional group (adapted and modified from (Quideau et al., 2011)). The planar aromatic nucleus combines its hydrophobic character with the hydrophilic character of the polar hydroxy substituent. The hydroxy group can act either as a hydrogen-bond donor or as a hydrogen-bond acceptor. The existence of two hydroxy groups on the phenyl ring enhances the ability for chelating metal ions from cationic nutrient, for example Ca, Mg, Mn, Fe or Cu.

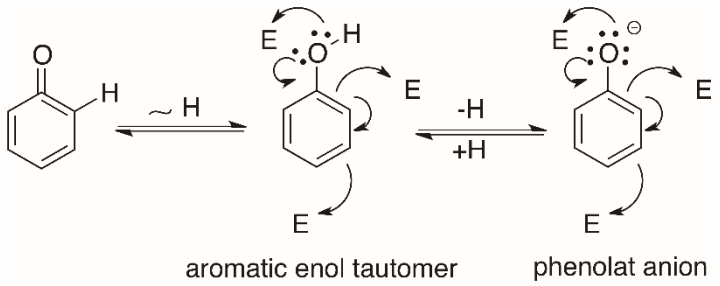

Figure 1.7 Chemical properties of the phenol functional group (adapted and modified from (Quideau et al., 2011)). Phenol is a very stable enol because of the aromaticity of its benzene ring. The stabilized enol tautomer is a soft nucleophile, which can be transformed into a harder nucleophile through deprotonation resulting into a phenolat anion. E = electrophile.

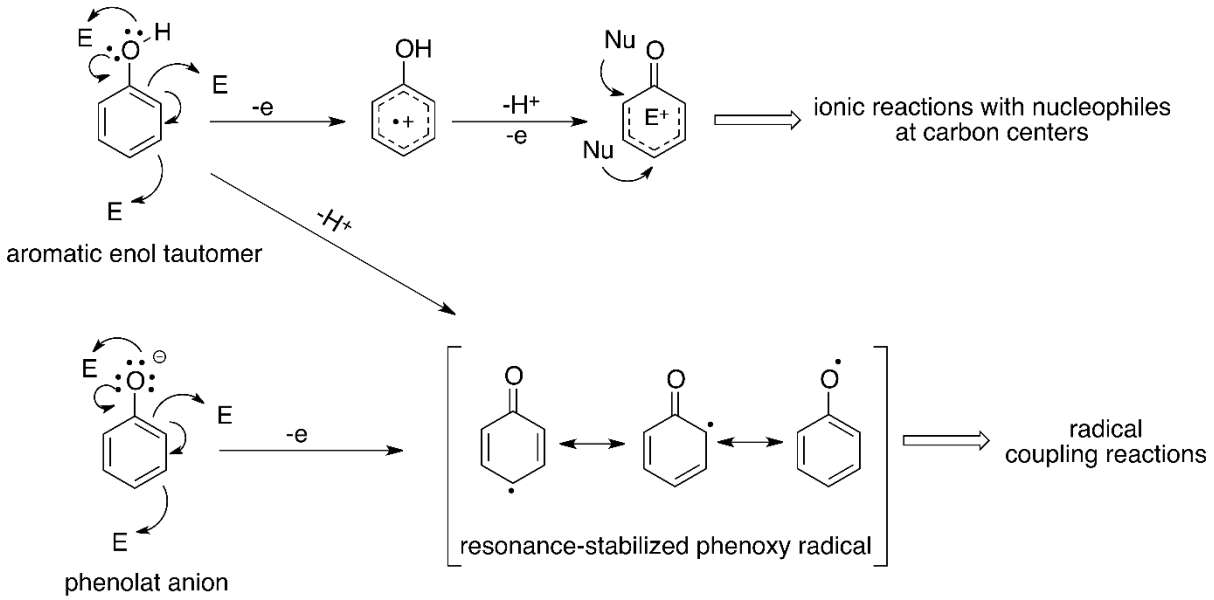

Figure 1.8 Basic reactions of the enolic form and phenolat anion (adapted and modified from (Quideau et al., 2011)). The phenolic "umpolung" forms a phenoenium cation that reacts with nucleophiles at *ortho*- and *para*-carbon centres. The release of a hydrogen atom of the enol tautomer leads to stabilized radicals. Additionally, phenolat anions can be easily oxidized through one-electron processes also generating delocalized radicals, which can undergo coupling reactions through carbon-oxygen or carbon-carbon bond-forming events, leading to polyphenols that are more complex. Both processes underlie the health benefiting antioxidant properties of plant phenols.

Phenolic alcohols and their secoiridoid derivatives

The phenolic alcohols hydroxytyrosol (3,4-dihydroxyphenylethanol) and tyrosol (*p*-hydroxyphenylethanol) are exclusively present in olives either as free compounds or linked to elenolic acid or its dialdehydic form, resulting to the following secoiridoid derivatives: oleuropein and oleuropein aglycone, oleuroside, oleacein, ligstroside and ligstroside aglycone, ligustaloside B, and oleocanthal (see Figure 1.9). Iridoids are a class of monoterpenoids bearing ten carbon atoms. A structural characteristic of these compounds is the cis-fused cyclopentapyran system, existing as glycosides or aglycones in the form of secoiridoids. In particular, oleuropein is the ester of elenolic acid with hydroxytyrosol and ligstroside is the ester of elenolic acid with tyrosol, both being the parent compounds of the less polar oleuropein aglycone and ligstroside aglycone. The aglycones are formed by removal of the glucose moiety. Oleuropein aglycone and ligstroside aglycone and their various derivatives are present in olive oil, whereas the polar glycosides oleuropein and ligstroside are mainly present in olives. Therefore, it has also to be noted that EVOO ordinarily does not contain ligstroside, since this

polyphenol can only be detected in large quantities during the early ripening period of olive fruits (Deiana et al., 2019).

It has to be considered that the contents of polyphenols in EVOO varies from 50 to 800 mg/kg, depending on the variety, the area of cultivation and climate, the time of harvest, the ripeness of the olive, and the production process (Visioli and Galli, 1995; Deiana et al., 2019). For example the amount of oleocanthal varies between 0.02% and 10% (Impellizzeri and Lin, 2006; Karkoula et al., 2012, 2014). Therefore, it is essential to test pure compounds to reveal a basic understanding of the cause-effect relationships.

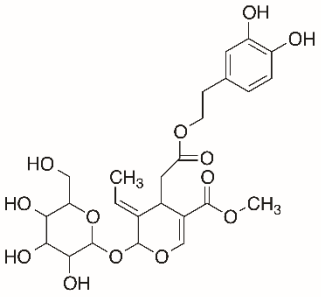

Oleuropein

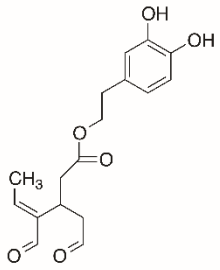

Oleacein

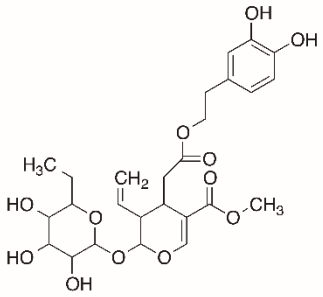

Oleuroside

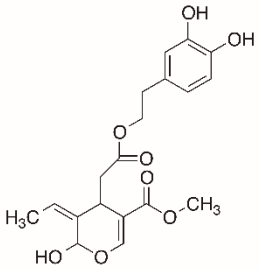

Oleuropein aglycone

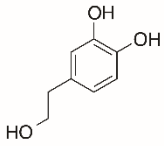

Hydroxytyrosol

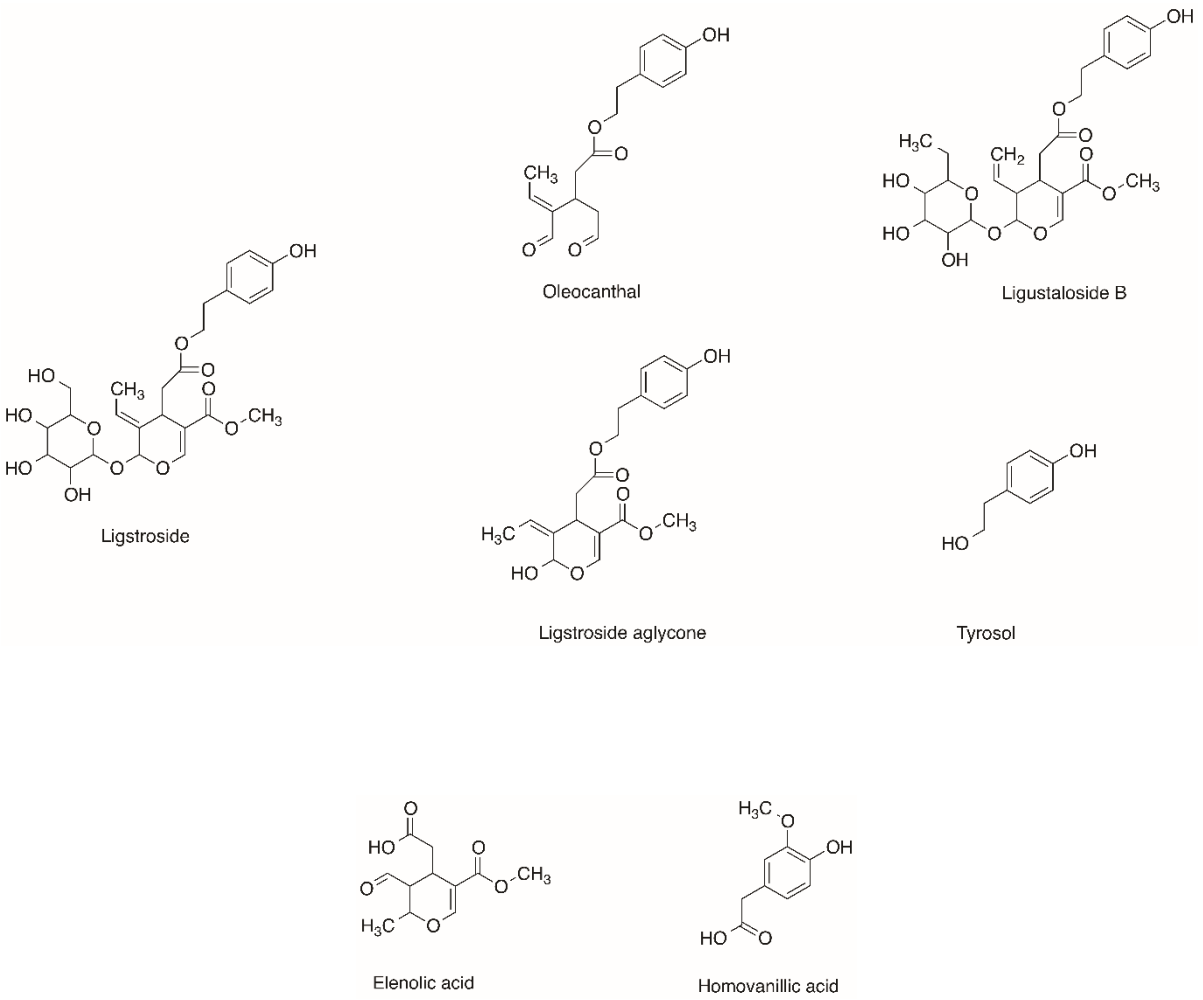

Figure 1.9 Chemical structures of secoiridoid derivatives. Chemical structures of secoiridoid derivatives present in olives, in their hydrolysed form hydroxytyrosol and tyrosol, and their two metabolites elenolic acid and homovanillic acid.

Bioavailability

The first requirement for a dietary compound to be a promising candidate is that it reaches the systemic circulation and the specific targets where it can exert its biological action. Generally, it is known, that polyphenols undergo phase I (hydroxylation) and phase II (conjugation) metabolism to be modified into their glucuronidated, methylated and sulfated form in order to be absorbed. Most of the studies regarding the bioavailability of phenols in olives or EVOO has been mainly focused on hydroxytyrosol and tyrosol, firstly determined in humans by Visioli et al. (Visioli et al., 2000). Additional human studies could demonstrate as well a dose-dependent absorption over 50% and a complex metabolism of olive phenols (Vissers et al., 2002; Suárez et al., 2011). The acidic environment of the stomach partly modifies olive polyphenols. This is

especially the case for aglycone secoiridoids. Hydrolysation of aglycones leads to free hydroxytyrosol and tyrosol. Still, some remain intact and enter the small intestine as secoiridoid aglycones (Corona et al., 2006). Conversely, secoiridoids bearing the sugar moiety are not subjected by gastric hydrolysis and enter the small intestine unmodified (Vissers et al., 2002). Due to a rapid increase of hydroxytyrosol and tyrosol in plasma (1 h) and urine (2 h), it is suggested that the small intestine is the main side of absorption. Analyses of plasma and urine had shown a primary metabolization to *o*-glucuronidated conjugates and in a less amount to *o*-methylated or sulfonated conjugates as well as to the two metabolites homovanillic acid, and homovanillyl alcohol (Miró-Casas et al., 2003; Suárez et al., 2011; Rubió et al., 2012). Additionally, Corona et al. had shown, that secoiridoids which are not absorbed by the small intestine, undergo degeneration by the colonic microflora ending up as hydroxytyrosol (Corona et al., 2006). Notably, it has been shown, that oleocanthal is able to cross the blood-brain barrier of mice brains (Abuznait et al., 2013; Qosa et al., 2015).

However, the exact absorption mechanism in humans is still not fully understood yet.

Most polyphenols are weakly absorbed and quickly metabolized. Anyhow, they might have beneficial effects on prevention of diseases that develop over a long period, by a daily intake and therefore being present in low but constant doses in the organism (Quideau et al., 2011).

Serreli and Deinana et al. calculated if a person consumed 25-50 ml EVOO a day, the intake of polyphenols would be around 9 mg/day. It has been estimated, that 1 mg is represented by hydroxytyrosol and tyrosol, whereas the remaining 8 mg are related to their elenolic esters and to oleuropein aglycones and ligstroside aglycones (Serreli and Deiana, 2018). It has been shown that after an intake of 25 ml/day EVOO, which is lower than the traditional daily consumption in Mediterranean areas, 98% of olive polyphenols are present in human plasma and urine as phase II metabolites, predominant as glucuronides and sulfated conjugates (Miro-Casas et al., 2003). Thus, the cited calculations only represent an approximation to the real situation.

1.4 Cellular models for AD

Central nervous system disorders are of high complexity. Since there is no proper cure, it is of high interest to gain a better understanding of their pathogenesis and to assess potential novel therapeutics. As mentioned in chapter 1.1, AD is characterized by impaired neuronal function

due to a progressive loss of neurons in the brain. Additionally, one of the multiple pathological hallmarks of the disease is the neuronal accumulation of amyloid plaques in affected brain regions. Since it is difficult to arrange or work on the human brain, experimental models are critical. Regarding AD animal models, research has focused on genetically-modified mice (transgenic or knockout), which for example express high levels of APP or PSEN1 and show other hallmarks of AD including plaque deposition and cognitive deficits, but notably reflect the inherited form of early-onset AD, which comprises only around 5% of all AD cases. Although, these models provide important insights into AD, researchers seek to create *in vivo* models, which reflect the more common, sporadic form of AD. Besides a range of transgenic animal models there are various *in vitro* cell lines used in AD investigations. Cell culture models provide a relatively simple, less invasive and economical method to study interactions of cellular material and drug. *In vitro* models are a good primary tool to investigate the disease pathology and especially for drug screening to support further animal and human investigations.

As in all neurodegenerative disorders neurons in the human brain are primarily affected. Obtaining human cells for *in vitro* investigations for AD is quite challenging. In 1962, CNS organotypic culture was firstly isolated from rat hypophysis tissue (Bousquet and Meunier, 1962). Since then, neuronal cultures have been prepared from brain slices (LaVail and Wolf, 1973; Whetsell and Schwarcz, 1983; Robertson et al., 1997). The possibility to prepare *in vitro* cultures of neuronal cells was fundamental in understanding the functioning of the nervous system. Although primary cells are barely altered and represent the organism the closest, the culture of neuronal cells is challenging since mature neurons do not undergo cell division. Additionally they are difficult to prepare and their variability restricts the reproducibility in experiments (Walsh et al., 2005). Furthermore, primary neuronal cells need to be separated from astrocytes and oligodendrocytes, as much as possible. Other important limitations are the lack of availability and quality of the post-mortem tissue. One way to overcome these limitations is the use of immortalized cell lines derived from neuronal tumours. Permanente cell lines give unlimited cell numbers and ideally do not vary between cultures or are rather homogenous. On the other hand, there are also some disadvantages as secondary cell lines often present genetic and metabolic differences compared to the cell type from which they were derived (Gordon et al., 2014). To get a more neuronal phenotype, culture conditions can be changed, e.g. addition of specific growth factors.

SH-SY5Y cells is one such cell line which is widely used as an *in vitro* model for AD and generally in research on neuronal cells (Gordon et al., 2013; Dubey et al., 2019). Additionally, the neuroblastoma cell lineage is frequently chosen because of its human origin and its catecholaminergic- neuronal properties (Xicoy et al., 2017). Under normal culture conditions, SH-SY5Y cells are undifferentiated monitoring a neuroblast-like morphology and express immature neuronal markers. One of several methods to differentiate SH-SY5Y cells is the addition of retinoic acid, which is marked by a morphological change similar to primary neurons, an increased expression of mature neuronal markers, and a partly inhibition of cell growth (Påhlman et al., 1984). As differentiated cells show problems in stability, variability and quantity of cells, the use of immortalized neuronal cells appear as an excellent alternative (Allen et al., 2005). Common used immortalized neuronal *in vitro* systems such as PC12 or SH-SY5Y cells can be transfected with wild-type amyloid precursor proteins, tau or mutant forms of those (Löffler et al., 2012; Stockburger et al., 2014b; Hagl et al., 2015b; Pohland et al., 2018). Transfection with APP mutations leads to an overproduction of Aβ. PC12 is a rat cell line that was derived from a pheochromocytoma of the adrenal medulla (Greene and Tischler, 1976). PC12 cells, stably transfected with the Swedish double mutation of APP express Aβ in low levels and are therefore a culture model for early stages of AD or late-onset AD. These cells exhibit impaired mitochondrial function and abnormal mitochondrial biogenesis (Hagl et al., 2015b). HEK293 a human, actually a non-neuronal cell line but with immature neuronal characteristics, stably transfected with Swedish mutant APP produce high amounts of Aβ and is thus more suitable to model early-onset AD (Citron et al., 1992; Gordon et al., 2013).

In recent years, stem cells that are among others involved in generating differentiated neurons gain much attention, as they are capable of long-term self-renewal in contrast to mature neurons, as mentioned above. Induced pluripotent stem cells (iPSC) have been generated from human donor cell types, such as fibroblasts or blood cells. Several groups have produced iPSCs from patients with familial and patients with sporadic AD. Both cultures showed an excess of Aβ and hyperphosphorylated tau compared to aged-control iPSCs (Yagi et al., 2011; Israel et al., 2012; Kondo et al., 2013; Muratore et al., 2014). iPSCs are a promising tool for the investigation of AD pathology but also bare limitations. Individual iPSCs vary in their phenotype due to inter-patient variations, and there is still a lack of standardized protocols to generate and maintain these cells, what might change in future.

In the last few years, the development of three-dimensional (3D) culture models became increasing popular as they overcome the limitations of the previous discussed *in vitro* models by offering a physiological environment of specific tissues or cells. These 3D models can be produced either with hydrogels or inert matrices or without a scaffold. Scaffold-free methods rely on iPSCs to self-assemble what makes it possible to create organ-like structures, known as organoids. In 2016, Raja et al. generated brain organoids from iPSCs of patients with familial AD. These brain organoids reproduced extracellular aggregation of Aβ plaques and intracellular aggregation of tau. Notably, this is the first time that both AD hallmarks were replicated *in vitro* and which furthermore, have never been reported in mouse models (Raja et al., 2016). Since this technology is quite new, there are still disadvantages or limitations.

An overview of the different *in vitro* cell lines used in AD investigations was recently published by Dubey et al. (Dubey et al., 2019).

Generally, it must be considered that animal models have non-physiological expression of Aβ or tau - Aβ formation and accumulation is physically and biochemically different in rodents in comparison to humans, and hence difficult to interpret downstream pathological changes. The poor success rate of clinical trials can be partly explained by the translation of animals to humans (Schneider et al., 2014; Banik et al., 2015). Additionally, non-human *in vitro* cultures have traditionally been more widely used. Human derived cells express a number of human specific proteins that would not be present in rodent cultures. However, the use of human derived tissue and cell lines or human stem cells is always to favour. Although the development of 3D-culture models represent roughly the complexity of human brain and therefore provide a new tool to model normal and pathological brain, there are still many challenges and limitations.

Immortalized human neuronal cell lines have the advantage of allowing a high-throughput screening of new substances, easy to handle and have a good reproducibility in experiments. Additionally, e.g. SH-SY5Y cells have a neuroblast-like morphology, are positive for tyrosine hydroxylase (TH) and dopamine-β-hydroxylase characteristic of catecholaminergic neurons, despite having the disadvantage being of cancerous origin. Furthermore, immortalized cells are always accessible and economical. Novel therapeutics can be tested quickly and rigorously such that the effects of potential drugs can be evaluated and their mechanism identified, and are therefore a good primary tool.

The SH-SY5Y neuroblastoma cell line is well characterized and favoured for the *in vitro* use in neuroscience, especially in neurodegenerative research. SH-SY5Y cells are originally derived from a bone tumor biopsy and a subline of the parental SK-N-SH line, which were subcloned three times (SH-SY to SH-SY5 and last to SH-SY5Y) (Kovalevich and Langford, 2013). As mentioned before, SH-SY5Y cells can be obtained in both, undifferentiated and differentiated form. As well in their undifferentiated form, SH-SY5Y cells have a neuroblast-like morphology and express immature neuronal markers (Påhlman et al., 1984). Briefly, they resemble mainly immature cholinergic neuronal cells, what makes them very suitable in studying the development and drug discovery of AD (Dubey et al., 2019). As a relevant cellular model for AD, SH-SY5Y cells can be stably transfected with key proteins of AD such as, human native tau (hTau40), mutant tau (P301L) or wild type amyloid precursor protein APP. It has been demonstrated, that APP transfected cells show elevated Aβ levels and impaired mitochondrial functions. In particular decreased ATP level, impaired mitochondrial membrane potential, and decreased mitochondrial respiration. Additionally, mitochondrial dynamics such as fission and fragmentation processes were altered (Rhein et al., 2009a; Stockburger et al., 2014b). Another study reported decreased mitochondrial DNA transcripts in APP transfected SH-SY5Y cells (Lopez Sanchez et al., 2017). Furthermore it has been shown that Bcl-2 levels and proteasome activity were decreased together with increased oxidative stress (Matsumoto et al., 2006). The increasing Aβ production together with mitochondrial dysfunction in APP transfected SH-SY5Y cells is well established. Taken together the cell line is a well-suited model for *in vitro* investigations in AD together with studying mitochondrial dysfunction, which arises mainly in the early stages of the progression of AD. The mild APP overexpression and the slightly elevated Aβ production make APP transfected SH-SY5Y cells a useful neuronal model for the early stages of late-onset AD.

2 Aim of the thesis

With increasing life expectancy and the consequential demographical shift towards an increase in population and ageing, the prevalence of neurodegenerative diseases such as Alzheimer's disease (AD) rises. To date, nearly 50 million people worldwide are suffering from dementia and the global number of patients is expected to triple by 2050. Despite extensive research into the pathology, AD, the most common form of dementia cannot be cured yet. Over 25 years, AD research has focused on the amyloid hypothesis, which assumes that the accumulation of the peptide amyloid-β is the main cause of the disease. One reason for the failure of clinical trials is thought to be that drugs had been administered too late in the disease progression. Currently, research is based on a number of cell and animal models, which are mainly useful for the familial form of AD. This form of AD only represents a small percentage of AD. With more than 90% of all AD cases, late-onset AD is much more common. Both, to investigate new drugs and to understand the pathology itself the need of models for the most frequent form of AD, late-onset AD is necessary. Therefore, in the present thesis a cell model should be established, in which a particular mild Aβ expression is present. These mild changes are supposed to be representative for the late-onset form of AD, before the onset of typical AD symptoms.

It is also becoming clear that it is of high importance to intervene in an early stage of AD. AD is intricate because of its multifactorial pathophysiological events including mitochondrial dysfunction. Mitochondrial dysfunction is increasingly recognized as one of the early events in the progression of AD. Aberrant bioenergetics is likely to play an important role in AD and ageing. In particular, reduced oxygen consumption, ATP production and downregulation of mitochondrial biogenesis have been observed in cell and animal models of AD. For this reason, mitochondrial parameters – in particular mitochondrial function and mitochondrial molecular mechanisms should be focused in this cell model.

In Mediterranean regions the prevalence of AD is low compared to those of other countries. Systematic reviews and meta-analysis have elaborated that the Mediterranean diet (MedDiet) lowers the incidence of AD. One integral component of the MedDiet is the high intake of extra virgin olive oil (EVOO). The health promoting properties of olive polyphenols and their metabolites have been frequently investigated in mixtures and extracts. However, for a basic understanding of the cause-effect relationships it is essential to test pure compounds. In a cooperation project with the university TU-Darmstadt and the company N-Zyme BioTec, supported by the German Ministry of Education and Research (BMBF #031A590C),

secoiridoid derivatives were obtained in a novel biotechnological and preparative approach. The partners produced starting from the precursor molecules oleuropein and ligstroside the functional secoiridoid derivatives ligstroside aglycone, oleocanthal, oleuropein aglycone, oleacein, oleuroside, ligustaloside B, their hydrolysis products tyrosol and hydroxytyrosol and two metabolites elenolic acid and homovanillic acid. The synthesized substances were purified by N-Zyme BioTec with the Fast Centrifugal Partition Chromatography (FCPC) in combination with the preparative RP-HPLC and characterized by mass spectrometry and NMR analysis, whereas product purities up to 99% should be achieved.

Accordingly, we tested ten highly purified olive secoiridoid derivatives and two metabolites which have been isolated from olive leaves on mitochondrial function in the established late-onset AD cell model. From the previous screening of these 12 substances, detailed investigations of the four best hit-substances with regard of their effectiveness in improving mitochondrial function should be examined.

3 Materials and Methods

3.1 Materials

3.1.1 Devices

Device	Name	Company	City, Country
Autoclave	Bioklav	Schütt Labortechnik	Göttingen, Germany
Balance	Precision balance AEJ200-5CM	Kern & Sohn GmbH	Balingen-Frommern, Germany
Blotting Chamber	Mini Protean® 3 System	Bio-Rad	München, Germany
Blotting System	Criterion™ Blotter	Bio-Rad	München, Germany
Centrifuge	Heraeus Megafuge 16 R	Thermo Fisher Scientific	Waltham, USA
Centrifuge	Heraeus Fresco 21 Centrifuge	Thermo Fisher Scientific	Waltham, USA
Centrifuge	GS-6R, Microfuge R	Beckman	Krefeld, Germany
Freezer (-20°C)	GNP 5255 Index 20A/001	Liebherr International Deutschland GmbH	Biberach an der Riβ, Germany
Freezer (-80°C)	TSX SERIES with VDRIVE	Thermo Fisher Scientific	Waltham, USA
Freezing Container	Nalgene®, Mr. Frosty	Thermo Fisher Scientific	Waltham, USA
Fridge (4°C)	3130 Index 20B/001	Liebherr International Deutschland GmbH	Biberach an der Riβ, Germany
Hamilton Syringe	Hamilton Syringe gastight, #1701, #1702, # 1705, #1725	Hamilton	Höchst, Germany
Imaging System	ChemiDoc™ Touch Imaging System	Bio-Rad	München, Germany
Incubator	Midi 40 CO_2 Incubator	Thermo Fisher Scientific	Waltham, USA
Incubator	BB6220	Heraeus	Hanau, Germany
Lab Homogenizer	Ultrasonic Processor UP50H	Hielscher Ultrasonics GmbH	Teltow, Germany

Laminar air flow work bench	MSC Advantage	Thermo Fisher Scientific	Waltham, USA
Microscope	Axiovert S100	Carl Zeiss AG	Oberkochen, Germany
Microscope	TCS SP5	Leica	Solms, Germany
Multichannelpipette	Xplorer 300 µL	Eppendorf	Hamburg, Germany
Multireader	Clariostar Viktor X3 2030	BMG Labtech Perkin Elmer	Ortenberg, Germany Rodgau-Jügeshein, Germany
Nanodrop	Nanodrop One	Thermo Fisher Scientific	Waltham, USA
Neubauer counting chamber	Neubauer counting chamber	Labor Optik	Lancing, GB
Oxygraph	Oxygraph 2k	Oroboros	Innsbruck, Austria
PCR Cycler	T100™ Thermal Cycler	Bio Rad	München, Germany
PCR workstation pipette	PCR workstation Finnpipette®	Thermo Fisher Scientific	Waltham, USA
pH-Meter	pH Meter HI2210	Hanna Instruments Deutschland GmbH	Vöhringen, Germany
Photometer	Spectrophotometer Genesys 10S UV-VIS	Thermo Fisher Scientific	Waltham, USA
Pipette	Research Plus 100-1000 µL	Eppendorf	Hamburg, Germany
Pipette	Pipete P2, P20, P2000	Gilson	Limburg, Germany
Pipette	Accu-jet® pro	Brand	Wertheim, Germany
Plate Stirrer	LAB DICS SO40	VWR International	Radnor, USA
Plate Stirrer	VARIOMAG MONO	H+P Labortechnik	Oberschleissheim, Germany
Protein Detection System	SNAP i.d. 2.0	Merck KGaA	Darmstadt, Germany
Real-time PCR System	CFX Connect™ Real-Time System	Bio-Rad	München, Germany
Rocking Shaker	Rocker 2D basic	IKA®-Werke GmbH & CO KG	Staufen, Germany
Thermo Shaker	PHMT-PSC24N	Grant Instruments	Shepreth, UK
Thermomixer	PSC24N Thermo-Shaker	Grant bio	Cambridgeshire, UK

Vacuum pump	Diaphragm vacuum pump	Vaccubrand GmbH & Co	Wertheim, Germany
Vacuum Pump	Millivac-Mini Vacuum Pump, XF5423050	Merck KGaA	Darmstadt, Germany
Vortex	Vortex-Genie 2®	Scientific Industries	Bohemia, USA
Walter filtration system	MilliQ Academic	Millipore	Schwalbach, Germany
Water bath	WNB22	Memmert	Schwabach, Germany

3.1.2 Consumables

Material	**Name**	**Company**	**City, Country**
24-well culture plate	Cellstar® 24-well cell culture plate, sterile	Greiner Bio-One	Frickenhausen, Germany
96-well microtiter plate	Microtiterplate white walled (96-well), sterile	Sigma-Aldrich	Steinheim, Germany
96-well PCR microtiter plate	Hard-Shell® PCR Plates 96-well, thin wall, sterile	Bio-Rad	München, Deutschland
Cell culture flask	Cellstar® Cell culture flask 250 ml, sterile	Greiner Bio-One	Frickenhausen, Germany
Centrifuge tubes	Centrifuge tubes	Greiner Bio-One	Frickenhausen, Germany
Disposable gloves	Vasco® Nitril white	B. Braun	Melsungen, Germany
Distritips	Distritips (125 µl, 1250 µl, 12.5 ml), sterile	Gilson	Middleton (WI), USA
Filter paper	Criterion™ Blot Filter Paper	Bio-Rad	München, Germany
Serological pipettes	Cellstar® Serological pipettes (5, 10, 25, 50 ml)	Greiner Bio-One	Frickenhausen, Germany
Single-use needles	Single-use hypodermic needles Sterican®	B. Braun	Melsungen, Germany

Syringe 1 ml	Injekt®-F Solo	B. Braun	Melsungen, Germany

3.1.3 Chemicals

Chemical	**Company**	**City, Country**
4-(2-hydroxyethyl)-1-piperazineethanesulfonic acid (HEPES)	Merck KGaA	Darmstadt, Germany
5,5‘-dithiobis-(2-nitrobenzoic acid) (DTNB)	Sigma-Aldrich	Steinheim, Germany
Acetyl coenzyme A	PanReac AppliChem	Darmstadt, Germany
Acrylamide/Bis-Solution (30%)	Bio-Rad	München, Germany
Adenosine diphosphate (ADP) (Sigma-Aldrich, Steinheim)	Sigma-Aldrich	Steinheim, Germany
Ammonium persulfate (APS)	Bio-Rad	München, Germany
Antimycin A	Sigma-Aldrich	Steinheim, Germany
Aprotinin	Sigma-Aldrich	Steinheim, Germany
Bovine serum albumine, essentially fatty acid free (BSA)	Sigma-Aldrich	Steinheim, Germany
Calcium chloride	Merck KGaA	Darmstadt, Germany
Carbonyl cyanide 4-trifluoromethoxyphenylhydra-zone (FCCP)	Sigma-Aldrich	Steinheim, Germany
Cell extraction buffer	Thermo Fisher Scientific Inc.	Waltham, USA
Cytochrome c from equine heart	Sigma-Aldrich	Steinheim, Germany
Digitonine	Sigma-Aldrich	Steinheim, Germany
Dimethylsulfoxid (DMSO)	Merck KGaA	Darmstadt, Germany
Disodium phosphate	Merck KGaA	Darmstadt, Germany
Dithionite	Merck KGaA	Darmstadt, Germany
Dulbecco’s Modified Eagle Medium (DMEM)	Invitrogen by Thermo Fisher Scientific Inc.	Waltham (MA), USA
Dulbecco’s phosphate buffered saline (PBS)	Gibco	Darmstadt, Germany
Ethanol (>99%)	Merck KGaA	Darmstadt, Germany

Ethanol (70%)	Roth	Karlsruhe, Germany
Ethylene glycol tetraacetic acid (EGTA)	Sigma-Aldrich	Steinheim, Germany
Ethylenediaminetetraacetic acid (EDTA)	Merck KGaA	Darmstadt, Germany
Fetal calf serum (FCS)	Sigma-Aldrich	Steinheim, Germany
Glucose	Merck KGaA	Darmstadt, Germany
Glutamate	Sigma-Aldrich	Steinheim, Germany
Glycine	Roth	Karlsruhe, Germany
Hanks' balanced salts	Sigma-Aldrich	Steinheim, Germany
Hydrochloric acid	VWR-International	Radnor (PA), USA
Hydrochloric acid 37% (HCl)	Merck KGaA	Darmstadt, Germany
Hygromycin B (50 mg/ml)	Invitrogen by Thermo Fisher Scientific Inc.	Waltham (MA), USA
Isopropanol	Merck KGaA	Darmstadt, Germany
iTaq™ Universal SYBR® Green Supermix	Bio-Rad	München, Germany
K-lactobionate	Sigma-Aldrich	Steinheim, Germany
Leupeptin	Sigma-Aldrich	Steinheim, Germany
Luminata™ Crescendo Western Horseradish Peroxidase (HRP) substrate	Merck KGaA	Darmstadt, Germany
Magnesium chloride hexahydrate	Merck KGaA	Darmstadt, Germany
Magnesium sulfate heptahydrate	Merck KGaA	Darmstadt, Germany
Malate	Sigma-Aldrich	Steinheim, Germany
MEM vitamin solution 100x	Gibco by Thermo Fisher Scientific Inc.	Waltham (MA), USA
Methanol	Merck KGaA	Darmstadt, Germany
Minimun Essential Media (MEM) Non-Essential Amino Acids (NEAA) 100x	Gibco by Thermo Fisher Scientific Inc.	Waltham (MA), USA
Monopotassium phosphate	Merck KGaA	Darmstadt, Germany
N, N, N′, N′-tetramethylethylendiamine (TEMED)	Bio-Rad	München, Germany
Non-fat dried milk powder	Sigma-Aldrich	Steinheim, Germany
NuPage® Antioxidant	Invitrogen by Thermo Fisher Scientific Inc.	Waltham (MA), USA

NuPage® LDS Sample Buffer 4x	Invitrogen by Thermo Fisher Scientific Inc.	Waltham (MA), USA
NuPage® Sample Reducing Agent 10x	Invitrogen by Thermo Fisher Scientific Inc.	Waltham (MA), USA
NuPage® Transferbuffer 20x	Invitrogen by Thermo Fisher Scientific Inc.	Waltham (MA), USA
Oligomycin	Sigma-Aldrich	Steinheim, Germany
Oxalacetate	Sigma-Aldrich	Steinheim, Germany
Penicilin/Streptomycin (10 000 U/ml)	Gibco by Thermo Fisher Scientific Inc.	Waltham (MA), USA
Pepstatin	Sigma-Aldrich	Steinheim, Germany
Phenylmethylsulfonylfluorid (PMSF)	Sigma-Aldrich	Steinheim, Germany
Potassium chloride	Merck KGaA	Darmstadt, Germany
Precision Plus Protein All Blue Standards	Bio-Rad	München, Germany
Precision Protein™ Strep Tactin-HRP Conjugate	Bio-Rad	München, Germany
Protease Inhibitor Cocktail Complete	Roche	Basel, Switzerland
Rhodamine-123	Sigma-Aldrich	Steinheim, Germany
RNAprotect Cell reagent	Qiagen N.V.	Hilden, Germany
Rotenone	Sigma-Aldrich	Steinheim, Germany
Sodium ascorbate	Sigma-Aldrich	Steinheim, Germany
Sodium azide	Sigma-Aldrich	Steinheim, Germany
Sodium chloride	Merck KGaA	Darmstadt, Germany
Sodium deoxychalat	Sigma-Aldrich	Steinheim, Germany
Sodium dodecyl sulfate (SDS)	Merck KGaA	Darmstadt, Germany
Sodium hydroxide	Merck KGaA	Darmstadt, Germany
Sodium orthovanadate	Sigma-Aldrich	Steinheim, Germany
Sodium pyrophosphate	Sigma-Aldrich	Steinheim, Germany
Sodium pyruvate 100x (100 nM)	Gibco by Thermo Fisher Scientific Inc.	Waltham (MA), USA
Succinate	Sigma-Aldrich	Steinheim, Germany
Sucrose	ROTH	Karlsruhe, Germany

Taurine	Sigma-Aldrich	Steinheim, Germany
Triethanolamine	Sigma-Aldrich	Steinheim, Germany
Tris(hydroxymethyl)aminomethan (Tris)	Merck KGaA	Darmstadt, Germany
Triton X-100	Sigma-Aldrich	Steinheim, Germany
Trypan blue	Sigma-Aldrich	Steinheim, Germany
Trypsin-EDTA (0.05%)	Gibco by Thermo Fisher Scientific Inc.	Waltham (MA), USA
Tween™20	Sigma-Aldrich	Steinheim, Germany
Urea	Merck KGaA	Darmstadt, Germany
β-Mercaptoethanol	PanReac AppliChem	Darmstadt, Germany

3.1.4 Kits

Kit	**Company**	**City, Country**
ViaLight Plus bioluminescence kit	Lonza	Walkersville, USA
Pierce™ BCA Protein Assay Kit	Thermo Fisher Scientific Inc.	Waltham, USA
RNeasy® Mini Kit (250)	Qiagen N.V.	Hilden, Germany
Turbo DNA-free™ Kit	Thermo Fisher Scientific Inc.	Waltham, USA
Human Aβ1-40 ELISA Kit	Elabscience	Houston, USA

3.1.5 Buffer, solutions and media

All buffers were produced in ultrapure water (Milli-Q, Millipore, Billerica, USA), which is referred to as H_2O in the following.

3.1.5.1 General buffers and solutions

Tris buffer

2.42 g Tris were dissolved in 1.0 L H_2O and pH was adjusted to 7.4 at 4 °C with HCl (1N).

Phosphate buffer saline (PBS)

100 ml of Dulbecco's PBS (10x) were diluted in 900 ml H_2O to obtain a 1x work solution.

HBSS buffer

HBSS	9.5 g
HEPES	2.4 g
$CaCl_2 \cdot 2H_2O$	0.147 g
$CgSO_4 \cdot 7H_2O$	0.246 g

The substances were dissolved in 1.0 L H_2O and adjusted to pH 7.4 at 37 °C using HCl (1N) and NaOH (1N). HBSS was stored at 4 °C.

Trypan blue solution (0.4%)

100 mg of trypan blue were dissolved in 100 ml PBS (1x).

3.1.5.2 Cell culture medium for SH-SY5Y-MOCK and SH-SY5Y-APP$_{695}$

Cell culture medium

DMEM	500 ml
FCS	10%
Hygromycin B	0.3 mg/ml
Sodium pyruvate	5 ml
NEAA	5 ml
Pen/Strep	60 U/ml
Vitamins	5 ml

The indicated volumes are required to produce full cell culture medium. For the production of reduced cell culture medium, FCS content was lowered to 2%. Cell culture medium was stored at 4 °C.

Freezing medium consisted of 50% FCS, 40% DMEM and 10% DMSO (sterile filtered). Freezing medium was stored at -20 °C.

3.1.5.3 Buffers for the determination of Citrate synthase activity

Tris HCl buffer (1.0 M)

12.114 g Tris were dissolved in 100 ml H_2O and adjusted to pH 8.1 with HCl (37%). Tris HCl buffer was stored at 4 °C.

Triethanolamine HCl buffer (0.5 M)

8.06 g Triethanolamine were dissolved in 100 ml H_2O and adjusted to pH 8.0 with HCl (37%). 186.1 mg of EDTA were added. The buffer was stored at 4 °C.

Triton X 100 (10%)

10 g Triton X-100 were dissolved in 90 ml H_2O. The storage was carried out at 4 °C.

Oxalacetate solution (10 mM)

5.94 mg Oxalacetate were dissolved in 4.5 ml Triethanolamine HCl buffer (0.1 M).

DTNB solution (1.01 mM)

3.6 mg DTNB were dissolved in 9 ml Tris buffer.

Citrate synthase reaction medium

DTNB	0.1 mM
Triton-X-100	10%
Oxalacetic acid	10 mM
Acetyl coenzyme A	12.2 mM

MIR05

EGTA	0.5 mM
$MgCl_2 \cdot 6\ H_2O$	3 mM
*K-Lactobionat	60 mM
Taurine	20 mM
Sucrose	100 mM
BSA	1 g/l
H_2O ad	1 l

pH was adjusted to 7.1 at 30 °C with KOH (5 N) and MIR05 was stored at -20 °C.

*K-Lactobionat stock solution

35.83 g K-Lactobionat were dissolved in 100 ml H_2O and pH was adjusted to 7.0 with KOH. H_2O was added to reach a final volume of 200 ml.

Lysis buffer

Buffer 1

EDTA	1 nM
Triton X-100	0.5%
NaF	5 mM
PBS (1x) ad	250 ml

Buffer 2

Urea	6 M
Sodium pyrophosphat	2.5 mM
Sodium orthovanadate	1 mM
Sodium deoxycholat	0.5%
Sodium dodecylsulfate	0.5%
Buffer 1 ad	100 ml

To the appropriate amount of buffer 2 shortly before use, following substances were added:

Aprotinin	1.7 mg/ml
Leupeptin	5 mg/ml
Pepstatin	100 mM

3.1.5.4 Buffers and solutions for Western blotting

Lower buffer for gel casting

45.425 g Tris and 1 g SDS were dissolved in 250 ml H_2O. pH was adjusted to 8.8 with HCl (37%). The lower buffer was stored at 4 °C.

Upper buffer for gel casting

6.04 g Tris and 0.4 g SDS were dissolved in 100 ml H_2O. pH was adjusted to 6.8 with HCl (37%). The upper buffer was stored at 4 °C.

Separating gel (for 1.5 mm SDS gels)

	7%	10%	12%	15%	
H_2O	4.19	3.4	2.81	1.27	ml
Lower buffer	2.15	2.15	2.15	2.15	ml
Acrylamide	1.92	2.74	3.29	4.13	ml
TEMED	4.13	4.13	4.13	4.13	µl
APS (10%)	41.25	41.25	41.25	41.25	µl

APS (10%) was prepared on the day of experiment.

Stocking gel

H_2O	2.64 ml
Upper buffer	1.07 ml
Acrylamide	412.5 µl
TEMED	4.13 µl
APS (10%)	20.63 µl

APS (10%) was prepared on the day of experiment.

Electrode buffer (10x) for gel electrophoresis

Tris	30.3 g
SDS	10 g
Glycin	144.7 g
H_2O ad	1.0 l

For gel electrophoresis the buffer was used 1x.

Transfer buffer

	1 gel	2 gels
H_2O	850 ml	750 ml
Methanol	100 ml	200 ml
NuPage Transfer Buffer (20x)	50 ml	50 ml
NuPage Antioxidant	1 ml	1 ml

TBST (10x)

Tris	24.2 g
NaCl	80 g
HCl (37%)	13 ml
Tween20	5 ml
H_2O ad	1.0 l

TBST (10x) was stored at room temperature and diluted 1:10 prior to use.

Stripping buffer

8.0g glycine were dissolved in 1.0 l H_2O and 2.5 ml HCl (37%) were added.

3.1.6 Primer

Primer	Sequence (3´-5´)	Product size (bp)	Company	City, Country
ACTB	Fwd: GGA CTT CGA GCA AGA GAT GG Rvs: AGC ACT GTG TTG GCG TAC AG	234	Biomol GmbH	Hamburg, Germany
ATP5D	Fwd: GGA AGC TCC TCC TCA GCT TT Rvs: CAG GCT TCC GGG TCT TTA AT	198	Biomol GmbH	Hamburg, Germany
CAT	Fwd: ACT TCT GGA GCC TAC GTC CT Rvs: CGC ATC TTC AAC AGA AAG GT	200	Biomol GmbH	Hamburg, Germany
COX5A	Fwd: GCA TGC AGA CGG TTA AAT GA Rvs: AGT TCC TCC GGA GTG GAG AT	152	Biomol GmbH	Hamburg, Germany
CREB1	Fwd: TGG AGT TGT TAT GGC ATC CT Rvs: ATT TTC AAG CAC TGC CAC TC	169	Biomol GmbH	Hamburg, Germany

CS	Fwd: CCA TCC ACA GTG ACC ATG AG Rvs: CTT TGC CAA CTT CCT TCT GC	186	Biomol GmbH	Hamburg, Germany
GAPDH	Fwd: GAG TCA ACG GAT TTG GTC GT Rvs: TTG ATT TTG GAG GGA TCT CG	238	Biomol GmbH	Hamburg, Germany
GPx1	Fwd: GCT TCC AGA CCA TTG ACA TC Rvs: GTG TTC CTC CCT CGT AGG TT	170	Biomol GmbH	Hamburg, Germany
NDUFV1	Fwd: CGC CAC CTA GCG TCT CTA TC Rvs: TGA AAA TCC GGT CTT CAT CC	213	Biomol GmbH	Hamburg, Germany
NRF1	Fwd: GTA ACC CTG ATG GCA CTG TC Rvs: TCT GGA TGG TCA TCT CAC CT	183	Biomol GmbH	Hamburg, Germany
PGC-1α	Fwd: TGC CCT GGA TTG TTG ACA TGA Rvs: TTT GTC AGG CTG GGG GTA GG	20	Biomers.net GmbH	Ulm, Germany
PGK1	Fwd: CTG TGG GGG TAT TTG AAT GG Rvs: CTT CCA GGA GCT CCA AA	198	Biomol GmbH	Hamburg, Germany
SIRT1	Fwd: TGT GGT AGA GCT TGC ATT GA Rvs: GCC TGT TGC TCT CCT CAT TA	153	Biomol GmbH	Hamburg, Germany
SOD2	Fwd: TGT CAC CCA GTG GTT TTT GT Rvs: GCC CTG CAA ATA AAC ATC CT	152	Biomol GmbH	Hamburg, Germany
TFAM	Fwd: TCC CCC TTC AGT TTT GTG TA Rvs: ATC AGG AAG TTC CCT CCA AC	189	Biomol GmbH	Hamburg, Germany

Primer	**Efficiency (%)**	**R^2**	**Dynamic Range**	**Melting Point (°C)**	**Conc. (µM)**	**Annealing Time (s)**	**Annealing Temperature (°C)**
ACTB	93.3	0.999	100 ng-1 pg	84	200	30	58
ATP5D	104.3	0.987	100 ng-1 pg	89	200	45	58
CAT	101.9	0.997	50 ng-0.5 pg	79.5	150	30	56
COX5A	97.1	0.996	100 ng-1 pg	91	200	45	58
CREB1	100.0	0.997	100 ng-1 pg	780	200	45	58
CS	92.7	0.997	100 ng-1 pg	983	400	30	58
GAPDH	91.8	0.993	100 ng-1 pg	80.5	200	30	58
GPx1	89.9	0.997	5 ng-5 pg	84.5	400	45	57

NDUFV1	96.2	0.992	100 ng-1 pg	78.5	200	30	58
NRF1	98.4	0.996	100 ng-1 pg	78	200	45	58
PGC-1α	98.8	0.994	100 ng-1 pg	76	200	30	60
PGK1	90.7	0.997	100 ng-1 pg	82.5	200	30	58
SIRT1	102.9	0.998	100 ng-1 pg	76	200	45	58
SOD2	92.7	0.997	50 ng-0.5 pg	79	100	45	58
TFAM	89.0	0.998	100 ng-1 pg	77.5	400	30	58

3.1.7 Antibodies

Primary antibodies were purchased from Abcam (Cambridge, UK) with the exception for GAPDH, which was purchased from Merck KGaA (Darmstadt, Germany).

Primary antibody	**Secondary antibody**	**Primary antibody dilution**	**Band size**
Citratsynthase	Rabbit	1:1000	52 kDa
CREB1	Rabbit	1:1000	43 kDa
GAPDH	Mouse	1:300	37 kDa
Total OXPHOS	Mouse	1:208	21, 24, 30, 50 and 60kDa
PGC-1α	Goat	1:500	100 kDa
pCREB	Rabbit	1:500	37 kDa
TOM22	Mouse	1:1000	15 kDa
Tubulin	rat	1:10000	52 kDa

Secondary antibody	Company	City, Country
Goat Anti-mouse IgG, H&L Chain Specific Peroxidase Conjugate	Merck KGaA	Darmstadt, Germany
Goat Anti-rabbit IgG, H&L Chain Specific Peroxidase Conjugate	Merck KGaA	Darmstadt, Germany
Goat Anti-Rat IgG, H&L Chain Specific Peroxidase Conjugate	Merck KGaA	Darmstadt, Germany
Goat Anti-Goat IgG, H&L Chain Specific Peroxidase Conjugate	Merck KGaA	Darmstadt, Germany

3.1.8 Cell lines

3.1.8.1 SH-SY5Y-MOCK

SH-SY5Y is a human cell line which was derived by subcloning from the parental metastatic bone tumor biopsy cell line SK-N-SH (Biedler et al., 1978). SH-SY5Y cells are widely used as an *in vitro* model for AD and in research in neuronal cells. They have a neuroblast-like morphology and grow adherent. SH-SY5Y-MOCK cells are transfected with the mammalian empty vector pCEP4 harbouring the Hygromycin B resistance gene and served as control cells.

3.1.8.2 SH-SY5Y-APP$_{695}$

SH-SY5Y-APP$_{695}$ cells are stably transfected with the DNA constructs harbouring the human wild-type APP$_{695}$ gene. Anne Eckert (Basel, Switzerland) and Tobias Hartmann (Homburg/Saar, Germany) kindly donated both cell lines.

3.2 Methods

3.1.1 Cell culture

3.1.1.1 Thawing cells

The cells stored in liquid nitrogen were gently thawed in a water bath (37 °C) until only a small amount of medium was frozen. 1 ml of preheated culture medium (37 °C) was added to the cell suspension before it was transferred into a falcon tube containing 10 ml of culture medium (37 °C). The cell suspension was centrifuged (1000 rpm, 5 min), the supernatant was aspired and the cell pellet was dissolved in 12 ml cell culture medium. Cells were placed in the incubator for at least 24 h.

3.1.1.2 Splitting cells

When cells reached a confluence of approximately 80%, cells were sub-cultivated. Cell culture medium was aspirated from the flask with a sterile autoclaved glass pipette. 10 ml PBS were gently added to the wall of the flask and after 1 minute removed. 1 ml of trypsin-EDTA was added to detach the cells from the culture flask. After max. 3 minutes, the reaction of trypsin was neutralized by adding 9 ml of culture medium (37 °C). Cells were completely detached by rinsing multiple times. The resulting 10 ml of cell suspension were divided into new flasks containing 12 ml of culture medium (37 °C). Depending on the confluence of the cells, cells were split between ratios of 1:2 to 1:10.

3.1.1.3 Seeding cells

Cells were seeded when they reached a confluence of 70-80%. The old culture medium was aspirated and cells were washed with 10 ml PBS and detached with 1 ml of trypsin-EDTA. 9 ml of culture medium (37 °C) were added to stop the reaction and to detach all cells from the

flask. The cell suspension was centrifuged (1000 rpm, 5 min, room temperature). After aspiring the supernatant, the remaining cell pellet was resolved in 1 ml cell culture medium (37 °C). Counting of cells was determined with the help of a Neubauer counting chamber, for which 10 µl of the cell suspension were stained with 90 µl of trypan blue (0.4%). Cell count was adjusted to 1 million cells per ml with reduced culture medium (37 °C). Depending on the experimental setup, the desired cell count was sown in the respective corresponding plate and placed in the incubator.

3.1.1.4 Incubation of cells

For the determination of ATP concentration

20 000 cells/well were seeded in a 96-well plate and grown for 24 h. 12 wells per concentration and substance (each of 1 µL volume) were incubated. For medium control for one entire 96-well plate, another 12 wells were incubated with 1 µl of cell culture medium. Four wells were incubated with EtOH in the respective concentration for solvent control. The plate was placed in the incubator for 1 h. After 1 h rotenone (25 µM) was added to six of the medium control wells and six of the substance wells of each concentration. The remaining wells were filled with the same amount of cell culture medium to reach equal volumes in each well. The plate was placed for another 24 h in the incubator.

For measurement of mitochondrial respiration

Cell culture flasks with a confluence of 60-70% were incubated with the respective substance (0.05 µM) by replacing the old cell culture medium with 24.75 ml new cell culture medium (37 °C) and adding 250 µl of the respective substance or EtOH as solvent control. Cells were placed in the incubator for 24 h.

For qPCR and Western Blot analysis

250 000 cells/well were seeded in a 6-well plate and grown for 24 h. Old culture medium was aspirated and 1.88 ml new culture medium and 20 µl of the respective substance (0.05 µM), EtOH solvent control or medium control, two wells each, were added. Cells were placed in the incubator for 24 h.

For measurement of $A\beta_{1-40}$ concentration

Cell culture flasks with a confluence of 70% were incubated with the respective substance (0.05 µM) by replacing the old culture medium with 9.9 ml new reduced culture medium (37 °C) and 100 µl of the respective substance of EtOH as solvent control. Cells were placed in the incubator for 24 h.

3.1.1.5 Harvesting cells for measurement of mitochondrial respiration

After 24 h incubation with the respective substance, old cell culture medium was aspirated and cells were washed with 10 ml PBS. Cells were detached from the flask by rinsing with MIR05 (37 °C) and then centrifuged (1000 rpm, 5 min, room temperature). The supernatant was discarded and the remaining cell pellet was resolved in MIR05 (37 °C). 10 µl of the cell suspension were stained with 90 µl trypan blue (0.4%) and counted with the Neubauer cell count chamber. Cell count was adjusted to 1 mio cells per ml with MIR05.

3.1.1.6 Harvesting cells for qPCR analysis

After 24 h incubation old cell culture medium was aspirated and cells were washed with ice-cold PBS. Cells were detached with 2 ml cell culture medium (ice-cold) and two wells were pooled. Cell suspension was centrifuged (1000 rpm, 4 °C, 5 min). After discarding the supernatant, the remaining cell pellet was redissolved in 300 µl RNA-Protect, thoroughly mixed and stored at -80 °C.

3.1.1.7 Harvesting cells for Western Blot analysis

After 24 h incubation, old cell culture medium was aspirated and cells were washed with ice-cold PBS. Cells were detached with 200 µl of ice-cold lysis buffer and stored at -80 °C.

3.1.1.8 Harvesting cells for determination of $A\beta_{1-40}$ concentration

After 24 h incubation cells were transferred into a 15 ml tube, centrifuged (300 g, 7 min, room temperature) and the medium was aspirated. The cell pellet was resuspended in ice-cold PBS, centrifuged (300 g, 7 min, 4 °C) and PBS was aspirated. Cells were stored at -80 °C.

3.1.1.9 Freezing cells

Cell culture flasks with a confluence of 80% were detached as described in chapter 3.2.1.2. Cell suspension was centrifuged (1000 rpm, 5 min), cell culture medium was aspirated, and the remaining cell pellet was redissolved in 1 ml freezing cell culture medium and quickly transferred in a cryo-vial on ice before it was stored in the freezing container Mr.Frosty™. Mr.Frosty™ is stored at -80 °C for 24 h and afterwards cells are stored in liquid nitrogen in the gas phase.

3.1.2 Determination of protein content

For the determination of protein content the bicinchoninic acid (BCA) method by using a kit was performed. The method is based on the reduction of Cu^{2+} ions which bind to proteins. Reduced copper gives a violet complex with BCA, which absorbs at 562 nm and can be measured photometrically. Bovine serum albumin was used to create a standard curve with six different concentrations (0, 0.1, 0.2, 0.33, 0.5, 1.0 mg/ml). Cell samples were thawed on ice, sonicated and diluted 1:5 with Tris buffer (20 mM). On a 96-well plate, 10 µl of each probe and standard was applied in triplets. Following procedures were conducted according to the instructions of the manufacturer.

3.1.3 Measurement of mitochondrial membrane potential

Rhodamin-123 (Rh123), a fluorescence dye was used to measure the membrane potential (MMP) of the cells. The cationic dye Rh123 is attracted to the negative potential across the inner mitochondrial membrane, is cell permanent and thus accumulates in active mitochondria. The cells were incubated with 0.4 µM Rh123 in an incubator (37 °C, 5% CO_2) for 15 min. The reaction was stopped by adding 500 µl HBSS (37 °C) into the wells. The 24-well plate was centrifuged (1500 rpm, 5 min, room temperature), medium was aspirated and cells were supplemented with 500 µl HBSS (37 °C). To determine MMP, fluorescence was read in four consecutive runs at an excitation wavelength of 490 nm and an emission wavelength of 535 nm (Victor X3 multilabel counter).

3.1.4 Measurement of ATP concentrations

The bioluminescence assay ViaLightTM Plus Kit (Lonza, Basel, Switzerland) was used to determine ATP levels, which is based on the production of light from ATP and luciferin in the

presence of luciferase. After the required incubation time, the 96-well plate was allowed to cool to room temperature for 10 min. 50 µl of lysis buffer were added to each well and incubated in the dark for 10 min. Afterwards, 100 µl of monitoring agent was applied to each well and under the protection of light incubated for 5 min. The luminescence was measured using a luminometer (Victor X3 multilabel counter). The emitted light is linearly related to ATP concentration. A standard curve was generated to determine ATP concentrations of the samples.

3.1.5 Measurement of mitochondrial respiration

Mitochondrial respiration was monitored at 37 °C, using the Oxygraph-2k (Oroboros, Innsbruck, Austria) and DatLab 7.0.0.2. The Oxygraph consists of two independent chambers with a Clark-type polarographic sensor where a membrane permeable to oxygen covers an electrode which is reducing oxygen. Oxygen concentration can be determined by the current that ensues. To analyse the function of the respiratory system, a complex protocol (elaborated by Prof. Dr. Erich Gnaiger) was applied including different substrates, uncouplers, and inhibitors. Before starting the measurement, 2.4 ml Mir05 (37 °C) were filled into the two chambers of the Oxygraph and allowed to equilibrate for at least 30 min. MIR05 was completely removed and replaced by 2.4 ml cell suspension containing 1 mio cells/ml MIR05. The oxygen consumption was allowed to stabilize to give endogenous respiration. Cell membranes were permeabilized with digitonin (10 µg/10^6 cells), leaving mitochondrial outer and inner membrane intact. OXPHOS respiration was determined with complex I related substrates glutamate (10 mM), malate (2 mM), and ADP (2 mM) followed by addition of succinate (10 mM). Oligomycin addition (2 µg/ ml) lead to measurement of leak respiration. Stepwise addition of FCCP showed the maximum capacity of the electron transfer system. By adding the complex I inhibitor rotenone complex II non-coupled respiration was measured. Inhibition of complex III by addition of antimycin A (2.5 µM) determines residual oxygen consumption (caused by enzymes which do not belong to the electron transfer system), which was subtracted from all respiratory states. Complex IV activity was achieved by adding N,N,N′,N′-tetramethyl-p-phenylenediamine (0.5 mM) and ascorbate (2 mM). Autoxidation rate was determined using sodium azide (≥100 mM). Complex IV respiration was additionally corrected for autoxidation. Figure 3.1 shows a typical measurement of mitochondrial respiration with an oxygraph 2k.

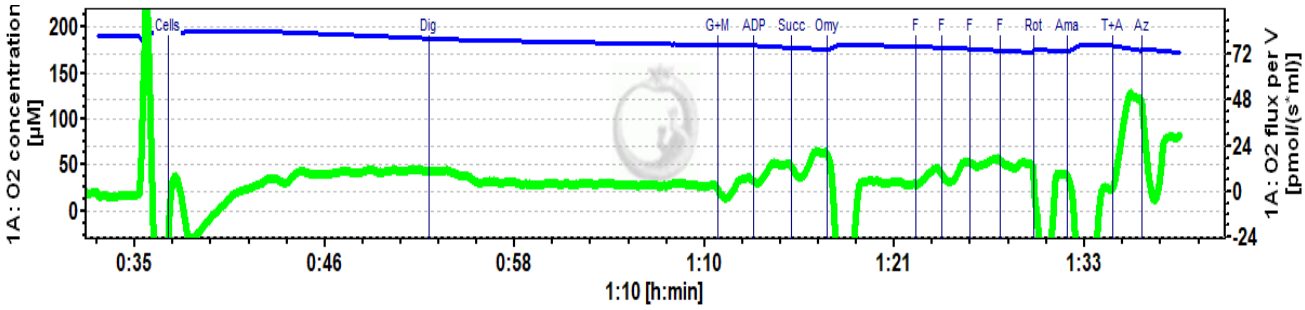

Figure 3.1 Example of a typical respiratory measurement of cells. The blue line shows the actual oxygen concentration, while the green trace displays the oxygen consumption. On the the x-axis the time scale of the measurement is depicted. Cells: addition of cell suspension; G+M: addition of glutamate and malate; ADP: addition of adenosine triphosphate; Succ: addition of succinate; Omy: addition of oligomycin; F: addition of carbonyl cyanide-4-(trifluoromethoxy)phenylhydrazone; Rot: addition of rotenone; Ama: addition of antimycin A; T+A: addition of tetramethylphenylenediamine and ascorbate; Az: addition of sodium azide

3.1.6 Measurement of citrate synthase activity

Citrate synthase (CS) is localized in the mitochondrial matrix, but nuclear encoded. Therefore, CS is commonly used as a quantitative marker for the content of intact mitochondria. The assay is based on the irreversible reaction from dithionitrobenzoic acid (DTNB) and acetyl coenzyme A (CoA-SH) to thionitrobenzoic acid (TNB) and CoA-S-S-TNB, catalysed by CS. TNB can be spectrometrically detected at 412 nm over 200 s. CS reaction medium was prepared (see section 3.1.5.3) and preheated at 30 °C for 5 min. 200 µl of the sample were added to the reaction medium, giving a total volume of 1 ml. The mixture was transferred to a quartz cuvette and CS activity was assessed using a photometer.

The specific enzyme activity was determined with the following formula:

$$v = \frac{r_A}{l \cdot \varepsilon_B \cdot v_B} \cdot \frac{V_{cuvette}}{V_{sample} \cdot \rho}$$

υ specific activity of TNB (1)

r_A rate of absorbance change (1/min)

l optical path length (1 cm)

ε_B extinction coefficient of TNB at 412 nm and pH=8.1 (13.6 mM^{-1} cm^{-1})

$V_{cuvette}$ volume of solution of the cuvette (1000 µl)

V_{sample} volume of the sample added to cuvette (200 µl)

ρ protein concentration (mg cm^{-3}) or density of cells (1 mio cells cm^{-3})

3.1.7 Quantitative real-time PCR

3.1.7.1 Isolation of mRNA from cells

Total RNA was isolated using RNeasy Mini Kit (Qiagen, Hilden, Germany). Cells were centrifuged (14 500 rpm, 10 min), supernatant was removed and cells were homogenized in 350 µl RLT buffer (+ 10% mercaptoethanol) by using a cannula to disrupt the cell structure. 350 µl ethanol (70%) were added, the cell suspension was transferred onto the RNeasy column and centrifuged (10 000 rpm, 30 s). The flow-through was discarded and a wash step was performed in which 700 µl RW1 buffer were applied and the column was centrifuged (10 000 rpm, 15 s). The flow-through was removed and two further washing steps followed, each with 500 µl RPE buffer. After the last wash step, the column was centrifuged (10 000, 2 min). The collection tube was discarded and the column was transferred to a fresh 1.5 ml reaction tube. To elute the mRNA, 50 µl RNase-free water was directly added to the spin column membrane and centrifuged (10 000 rpm, 1 min). Determination of the concentration and purity of the isolated RNA was performed with NanoDrop™ One (Thermo-Scientific) at the wavelengths of 230 nm, 260 nm and 280 nm. The purity was determined by the ratio A260/A280. A ratio of 1.8-2 is indicative of highly purified RNA. Lower ratio might arise of contamination with proteins or phenols. The ratio of A260/A230 is also calculated as indicator for contaminations. The values should be over 1.5.

To exclude contamination with genomic DNA, an additional DNase digestion was performed with the Turbo DNA-free™ Kit. For this purpose, RNA (< 200 µg/ml), 5 µl of the 10x TURBO DNase buffer and 1 µl TURBO DNase were added to 50 µl RNA (< 200 µg/ml). Subsequently, incubation was performed at 37°C for 25 min. At the end of the incubation period, 5 µl DNase Inactivation Reagent was added and incubated at room temperature for 5 min, thus the reaction was stopped. The samples were then centrifuged (10 000 g, 90 s, room temperature), the supernatant removed, and the concentration was determined by using NanoDrop™ One.

3.1.7.2 Synthesis of cDNA

Synthesis of the cDNA was performed using the iScript™ cDNA Synthesis Kit (Bio-Rad, Munich). To prepare the cDNA, the RNA aliquots were thawed and mixed with RNAse-free water (total volume 10 µl). To each sample, 10 µl Mastermix (5 µl RNase-free H_2O, 4 µl 5x iScriptase Reaction Mix and 1 µl iScript Reverse Transcriptase) were added. Subsequently, incubation was performed in the T100TM Thermocycler (BioRad) (5 min at 25 °C, 20 min at 46 °C and 1 min at 95 °C, lid temperature 105 °C). The cDNA was stored in aliquots (5 µl) at -80°C.

3.1.7.3 Procedure of quantitative real-time PCR

The mRNA expression (gene expression) was determined by quantitative real-time PCR (qPCR) with target specific primers and conducted using a CFX Connect™ Real-Time System (Bio-Rad, Munich). For this purpose, the cDNA aliquots were thawed and diluted with RNase –free H_2O (1:10). 8 µl of the master mix (5 µl SYBR Green Supermix, 1 µl primer stock (2 or 4µM), 2 µl RNase –free H_2O) were added onto a 96-well PCR plate. 2 µl of the diluted cDNA was added in triplets. RNase-free H_2O was used as a control. The PCR plate was sealed with an adhesive foil and incubated in a thermal cycler. The cycle conditions for the qRT-PCR are summarized in Table 3.1.

Table 3.1 Cycling conditions for qRT-PCR.

Cycling	Temperature (°C)	Time
Initial denaturation	95	3 min
Denaturation	95	10 s
Annealing	56-58	30 s / 45 s
Elongation	72	29 s
Number of cycles	45	

Depending on the primer used, the primer concentration, annealing time and temperature vary. Relative quantification was followed by a melting curve analysis to detect primer dimers or unspecific annealing of the primers. The melting curve was plotted at a temperature increase from 65 °C to 95 °C with a heating rate of 0.5 °C/5 s over a period of 5 min. Gene expression was analysed using the –(2ΔΔCq) method using BioRad CfX manager software and were normalized to the expression levels of GAPDH, beta-Actin and PGK.

3.1.8 Western Blot analysis

3.1.8.1 Gel casting

For gel casting a casting stand for 2 gels (Bio-Rad, Hercules, USA) was used. Gels with different acrylamide concentrations (7%, 10%, 12%, 15%) were cast, depending on the size of the proteins that should be detected. The required buffers and the composition of the gels are described in section 1.3.5.4. APS and TEMED were added just before casting the gels. The running gel was cast into the stand and covered with a layer of isopropanol to avoid drying-out. The gel was allowed to become solid for 45 min. Isopropanol was poured off, the stocking gel was cast on top of the running gel and a comb was added without bubbles. The gel was allowed to become solid for 45 min and stored at 4 °C for no more than 2 weeks

3.1.8.2 Gel electrophoresis

Cell samples were thawed on ice and homogenized by sonication. The samples were diluted in Tris buffer (20 mM) to adjust protein content to 10 or 20 µg. Sample buffer (1:3) and reducing agent (1:9) were added. The samples were incubated in a Thermo-Shaker (95 °C, 10 min) to disintegrate proteins. After a short centrifugation step, samples were loaded into the gels. To be able to identify the bands, a protein standard (Precision Plus Protein WesternC Standards, BioRad, Hercules, USA) was added into one pocket of the gel. Gels were run 20 min at 60V until the samples reached the running gel. Afterwards the voltage was increased to 120V for approximately 60 min to separate proteins in the gel.

3.1.8.3 Blotting on PVDF membrane

After the gel electrophoresis, proteins were blotted onto a carrier membrane using the blotting system Criterion™ Blotter. The PVDF membrane was activated in MeOH for 5 min. The filter papers and the pads were soaked in transfer buffer. The gel cassette was opened carefully, the collection gel was removed and the running gel was transferred to a damp filter paper. Afterwards, a pad was placed on the cathode side of the blot cartridge, followed by a filter paper on which the gel was placed. The activated PVDF membrane was carefully placed on the gel and covered with another filter paper. Air bubbles were removed with a blot roller. Finally, another cushion was placed on the sandwich. After the blot cartridge was closed tightly, a cooling element (-20°C) was put into the Criterion™ blotter and the chamber was filled with transfer buffer. It is important to note that protein transfer should be carried out at the low temperatures. The transfer was carried out at a voltage of 30 V for 90 min. Afterwards, the membranes were blocked for 30 min in a solution of skimmed milk powder (75 mg/ml H_2O). After removal of the blocking solution, the membrane was washed with water until the milky residue was completely removed. Until further use, the membrane was stored in TBST buffer (1x) at 4 °C.

3.1.8.4 Antibody incubation

Western Blots were incubated with all primary antibodies on a shaker plate overnight at 4 °C, with the exception of the loading controls GAPDH and tubulin which were incubated for 20 min or 30 min on a shaker plate at room temperature. The primary antibody solution was then poured off. Secondary antibodies were incubated using the SNAP i.d. 2.0 device (Merck KGaA, Germany). The loaded blot was inserted into the SNAP i.d. according to instructions and washed with 50 ml TBST (1x). The secondary antibody solution was added to the washed membrane. After an incubation period of 10 min the secondary antibody was aspirated and the blot was washed again. For the detection of the blot, 0.5 ml TBST (1x) were added to 1 ml of Luminata™ Crescendo Western HRP reaction reagent. The membrane was covered with the reaction reagent and incubated in the dark for 5 min. The detection of the protein bands was performed in ChemiDoc™ Touch Imaging System (Bio-Rad, Germany), (chemiluminescence / 20-120 s exposure).

3.1.9 Measurement of Amyloid-β_{1-40} level

$A\beta_{1-40}$ levels were determined using an enzyme-linked immunosorbent assay (ELISA) Kit (Elabscience Biotechnology Inc., USA). The kit uses the Sandwich-ELISA principle. The plate is pre-coated with a specific antibody to human $A\beta_{1-40.}$ The added sample then binds to the specific antibody. An enzyme-linked secondary antibody is applied as detection antibody directed against $A\beta_{1-40}$. Subsequently the bound antigen binds to the secondary antibody. In the last step, the bound enzyme activates the added dye, which can be detected photometrically to determine the presence and quantity of $A\beta_{1-40.}$ The ELISA was performed according to the manufacture's instructions. The concentration of $A\beta_{1-40}$ was measured in lysed cells. After 24 h treatment, cells were lysed by adding 600 µl Cell Extraction Buffer (Thermo-Scientific) with protease inhibitor cocktail (reconstitute to the manufacture´s guideline, Roche) and 1 mM PMSF to the cell pellet. Lysates were transferred into clean 1 ml reaction tubes, vortexed and incubated on ice for 30 min, with occasional vortexing. Then, lysates were centrifuged (13 000 g, 10 min, 4 °C) and transferred to a clean 1 ml reaction tube. Later on, protein content (see section 3.1.2) was determined. First, 100 µl of the prepared standard solution was applied to the first two columns of the pre-coated 96-well plate. 100 µl of samples were added to the other wells. The plate was covered with a sealer and incubated at 37 °C for 90 min. Afterwards, the liquid was removed and 100 µl of the biotinylated detection solution were added and incubated at 37 °C for 60 min. The solution was decanted from all wells and the plate was washed 3 times by adding 350 µl of wash buffer and 1-2 min incubation time. 100 µl of the secondary antibody (horseradish peroxidase conjugate solution) were applied to each well, the plate was covered and incubated at 37 °C for 30 min. The solution from each well was decanted and the wash process was repeated for five times as described above. 90 ml of substrate reagent was added and incubated at 37 °C for 15 min. Afterwards 50 µl of the stop solution were added to terminate the enzyme-substrate reaction and the colour turns from blue to yellow. The optical density was measured on a Spectrometer (ClarioStar Platereader, BMG, Ortenberg, Germany) at a wavelength of 450 nm. The measured values are proportional to the concentration of $A\beta_{1-40}$. By comparing the concentrations of the standard curve, the concentration of $A\beta_{1-40}$ can be calculated. The values were then normalized to protein content.

3.1.10 Statistical evaluation

Statistical analysis were performed using the software GraphPad Prism Version 8.0.1. Measured values are displayed as mean values with standard error of the mean value (± SEM). For the statistical verification of differences between two measurement groups the unpaired, two-sided *t*-test was used. For differences between more than two measurement groups a 1-way ANOVA with Tukey's Multiple Comparison Test was used.

4 Results

First, a cell model of late-onset AD was characterized by investigating differences in mitochondrial function between SH-SY5Y-MOCK vector transfected control cells and the corresponding transgenic cell line SH-SY5Y-APP$_{695}$ harbouring the neuronal form of human amyloid precursor protein (APP). In particular, we determined ATP levels, mitochondrial membrane potential, the capacity of respiratory chain complexes, mRNA level of genes involved in mitochondrial biogenesis, and genes of the respiratory system as well as their protein expression and A$\beta_{1\text{-}40}$ levels. Additionally, we simulated mitochondria related ageing processes by using rotenone to inhibit complex I of the respiration chain. Afterwards we assessed effects of ten highly purified olive polyphenols (hydroxytyrosol, tyrosol, oleacein, oleuroside, oleuropein, oleuroside aglycone, oleocanthal, ligstroside, ligstroside aglycone, ligustaloside B) and two metabolites (the plant metabolite elenolic acid and the mammalian metabolite homovanillic acid) in very low doses on mitochondrial function in SH-SY5Y-MOCK and SH-SY5Y-APP$_{695}$ cells. Figure 1 shows the experimental workflow that led to the identification of the compounds with the highest beneficial effects on mitochondrial function in SH-SY5Y-APP$_{695}$ cells.

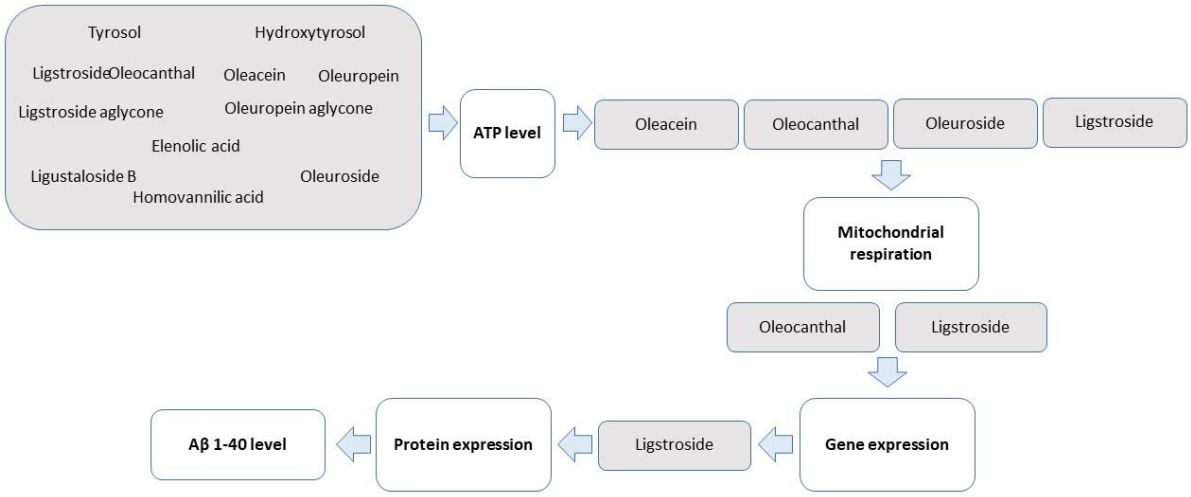

Figure 4.1 Workflow. Workflow of carried out experiments to identify the most promising compounds on mitochondrial promoting effects.

4.1 Characterization of the SH-SY5Y cell line as a model of late-onset AD

4.1.1 SH-SY5Y-APP$_{695}$ exhibit reduced ATP and MMP level

Mitochondrial dysfunction is characterized by reduced supply of the electrical and chemical transmembrane potential of the inner mitochondrial membrane and a reduced efficiency of oxidative phosphorylation which consequently leads to limited production of the critical metabolite ATP (Nicolson 2014). SH-SY5Y-APP$_{695}$ cells showed a significant reduced ATP production and a significant decrease of MMP level compared to control cells (see Figure 4.2 a and b).

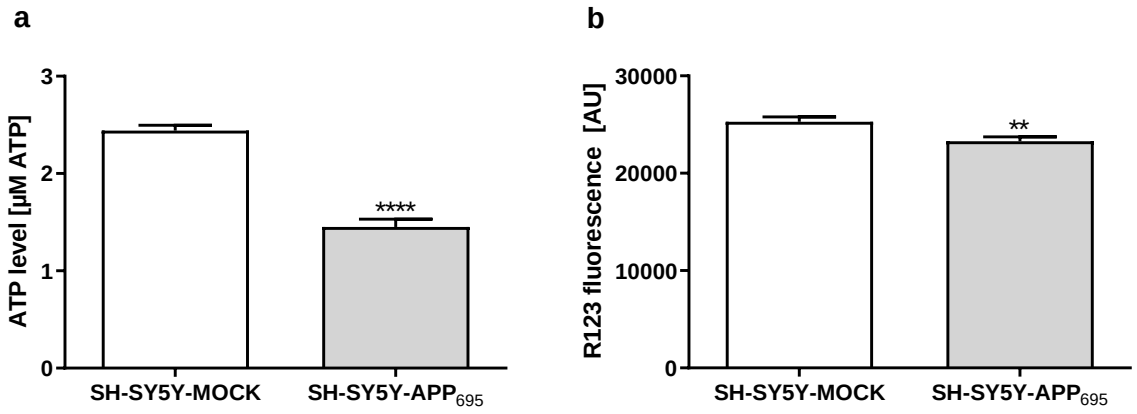

Figure 4.2 Comparison of ATP level and MMP in SH-SY5Y-MOCK control cells and APP transfected SH-SY5Y-APP$_{695}$ cells. ATP production was determined using the ViaLightKit (Lonza) by measuring bioluminescence after 48 h incubation. (a) SH-SY5Y-APP$_{695}$ cells exhibit reduced ATP levels compared to SH-SY5Y-MOCK control cells; mean ± SEM; student´s unpaired *t*-test (****p < 0.0001); n = 6. (b) Rhodamin-123 fluorescence of SH-SY5Y-MOCK and SH-SY5Y-APP$_{695}$ cells representing mitochondrial membrane potential (MMP); mean ± SEM; student´s unpaired *t*-test (**p < 0.01); n = 11.

4.1.1.1 Impaired mitochondrial respiration in SH-SY5Y-APP$_{695}$ cells

To assess activities of single complexes of the mitochondrial respiration chain a Clarke-electrode (Oroboros Oxygraph-2k) was used. A significant reduction of oxygen consumption was detected across all measured complexes in SH-SY5Y-APP$_{695}$ cells compared to control SH-SY5Y-MOCK cells (see Figure 4.3 a). The respiratory control ratio (RCR) indicates the coupling between oxygen consumption and oxidative phosphorylation (Hughey et al. 2011). RCR was calculated as ratio between uncoupled respiration and leak respiration after addition of oligomycin. The significant lower RCR in SH-SY5Y-APP$_{695}$ cells indicates a reduced ability to

couple mitochondrial respiration and phosphorylation – indicating mitochondrial dysfunction (Figure 4.3 b).

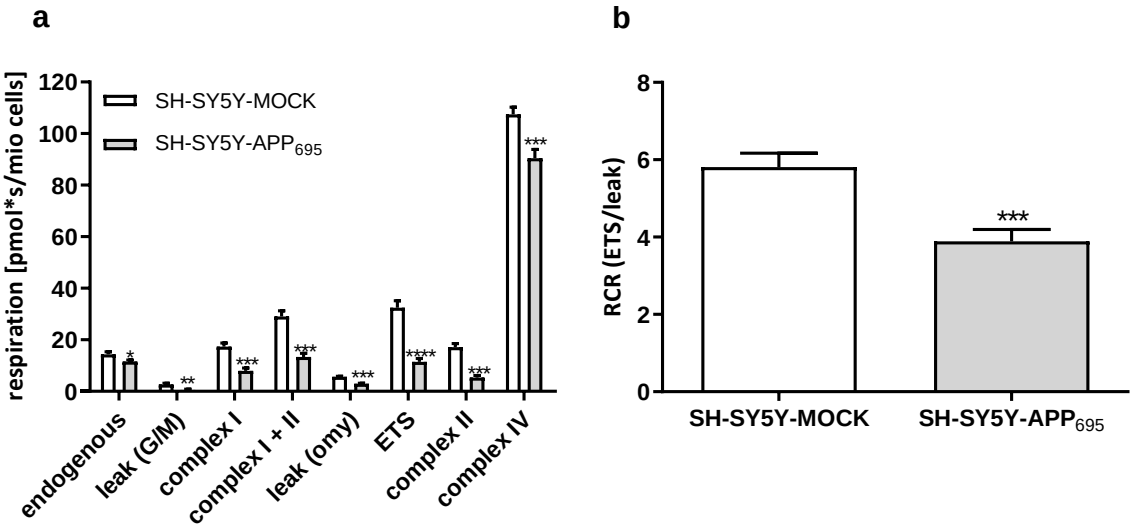

Figure 4.3 Mitochondrial respiration in SH-SY5Y-MOCK and SH-SY5Y-APP$_{695}$ cells. (a) SH-SY5Y-APP$_{695}$ cells showed an overall reduction of all measured respiratory states. For analyzing mitochondrial respiration, a solution of 10^6 cells/ml was used; mean ± SEM; student´s unpaired *t*-test (*p < 0.05, **p < 0.01, ***p < 0.001, ****p < 0.0001); n = 12. (b) SH-SY5Y-APP$_{695}$ cells have a significant lower RCR compared to SH-SY5Y-MOCK control cells, indicating a lower capacity for substrate oxidation and ATP turnover and a higher proton leak; mean ± SEM; students unpaired *t*-test (***p < 0.01); n = 10.

4.1.1.2 Alterations in mitochondrial gene expression in SH-SY5Y-APP$_{695}$ cells

To elaborate underlying molecular mechanisms, the expression of genes involved in mitochondrial biogenesis, mitochondrial function and antioxidative properties were determined in SH-SY5Y-MOCK control cells and SH-SY5Y-APP$_{695}$ cells. Gene expression of complex I, which is mainly associated with brain ageing and neurodegenerative diseases (Fiedorczuk and Sazanov 2018), was significantly reduced in SH-SY5Y-APP$_{695}$ cells (Figure 4.5 a). Additionally, mRNA levels of the antioxidative enzyme glutathione peroxidase 1 (GPx1) was significantly lower compared to SH-SY5Y-MOCK control cells (see Figure 4.5 b). CREB1, SIRT1, PGC-1α and TFAM which are involved in the mitochondrial biogenesis pathway, were numerically but not significantly decreased in SH-SY5Y-APP$_{695}$ cells (see Figure 4.4). mRNA expression levels of NRF1, COX5A, ATP5D, CS, CAT and SOD2 were unaffected compared to SH-SY5Y-MOCK cells (Table 4.1).

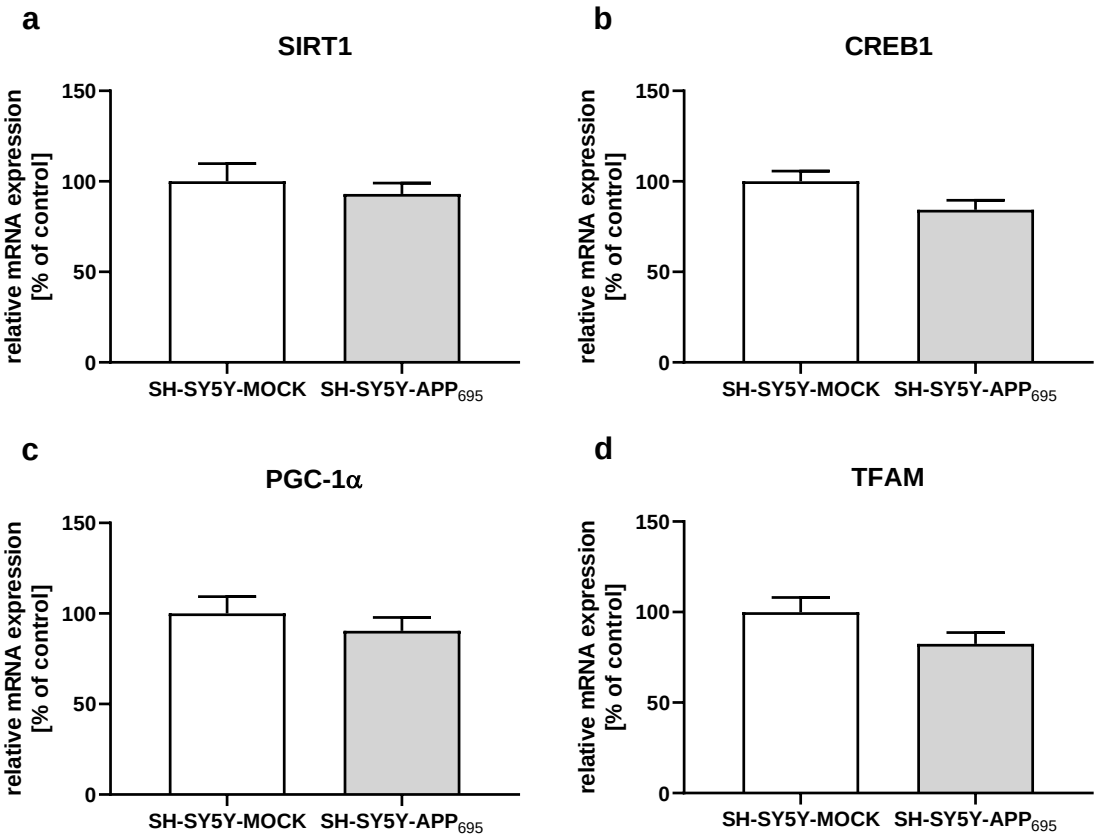

Figure 4.4 Relative mRNA expression in SH-SY5Y-MOCK and SH-SY5Y-APP$_{695}$ cells. Relative mRNA expression in SH-SY5Y-MOCK control cells (100%) compared to APP transfected SH-SY5Y-APP$_{695}$ cells. Cells were grown for 48 h and harvested with RNAprotect to provide immediate stabilization of RNA. (a) SIRT1 (b) CREB1 (c) PGC1-α and (d) TFAM, genes which are involved in the mitochondrial biogenesis pathway show a tendency towards lower mRNA expression. Data are represented as mean ± SEM; student´s unpaired t-test; n = 17.

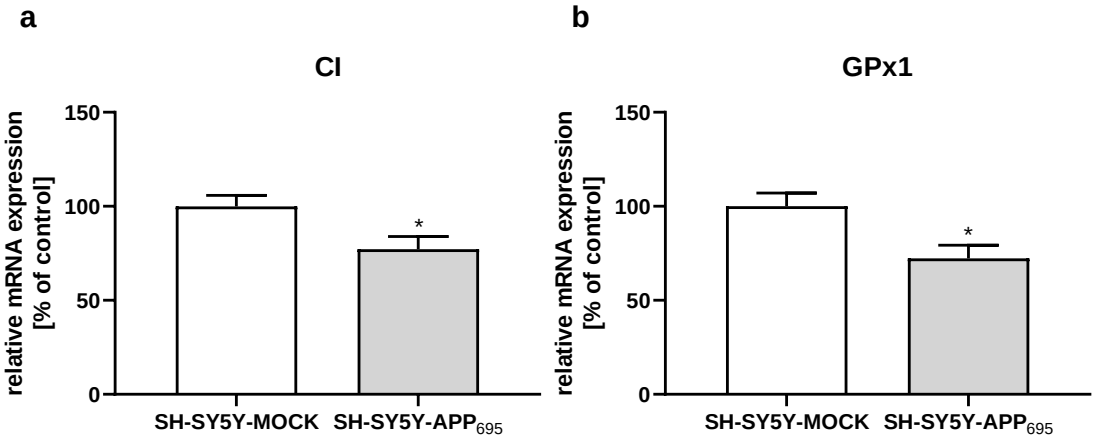

Figure 4.5 Relative mRNA expression of CI and GPx1 in SH-SY5Y-MOCK and SH-SY5Y-APP$_{695}$ cells. Relative mRNA expression in SH-SY5Y-MOCK control cells (100%) compared to APP transfected SH-SY5Y-APP$_{695}$ cells. (a) CI, which is associated with brain ageing and (b) GPx1, a gene of the mitochondrial oxidative defense system have both a significant lower mRNA expression compared to control cells. Data are represented as mean ± SEM; student´s unpaired t-test (*$p < 0.05$); n = 17.

Table 4.1 Relative normalized mRNA expression in SH-SY5Y-APP$_{695}$ cells. Relative normalized mRNA expression levels in SH-SY5Y-APP$_{695}$ cells determined using quantitative real-time PCR in comparison to SH-SY5Y-MOCK control cells (100%); mean ± SEM with student´s unpaired t-test (*$p < 0.05$); n = 17. Results are normalized to the mRNA expression levels of actin-β (ACTB), glyceraldehyde 3-phosphate dehydrogenase (GAPDH) and phosphoglycerate kinase 1 (PGK1).

	SH-SY5Y-APP$_{695}$
CS	97.1 ± 5.8
CREB1	84.4 (↓) ± 5.2
SIRT1	93.0 (↓) ± 6.1
PGC-1α	90.5 (↓) ± 7.3
NRF1	100.0 ± 10.6
TFAM	82.4 (↓) ± 6.3
CI	77.2 ↓* ± 6.8
COX5A	100.0 ± 6.2
ATP5D	102.4 ± 6.2
GPx1	72.3 ↓* ± 7.0
CAT	97.6 ± 13.1
SOD2	100.0 ± 7.8

4.1.1.3 Changes in protein biosynthesis in SH-SY5Y-APP$_{695}$ cells

Protein levels of the master regulator of mitochondrial biogenesis PGC-1α was significantly decreased in SH-SY5Y-APP$_{695}$ cells compared to control cells (Figure 4.6 c). Furthermore, protein levels of the transcription factor CREB were also significantly decreased, whereas the activated form (pCREB) showed only a numerically decrease of protein levels (Figure 4.6 a and b). Complexes II and III of the respiratory chain showed a significant decrease of protein levels in SH-SY5Y-APP$_{695}$ cells compared to SH-SY5Y-MOCK control cells (Figure 4.6 e and f). Complex I tended to be down regulated whereas protein levels of complexes IV and V as well as TOM22 and CS revealed no significant changes compared to SY5Y-MOCK cells (Table 4.2).

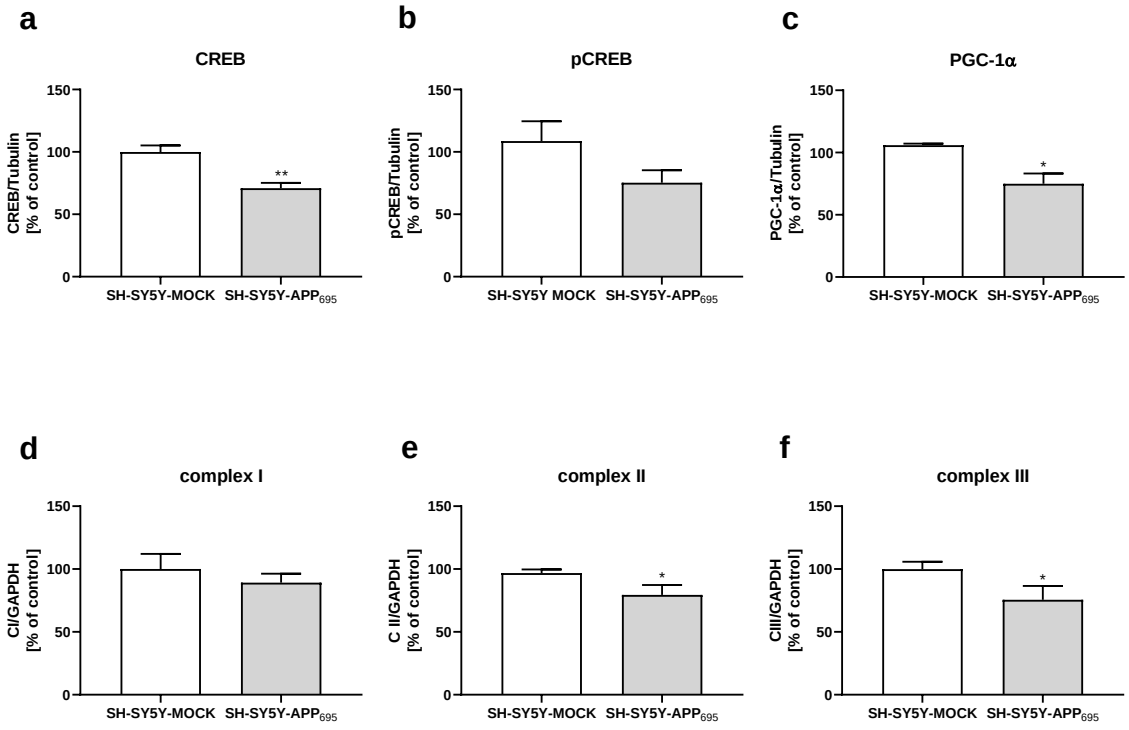

Figure 4.6 Protein levels in SH-SY5Y-MOCK control cells (100%) compared to SH-SY5Y-APP$_{695}$ cells. Cells were grown for 48 h and lysed. Proteins were separated by SDS-PAGE and blotted onto a PVDF membrane using a Blotting system. For further details see Materials and Methods; (a) The cellular transcription factor CREB is significantly downregulated, whereas the activated form (b) pCREB is numerically decreased; (c) the master regulator of mitochondrial biogenesis (c) PGC-1α is significantly decreased; (d) complex I tends to be lower expressed, whereas (e) complex II and (f) complex III are significantly lower than control cells. Data are represented as mean ± SEM with student´s unpaired *t*-test (*$p < 0.05$; **$p < 0.01$); n = 6; results are normalized to loading control tubulin or GAPDH.

Table 4.2 Protein levels in SH-SY5Y-APP$_{695}$ cells. Protein levels in SH-SY5Y-APP$_{695}$ cells determined using Western Blot analysis in comparison to SH-SY5Y-MOCK control cells (100%); mean ± SEM with student´s unpaired *t*-test (*p < 0.05; **p < 0.01); n = 6; results are normalized to loading control tubulin or GAPDH.

	SH-SY5Y-APP$_{695}$
CS	99.0 ± 6.37
TOM22	111.5 ± 7.74
CREB1	70.8 ↓** ± 4.23
pCREB	75.3 (↓) ± 10.02
PGC-1α	74.9 ↓* ± 8.35
CI	89.1 (↓) ± 7.18
CII	79.4 ↓* ± 7.89
CIII	75.6 ↓* ± 10.92
CIV	93.6 ± 6.24
CV	97.8 ± 9.93

4.1.1.4 Enhanced formation of Aβ$_{1-40}$ in SH-SY5Y-APP$_{695}$ cells

Since mitochondrial dysfunction is closely related with increased Aβ levels (Leuner et al. 2012; Grimm et al. 2016), the difference of Aβ expression between both cell lines was determined. As SH-SY5Y cells represent a human derived cell line, APP$_{695}$ is already expressed under normal conditions (SH-SY5Y-MOCK control cells). ELISA analysis of Aβ$_{1-40}$ levels in lysed cells demonstrated that Aβ$_{1-40}$ was 80-fold higher in the APP-overexpressing cell line compared to MOCK-transfected control cells (Figure 4.7).

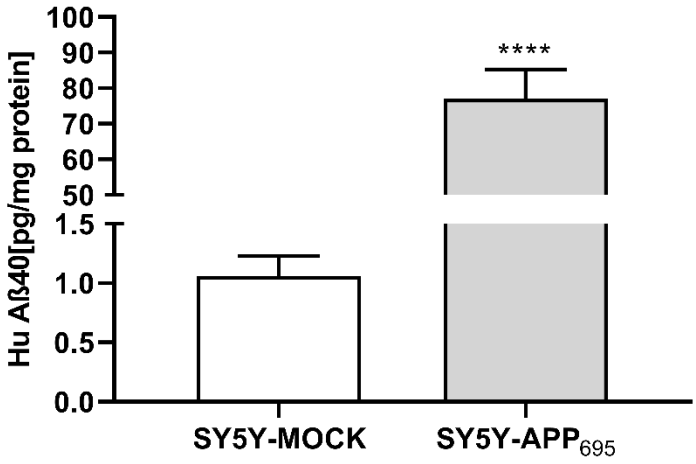

Figure 4.7 Comparison of human Aβ1-40 level in SH-SY5Y-MOCK and SH-SY5Y-APP$_{695}$ cells. Cells were grown for 48 h, lysed with a cell extraction buffer and Aβ levels were determined by ELISA, and normalized to protein content. SH-SY5Y-APP$_{695}$ cells show significantly increased A$\beta_{1\text{-}40}$ levels compared to SH-SY5Y-MOCK cells. Data are represented as mean ± SEM with students unpaired *t*-test; (****$p < 0.0001$); n = 8.

4.1.1.5 Complex I-inhibition as a model for simulating ageing processes in SH-SY5Y cells

As brain ageing is associated with a low activity of complex I of the mitochondrial respiration chain (Lenaz et al. 1997), SH-SY5Y-MOCK and SH-SY5Y-APP$_{695}$ cells were incubated with the complex I inhibitor rotenone, simulating this alteration. Additionally, complex I dysfunction is associated with increased ROS production (Leuner et al. 2012). The insult with rotenone led to a concentration dependant decrease of ATP- and MMP levels (Figure 4.8)

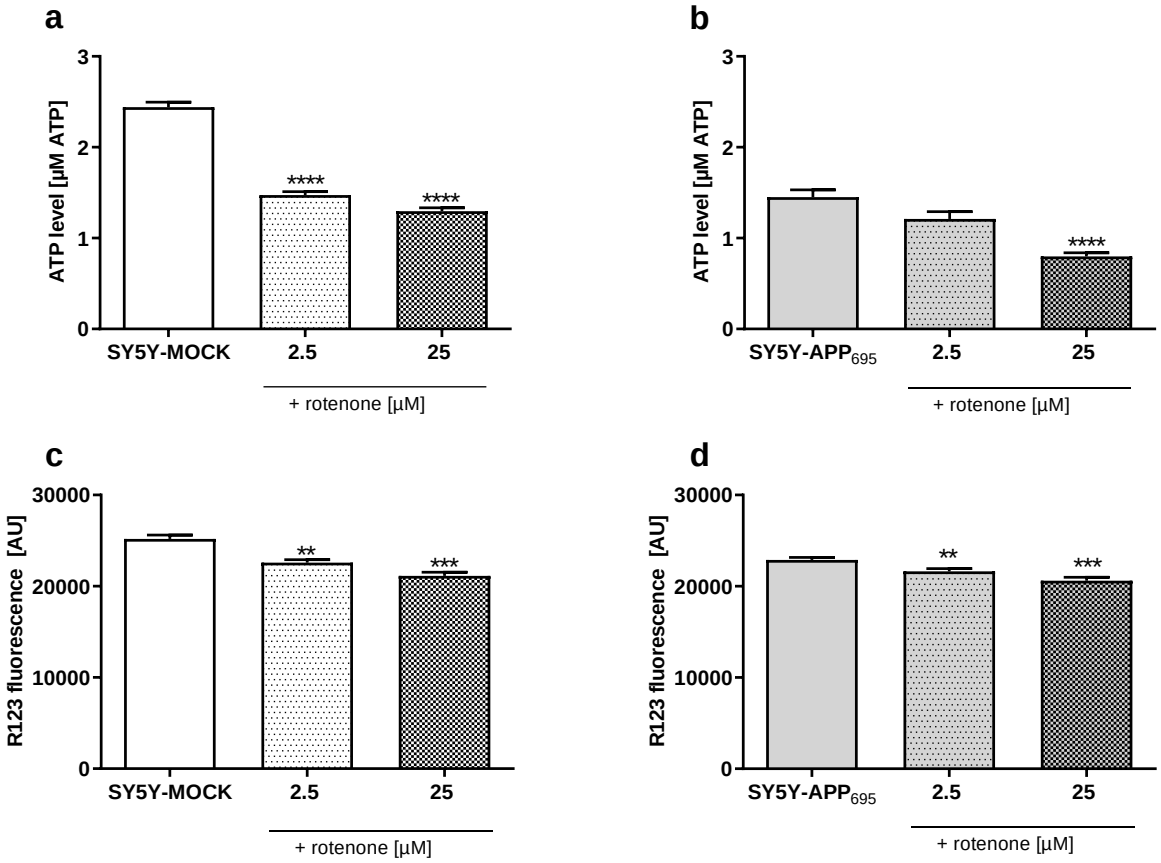

Figure 4.8 ATP level and MMP after complex I-inhibition in SH-SY5Y-MOCK and SH-SY5Y-APP$_{695}$ cells. 24 h Insult with rotenone (2.5 or 25 µM) in SH-SY5Y-MOCK cells lead to significantly decreased ATP level (a) and significantly decreased MMP level (c). In SH-SY5Y-APP$_{695}$ cells the complex I-inhibition with rotenone decreased ATP level (b) and significantly decreased MMP level (d); mean ± SEM; Data are represented as mean ± SEM; one-way ANOVA with Tukey´s multiple comparison post-hoc test (*p < 0.05, **p < 0.01, ***p < 0.001, ****p < 0.0001); n = 8-10.

4.2 Secoiridoid derivatives

All tested substances, apart from homovanillic acid (purchased from Sigma), were manufactured from N-Zyme BioTec GmbH (Darmstadt, Germany) through isolation from olive leaves, EVOO or enzymatically/chemically transformed. Verification of the isolated olive polyphenols or metabolites were accomplished by means of mass spectrometry and NMR analysis or with reference standard (see Table 4.3).

Table 4.3 Purification method, purity and identification of all tested polyphenols and metabolites. Data are provided by N-Zyme BioTec.

Substance	Purification	Purity (%)	Identification
Elenolic acid	FCPC, HPLC	> 92	MS, NMR
Hydroxytyrosol	FCPC	98	Reference
Ligstroside	FCPC	96	MS, NMR
Ligstroside aglycone	FCPC, HPLC	96	MS, NMR
Ligustaloside B	FCPC, HPLC	100	MS, NMR
Oleacein	HPLC	96	MS, NMR
Oleocanthal	FCPC	96	MS, NMR
Oleuropein	FCPC, HPLC	96	Reference
Oleuropein aglycone	FCPC	95	MS, NMR
Oleuroside	FCPC, HPLC	97	MS, NMR
Tyrosol	FCPC	98	Reference

4.2.1 Screening of olive polyphenols for ATP production

Olive polyphenol screening of 10 different purified secoiridoids (hydroxytyrosol, tyrosol, oleacein, oleuroside, oleuroside aglycone, oleuropein, oleocanthal, ligstroside, ligstroside aglycone and ligustaloside B) and two metabolites (the plant metabolite elenolic acid and the mammalian metabolite homovanillic acid) was carried out measuring ATP levels in SH-SY5Y-MOCK and SH-SY5Y-APP$_{695}$ cells in order to identify compounds with the highest beneficial effects on mitochondrial function. To determine the concentration with the highest positive effect, we firstly measured the influence of the two most simple phenolics hydroxytyrosol and tyrosol in concentrations between 0.5 and 50 µM on ATP levels in SH-SY5Y-MOCK cells (Figure 4.9). Additionally, we insulted SH-SY5Y-MOCK cells with rotenone in the concentration that has previously been proven suitable (25 µM) to assess if both phenolics can restore impaired ATP levels after insult with the complex I inhibitor rotenone.

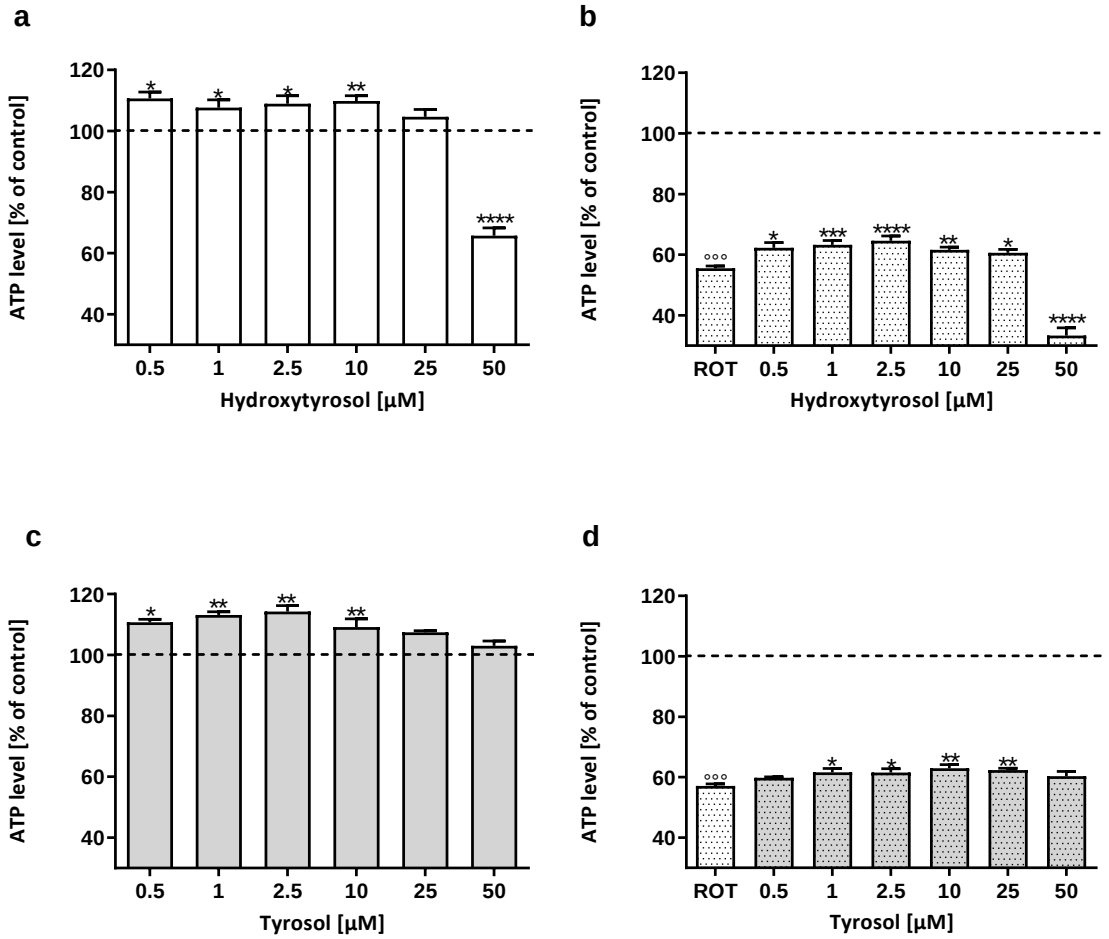

Figure 4.9 Effects of hydroxytyrosol and tyrosol on ATP levels in SH-SY5Y-MOCK cells. (a) ATP level of SH-SY5Y-MOCK cells after 24 h treatment with hydroxytyrosol or (c) Tyrosol in different concentrations (0.5-50 µM). (b) SH-SY5Y-MOCK cells after preincubation with hydroxytyrosol or (d) tyrosol for 1 h and insult with rotenone (25 µM) for 24 h; cells were normalized to cell medium control (100%); EtOH served as solvent control and had no influence on ATP level (data not shown); mean ± SEM; Data are represented as mean ± SEM; one-way ANOVA with Tukey´s multiple comparison post-hoc test (*$p < 0.05$, **$p < 0.01$, ***$p < 0.001$, ****$p < 0.0001$); n = 8.

Basal ATP levels were significantly increased by incubation with hydroxytyrosol (0.5, 1, 2.5 and 10 µM). The highest concentration (50 µM) led to a significant decrease of ATP levels, indicating toxic effects in high doses (Figure 4.9 a). Tyrosol treated cells showed positive significant effects in concentrations between 0.5 and 10 µM. The two highest concentrations 25 and 50 µM revealed no changes in ATP levels (Figure 4.9 c). Incubation with the complex I inhibitor rotenone (25 µM) led to significantly decreased ATP levels (around 60% of control cell level). Simultaneous incubation with rotenone and hydroxytyrosol (0.5-25 µM) or tyrosol (1-25 µM) were able to significantly prevent the rotenone-induced drop in ATP levels. The highest concentration of 50 µM tyrosol had no effect whereas 50 µM hydroxytyrosol had a

significant negative effect on rotenone-insulted ATP levels, leading to a reduction of 33% of control cell level (Figure 4.9 b and d).

Since low concentrations of hydroxytyrosol and tyrosol already showed positive effects and the two highest concentrations had no or even toxic effects on ATP levels, the remaining olive polyphenols and metabolites were used in concentrations of 0.05 to 10 µM.

Table 4.4 shows the influence of all tested substances on basal ATP levels and after 24 h insult with rotenone in SY5Y-MOCK cells. Ligstroside aglycone and oleuroside aglycone had no effect on ATP levels (data not shown). All remaining tested olive polyphenols had a significant positive effect on ATP levels. Considering the smallest concentration (0.05 µM) the increase ranged between 9 to 11% of control level. To study the potential protective activity of the olive polyphenols and metabolites against complex I inhibition, cells were additionally treated with 25 µM rotenone. Treatment with rotenone led to a significant decrease of ATP levels (61-69% of control level) in SH-SY5Y-MOCK cells. Regarding the smallest concentration of 0.05 µM only ligstroside, ligustaloside B, oleocanthal, oleuropein and oleuroside were able to protect complex I-insult significantly. Ligstroside and ligustaloside B showed the highest potential against rotenone insult. As 10 µM oleocanthal decreased basal ATP levels significantly, simultaneous incubation with rotenone also led to a significant negative effect.

Table 4.4 Effects of all tested substances on ATP levels in SH-SY5Y-MOCK cells. Results of test statistics after 24 h incubation with ligstroside, ligustaloside B, oleacein, oleocanthal, oleuropein, oleuroside and elenolic acid on ATP levels in SH-SY5Y-MOCK cells. ↑↓ = increase or decrease of ATP levels compared to EtOH control; Data are represented as mean ± SEM; one-way ANOVA with Tukey´s multiple comparison post-hoc test (*p < 0.05, **p < 0.01, ***p < 0.001, ****p < 0.0001); n = 9.

Compound	0.05 µM	0.1 µM	1 µM	2.5 µM	10 µM
Elenolic acid	108.1 ± 2.192 ↑**	114.5 ± 1.677 ↑****	112.1 ± 1.793 ↑****	114.8 ± 2.62 ↑****	100.3 ± 1.930 -
+ rotenone 67% insult	71.78 ± 2.205 -	74.86 ± 1.967 ↑**	71.57 ± 1.035 -	73.35 ± 2.251 ↑**	69.47 ± 1.685 -
Homovanillic acid	110.6 ± 2.491 ↑***	113.2 ± 1.665 ↑****	108.6 ± 2.371 ↑**	111.9 ± 2.842 ↑****	99.57 ± 2.185 -
+ rotenone 69% insult	72.73 ± 1.216 -	73.63 ± 1.419 ↑*	73.97 ±1.026 ↑**	72.86 ± 0.188 -	68.86 ± 1.828 -

Ligstroside	111.0 ± 0.775 ↑***	112.5 ± 0.717 ↑****	115.1 ± 2.162 ↑****	113.2 ± 1.599 ↑****	112.2 ± 1.266 ↑****
+ rotenone 67% insult	75.80 ± 1.068 ↑****	76.86 ± 1.203 ↑****	78.35 ± 1.201 ↑****	76.05 ± 0.688 ↑****	74.83 ± 0.472 ↑**
Ligustaloside B	109.6 ± 1.190 ↑**	110.8 ± 1.291 ↑***	111.1 ± 1.013 ↑****	113.1 ± 1.496 ↑****	111.5 ± 1.532 ↑****
+ rotenone 67% insult	74.32 ± 1.423 ↑**	74.57 ± 1.275 ↑***	75.15 ± 1.502 ↑***	76.96 ± 1.657 ↑****	76.45 ± 2.261 ↑****
Oleacein	111.1 ± 1.667 ↑****	113.7 ± 1.497 ↑****	114.8 ± 1.108 ↑****	113.6 ± 1.304 ↑****	96.68 ± 2.026 -
+ rotenone 62% insult	67.65 ± 1.610 -	71.36 ± 2.490 ↑**	70.33 ± 1.551 ↑*	69.37 ± 2.071 -	57.06 ± 1.668 -
Oleocanthal	108.9 ± 0.691 ↑***	110.1 ± 1.427 ↑****	111.7 ± 1.273 ↑****	107.1 ± 1.739 ↑**	74.15 ± 3.473 ↓****
+ rotenone 61% insult	69.89 ± 1.939 ↑*	71.63 ± 2.045 ↑**	70.04 ± 1.657 ↑*	66.88 ± 1.476 -	49.18 ± 2.498 ↓**
Oleuropein	109.3 ± 1.262 ↑***	109.3 ± 1.903 ↑***	112.0 ± 1.945 ↑****	111.0 ± 1.390 ↑****	107.5 ± 0.842 ↑*
+ rotenone 67% insult	74.21 ± 1.354 ↑***	73.49 ± 1.521 ↑**	74.79 ± 1.656 ↑****	73.79 ± 0.953 ↑***	71.68 ± 1.107 ↑*
Oleuroside	106.3 ± 1.956 -	109.0 ± 1.834 ↑**	108.8 ± 1.272 ↑*	110.8 ± 1.991 ↑***	108.4 ± 2.362 ↑*
+ rotenone 67% insult	74.14 ± 1.527 ↑**	73.81 ± 1.881 ↑**	74.52 ± 1.991 ↑**	75.56 ± 1.657 ↑***	72.33 ± 1.628 -

Table 4.5 shows the influence of all tested olive polyphenols and metabolites on basal ATP levels and on ATP levels with simultaneous rotenone-insult in SH-SY5Y-APP$_{695}$ cells. All tested compounds led to significant elevated ATP levels with the exception of ligstroside aglycone and oleuroside aglycone (data not shown). Oleuroside, oleacein, ligstroside and oleocanthal had a slightly higher effect regarding the smallest concentration of 0.05 µM on ATP levels compared to the other secoiridoids and metabolites and therefore identified as hit-substances. Insult of complex I led to a significant reduction of ATP levels (49-53%). With the exception of elenolic acid, oleacein and oleocanthal the remaining compounds showed a moderate protection against rotenone insult. The moderate protection could be due to the already impaired complex I respiratory capacity and the impaired complex I mRNA expression measured in SH-SY5Y-APP$_{695}$ cells (see Figure 4.3and Figure 4.5).

Figure 4.10 shows the effect of the four hit-substances oleacein, oleocanthal, ligstroside and oleuroside in the small concentration of 0.05 µM on ATP levels compared to solvent control. Followed determination of mitochondrial respiration was performed exclusively for oleacein, oleocanthal, ligstroside and oleuroside.

Table 4.5 Effects of all tested substances on ATP levels in SH-SY5Y-APP$_{695}$ cells. Results of test statistics after 24 h incubation with ligstroside, ligustaloside B, oleacein, oleocanthal, oleuropein, oleuroside and elenolic acid on ATP levels in SH-SY5Y-APP$_{695}$ cells. ↑↓ = Increase or decrease of ATP levels compared to EtOH control; Data are represented as mean ± SEM; one-way ANOVA with Tukey´s multiple comparison post-hoc test (*p < 0.05, **p < 0.01, ***p < 0.001, ****p < 0.0001); n = 9.

Compound	0.05 µM	0.1 µM	1 µM	2.5 µM	10 µM
Elenolic acid	108.2 ± 2.089 ↑*	113.6 ± 1.037 ↑***	110.5 ± 1.937 ↑**	109.9 ± 1.240 ↑**	103.3 ± 2.017 -
+rotenone 52% insult	56.13 ± 1.872 -	56.67 ± 1.928 -	57.32 ± 1.991 -	55.91 ± 1.924 -	54.01 ± 1.788 -
Hydroxy-tyrosol	110.3 ± 0.997 ↑***	110.0 ± 1.063 ↑****	110.5 ± 1.551 ↑****	110.1 ± 1.294 ↑****	103.1 ± 1.414 -
+rotenone 53% insult	63.95 ± 1.587 ↑****	63.49 ± 1.884 ↑****	62.69 ± 0.714 ↑***	63.59 ± 0.987 ↑****	59.08 ± 2.005 ↑*
Ligstroside	110.2 ± 1.154 ↑***	109.0 ± 1.723 ↑***	109.7 ± 1.515 ↑***	109.5 ± 1.276 ↑***	107.2 ± 1.290 ↑*
+rotenone 55% insult	61.82 ± 2.117 -	60.59 ± 2.250 -	63.32 ± 1.947 ↑*	62.99 ± 2.465 ↑*	62.73 ± 2.634 -
Ligustaloside B	106.2 ± 1.770 -	106.9 ± 2.221 ↑*	111.2 ± 0.961 ↑***	109.4 ± 1.283 ↑**	106.8 ± 1.683 -
+rotenone 53% insult	56.45 ± 0.912 -	59.20 ± 1.791 -	60.10 ± 1.545 ↑*	65.51 ± 2.372 ↑***	61.79 ± 2.559 ↑***
Oleacein	107.8 ± 0.691 ↑*	109.9 ± 1.427 ↑**	109.8 ± 1.273 ↑**	108.1 ± 1.739 ↑*	95.72 ± 3.473 -
+rotenone 50% insult	52.10 ± 0.6116 -	52.53 ± 18.24 -	52.69 ± 1.704 -	50.88 ± 1.468 -	40.71 ± 1.499 ↓***
Oleocanthal	109.5 ± 1.274 ↑***	111.6 ± 1.615 ↑****	112.8 ± 1.571 ↑****	108.4 ± 1.840 ↑**	56.56 ± 2.981 ↓****
+rotenone 49% insult	49.80 ± 1.273 -	50.17 ± 1.384 -	48.41 ± 1.513 -	42.33 ± 1.691 ↓*	26.99 ± 2.216 ↓****
Oleuropein	107.7 ± 1.231 ↑*	109.1 ± 2.012 ↑**	109.3 ± 1.760 ↑**	107.9 ± 1.611 ↑*	106.9 ± 2.097 ↑*

+rotenone 53% insult	59.57 ± 2.259 -	60.83 ± 2.249 ↑**	62.91 ± 2.285 ↑***	60.47 ± 2.210 ↑*	58.38 ± 1.920 -
Oleuroside	110.5 ± 1.777 ↑***	109.2 ± 1.833 ↑**	109.5 ± 1.486 ↑***	109.4 ± 2.013 ↑**	108.6 ± 1.964 ↑**
+rotenone 53% insult	58.39 ± 1.650 -	59.76 ± 0.9493 -	63.58 ± 1.337 ↑**	66.35 ± 2.380 ↑***	58.97 ± 1.051 -
Tyrosol	105.8 ± 1.987 -	108.3 ± 1.511 -	107.7 ± 1.639 -	107.4 ± 1.682 -	105.5 ± 1.475 -
+rotenone 53% insult	59.36 ± 1.369 -	59.23 ± 1.540 -	60.66 ± 2.206 ↑*	60.93 ± 1.970 ↑*	57.10 ± 1.897 -
Homovanillic acid	107.3 ± 2.297 -	111.3 ± 1.686 ↑**	106.2 ± 3.067 -	107.2 ± 2.035 -	103.1 ± 2.875 -
+rotenone 49% insult	55.87 ± 1.723 -	57.08 ± 1.845 -	56.34 ± 2.171 ↑*	61.18 ± 1.669 ↑*	55.01 ± 0.963 -

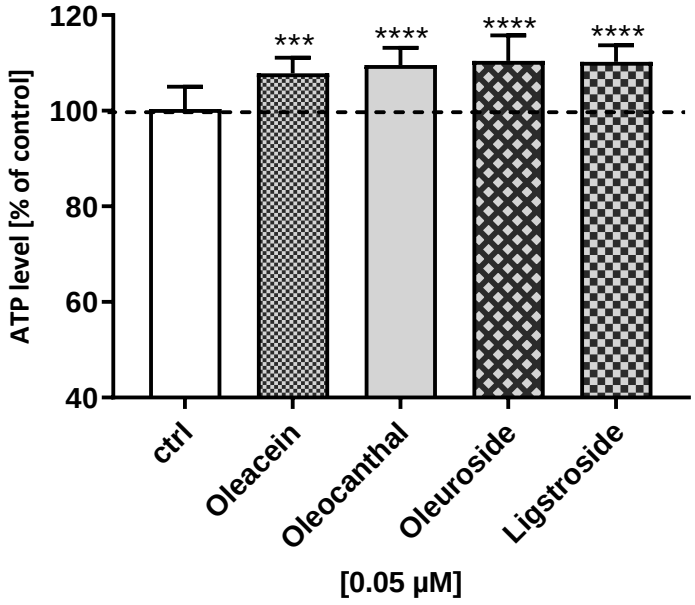

Figure 4.10 Effects of the four hit-substances on ATP level in SH-SY5Y-APP$_{695}$ cells. ATP levels after 24 h incubation with 0.05 µM oleacein, oleocanthal, oleuroside or ligstroside. The four hit-substances significantly increase ATP levels compared to solvent control (EtOH). Cell culture medium served as control for normalization (100%). Data are represented as mean ± SEM; one-way ANOVA with Tukey´s multiple comparison post-hoc test (∗∗∗p < 0.001, ∗∗∗∗p < 0.0001); n = 9.

4.2.2 Influence of the four hit-substances on mitochondrial respiration and CS activity in SH-SY5Y-APP$_{695}$ cells

Mitochondrial respiration was assessed after 24 h incubation with 0.05 µM oleocanthal, ligstroside, oleacein or oleuroside. Oleuroside revealed no changes in all measured respiratory states, whereas oleacein showed a significant increase in endogenous respiration (Figure 4.11 a and b). Ligstroside incubation led to a significant elevation of endogenous, complex I, complex I+II, leak (omy) and ETS respiration (Figure 4.11 c). Oleocanthal increased endogenous respiration, complex I and complex I+II respiration significantly (Figure 4.11 d). The respiratory ratio (RCR) was significantly increased after 24 h treatment with 0.05 µM oleuroside, indicating improved mitochondrial coupling. RCR of oleacein, ligstroside and oleocanthal was not different compared to control cells (data not shown).

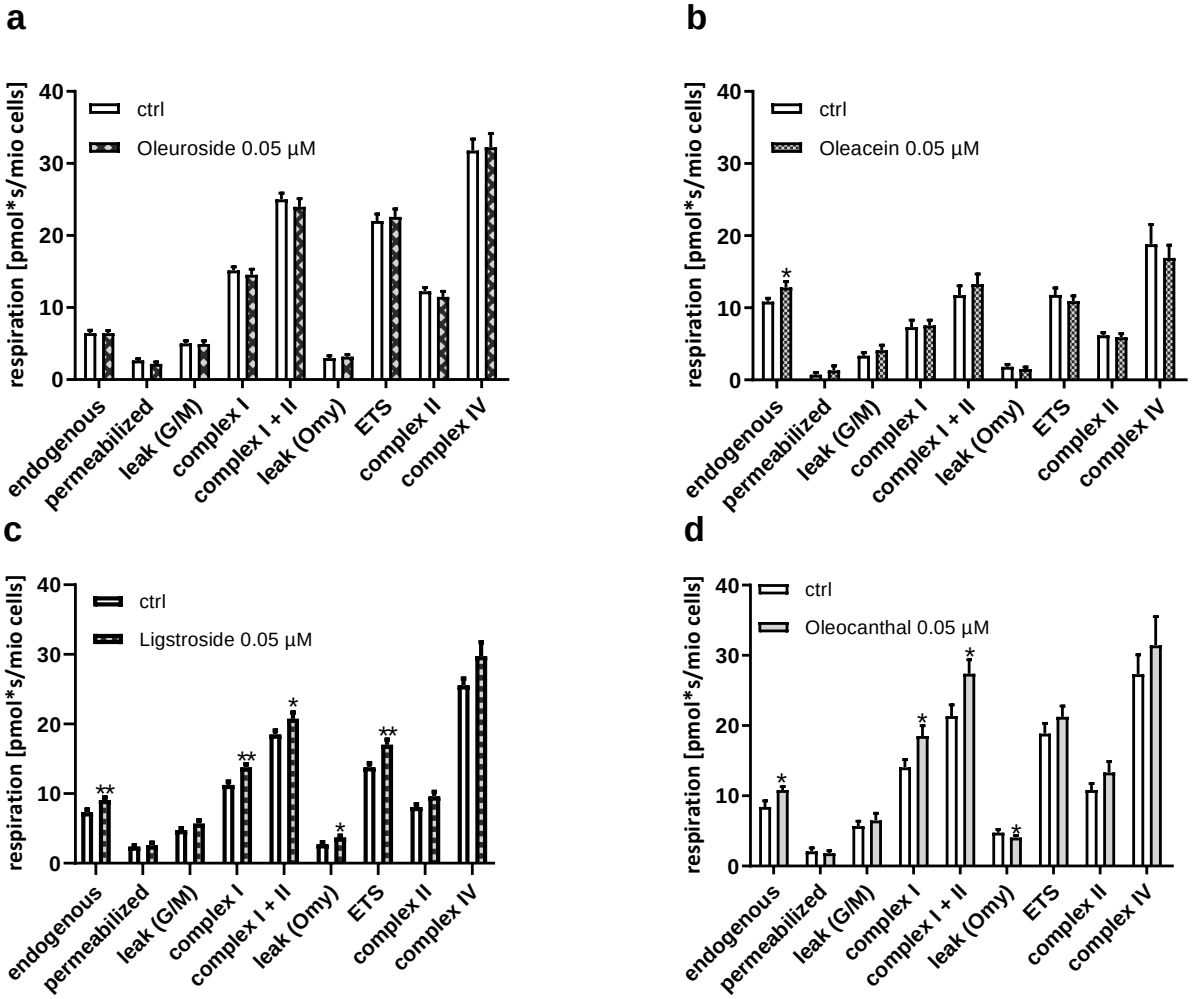

Figure 4.11 Mitochondrial respiration of the four hit-substances in SH-SY5Y-APP$_{695}$ cells. Mitochondrial respiration in SH-SY5Y-APP$_{695}$ cells after 24 h incubation with the respective olive

polyphenol (0.05 µM) or solvent control (EtOH). A solution containing 10^6 cells/ml was used for analyzing oxygen capacity. (a) Oleuroside had no influence on mitochondrial respiration. (b) Oleacein elevated endogenous respiration. All other complexes were unaffected. (c) Ligstroside treatment led to significant elevations of endogenous, complex I, coupled complex I+II, leak I (omy) respiration and increased capacity of the electron transfer system (ETS). (d) Incubation with oleocanthal elevated endogenous, complex I and coupled complex I+II respiration. Data are represented as mean ± SEM; student´s unpaired *t*-test (∗p < 0.05, ∗∗p < 0.01, ∗∗∗p < 0.001); n = 13.

Citrate synthase activity (CS) is a known marker for mitochondrial content (Larsen et al. 2012). CS was significantly increased after incubation with ligstroside or oleocanthal (Figure 4.12 c and d). Treatment with oleacein or oleuroside revealed no changes of CS activity (Figure 4.12 a and b).

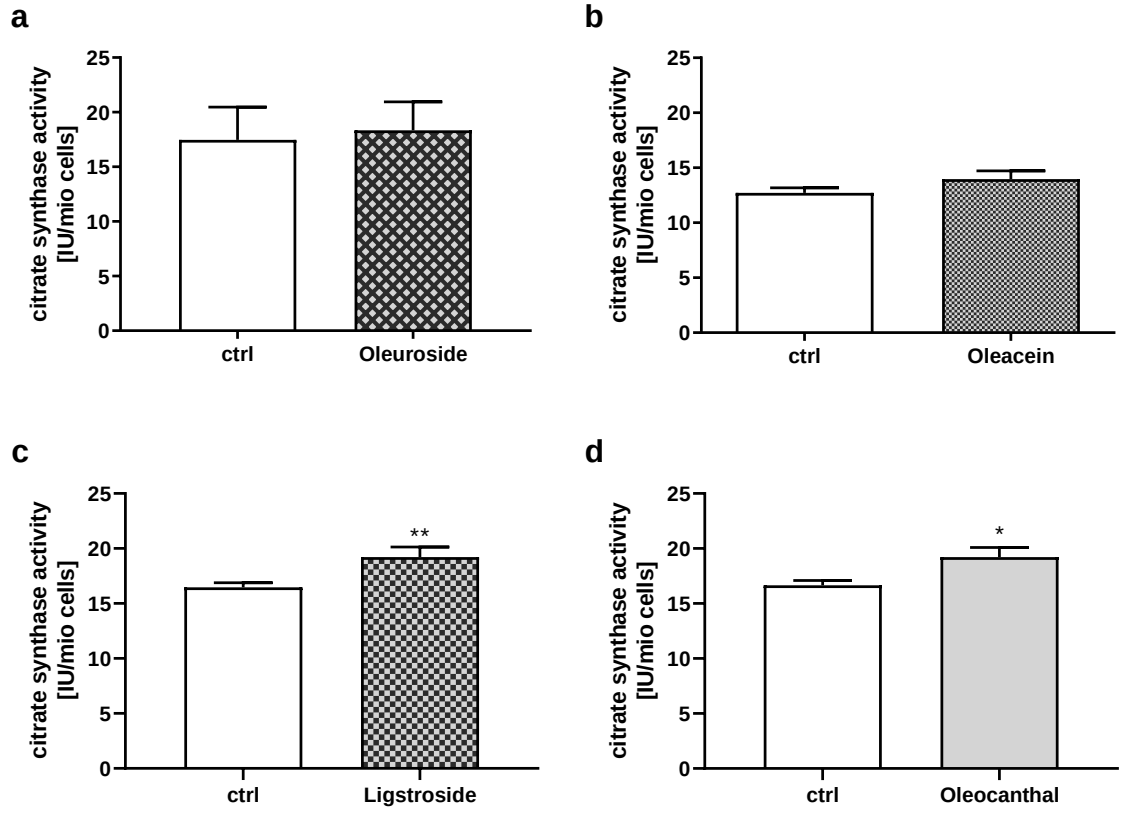

Figure 4.12 Citrate synthase activity of the four hit-substances in SH-SY5Y-APP cells. Citrate synthase activity of SH-SY5Y-APP_{695} cells after 24 h incubation with 0.05 µM (a) oleuroside (b) oleacein (c) ligstroside or (d) oleocanthal and EtOH as solvent control. CS activity was assessed spectrophotometrically at 412 nm. Data are represented as mean ± SEM; student´s unpaired *t*-test (∗p < 0.05, ∗∗p < 0.01); n = 13.

Normalizing respiration to CS activity gives information about the respiration of a single mitochondrion (Park et al. 2014). CS normalized respiration after oleuroside treatment was again unchanged (Figure 4.13 a), whereas oleacein treatment showed a significant increase of

the permeabilized and leak (G/M) state which is very likely due to a better integrity of the inner mitochondrial membrane (Brand und Nicholls 2011). CS normalized respiration after treatment with ligstroside showed similar results like cell count normalized respiration: endogenous, complex I, complex I+II respiration and ETS were significantly increased, only leak (omy) respiration was unchanged (Figure 4.13 c). Incubation with oleocanthal led to a significant increase in endogenous respiration whereas leak (omy) respiration was significantly decreased (Figure 4.13 d).

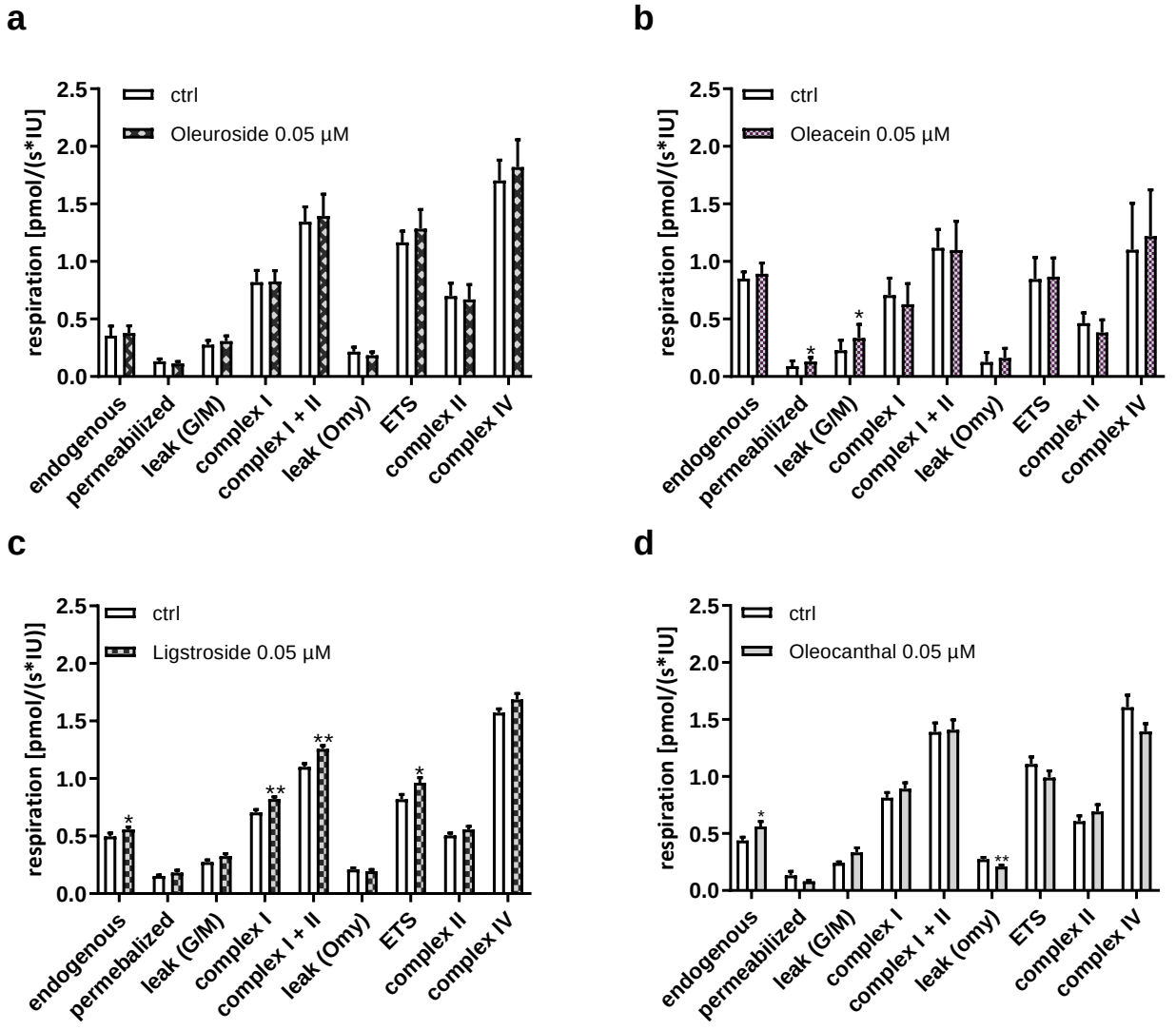

Figure 4.13 CS normalized mitochondrial respiration of the four hit-substances in SH-SY5Y$_{695}$ cells. CS normalized mitochondrial respiration of SH-SY5Y-APP$_{695}$ cells after 24 h incubation with (a) oleuroside (b) oleacein (c) ligstroside or (d) oleocanthal and EtOH as control, representing respiration of a single mitochondrion and consequently showing the functionality of the mitochondrion. Data are represented as mean ± SEM; student´s unpaired *t*-test (∗p < 0.05, ∗∗p < 0.01); n = 13.

Taken together, ligstroside and oleocanthal had the highest positive influence on mitochondrial respiration and CS activity. Therefore, following experiments were carried out exclusively for these two compounds. Additionally, we determined ATP levels after ligstroside or oleocanthal incubation in very small concentrations (nM scale) (Figure 4.14). Ligstroside has already a significant positive influence at 0.0001 µM and oleocanthal shows a significant increase at 0.001 µM.

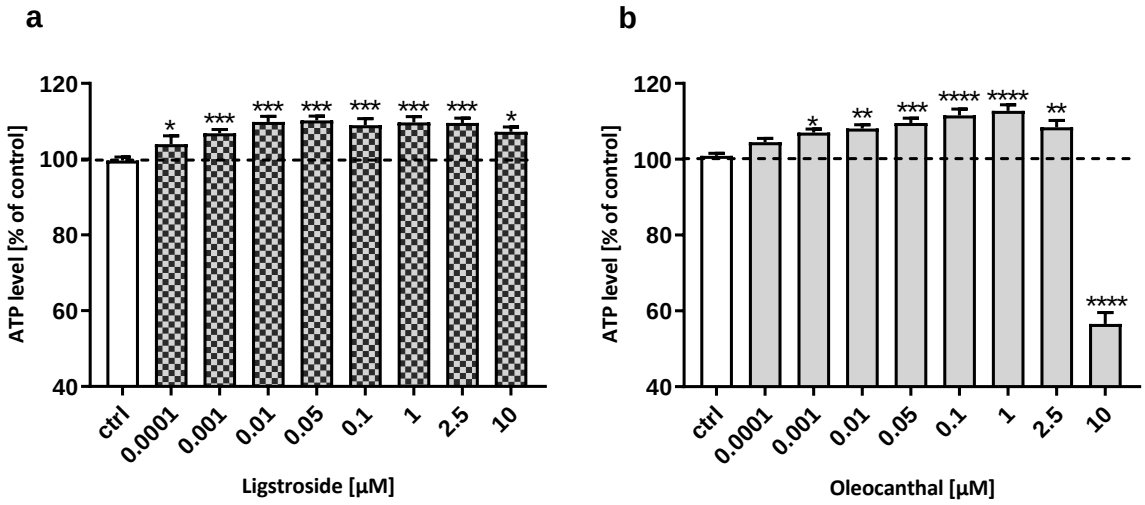

Figure 4.14 ATP-concentration-response curve of ligstroside and oleocanthal incubated SH-SY5Y-APP$_{695}$ cells. ATP level in SH-SY5Y-APP$_{695}$ cells after 24 h incubation with different concentration of (a) ligstroside and (b) oleocanthal. Ligstroside was able to significantly elevate ATP level in very small concentrations starting with 0.0001 µM, whereas oleocanthal significantly increased ATP level at a concentration of 0.001 µM. Data are represented as mean ± SEM; student´s unpaired *t*-test (∗p < 0.05, ∗∗p < 0.01, ∗∗∗p < 0.001, ∗∗∗∗p < 0.0001); n = 13.

4.2.3 Analysis of mRNA expression in oleocanthal and ligstroside incubated SH-SY5Y-MOCK cells

Oleocanthal elevated mRNA expression levels of SIRT1, NRF1 and complex I significantly compared to solvent control (Figure 4.15). On the other hand oleocanthal showed no significant effects on CS, CREB1, PGC-1α, TFAM, COX5A and ATP5D (Table 4.6). In contrast, ligstroside was able to upregulate all genes of the mitochondrial biogenesis pathway; SIRT1, CREB1, PGC-1α, NRF1 and TFAM were significantly increased (Figure 4.16). Additionally, complex I and COX5A were significantly elevated. Interestingly, ligstroside led to a significant decrease

of CS and ATP5D gene expression. Considering the antioxidative system, oleocanthal significantly increased SOD2 and CAT mRNA levels compared to solvent control, whereas GPx1 was numerically but not significantly increased (Figure 4.16). Ligstroside showed a significant positive effect on SOD2 and GPx1 mRNA expression, while mRNA expression of CAT remained unchanged (Figure 4.17).

Table 4.6 shows the influence of oleocanthal and ligstroside of all tested genes in SH-SY5Y-MOCK cells compared to solvent control.

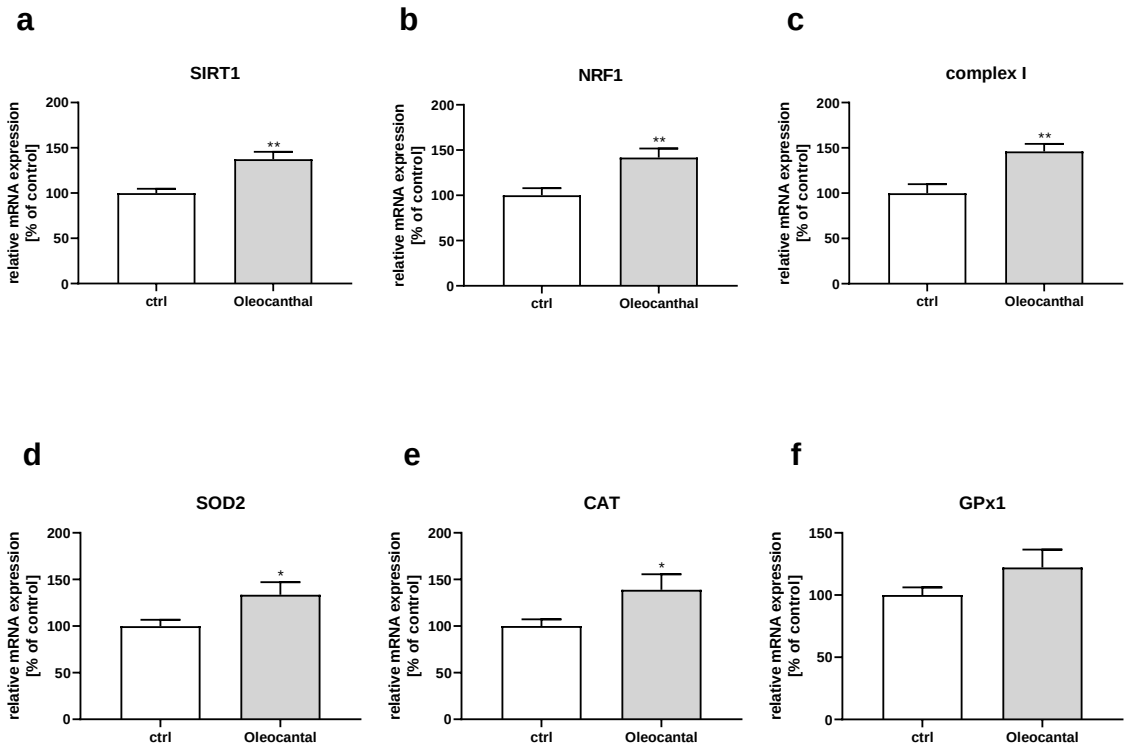

Figure 4.15 Relative mRNA level after treatment with oleocanthal in SH-SY5Y-MOCK cells. Relative mRNA expression after 24 h incubation with 0.05 µM oleocanthal in SH-SY5Y-MOCK cells. (a) SIRT1, (b) NRF1 genes of the mitochondrial biogenesis pathway are significantly elevated after oleocanthal treatment compared to control cells. (c) Complex I is significantly increased compared to control cells. (d) SOD2, (e) CAT and (f) GPx1 enzymes of the antioxidative defence system are significantly increased after oleocanthal treatment. Data are represented as mean ± SEM; one-way ANOVA with Tukey´s multiple comparison post-hoc test ($*p < 0.05$, $**p < 0.01$); n = 7.

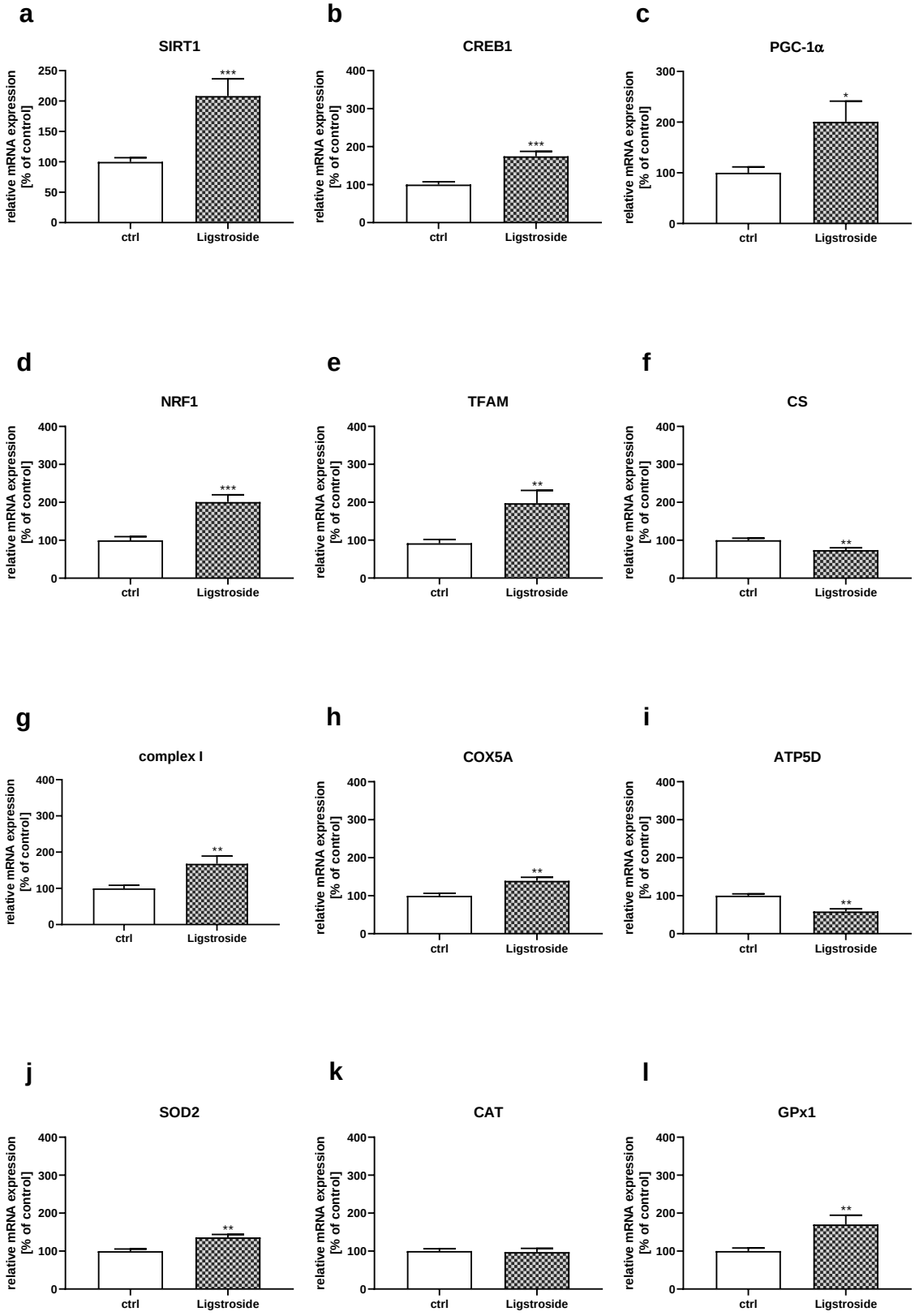

Figure 4.16 Relative mRNA level after treatment with ligstroside in SH-SY5Y-MOCK cells. Relative mRNA expression after 24 h incubation with 0.05 µM ligstroside in SH-SY5Y-MOCK cells. (a-e) Target genes of mitochondrial biogenesis are all significantly upregulated through ligstroside

incubation compared to solvent control; (f) CS activity is significantly decreased; (g-i) complex I and IV of the respiratory chain are significantly increased, whereas complex V is significantly downregulated; (j-l) SOD2 and GPx1 are significantly enhanced although CAT revealed no changes. Data are represented as mean ± SEM; one-way ANOVA with Tukey´s multiple comparison post-hoc test (∗p < 0.05, ∗∗p < 0.01, ∗∗∗p < 0.001); n = 7.

Table 4.6 Relative normalized mRNA expression of oleocanthal and ligstroside incubated SH-SY5Y-MOCK cells. Relative normalized mRNA expression levels in SH-SY5Y-MOCK cells after oleocanthal or ligstroside treatment determined using quantitative real-time PCR in comparison to solvent control (100%); n=7 mean ± SEM; one-way ANOVA with Tukey´s multiple comparison post-hoc test (∗p < 0.05, ∗∗p < 0.01, ∗∗∗p < 0.001); results are normalized to the mRNA expression levels of actin-β (ACTB), glyceraldehyde 3-phosphate dehydrogenase (GAPDH) and phosphoglycerate kinase 1 (PGK1).

	Oleocanthal	**Ligstroside**
CS	123.3 ± 14.8	74.1 ↓** ± 8.2
CREB1	89.0 ± 9.1	174.4 ↑*** ± 15.9
SIRT1	137.4 ↑** ± 8.9	267.2 ↑*** ± 46.1
PGC-1α	118.6 ± 15.9	200.7 ↑* ± 38.4
NRF1	141.8 ↑** ± 12.5	200.9 ↑*** ± 21.2
TFAM	103.6 ± 13.9	197.3 ↑** ± 35.3
CI	171.9 ↑** ± 25.8	167.8 ↑** ± 20.1
COX5A	84.5 ± 8.7	139.2 ↑** ± 11.6
ATP5D	116.8 ± 11.9	58.5 ↓** ± 8.6
GPx1	122.2 ± 15.0	170.2 ↑** ± 23.4
CAT	138.9 ↑* ± 18.1	97.5 ± 11.3
SOD2	133.6 ↑* ± 15.1	136.0 ↑** ± 9.4

4.2.4 Analysis of mRNA expression in oleocanthal and ligstroside incubated SH-SY5Y-APP$_{695}$ cells

Oleocanthal had no significant positive effect on mRNA expression in SH-SY5Y-APP$_{695}$ cells (Table 4.7). The antioxidant enzymes CAT and SOD2 were significantly decreased after incubation with both, oleocanthal and ligstroside, whereas ligstroside incubation led to a significantly increased mRNA expression of GPx1 compared to solvent control (Figure 4.17, Table 4.7). In contrast, CREB1 and SIRT1 were significantly increased after ligstroside

incubation (Figure 4.17). Moreover, ligstroside treated cells showed numerical elevations of NRF1 and TFAM gene expression compared to control cells (Table 4.7).

Table 4.7 Relative normalized mRNA expression levels of oleocanthal and ligstroside incubated SH-SY5Y-APP$_{695}$ cells. Relative normalized mRNA expression levels in SH-SY5Y-APP$_{695}$ cells after oleocanthal or ligstroside treatment determined using quantitative real-time PCR in comparison to solvent control (100%); n=7 mean ± SEM with one-way ANOVA with Tukey´s multiple comparison post-hoc test, (↑/↓) trend to increase/decrease; (∗p < 0.05, ∗∗p < 0.01, ∗∗∗p < 0.001); results are normalized to the mRNA expression levels of actin-β (ACTB), glyceraldehyde 3-phosphate dehydrogenase (GAPDH) and phosphoglycerate kinase 1 (PGK1).

	Oleocanthal	**Ligstroside**
CS	99.3 ± 15.7	63.6 (↓) ± 13.5
CREB1	88.5 ± 15.3	137.2 ↑* ± 12.9
SIRT1	70.1 ± 15.5	175.2 ↑** ± 17.7
PGC-1α	113.7 ± 32.6	138.9 (↑) ± 29.1
NRF1	75.3 ± 13.2	138.6 (↑) ± 20.7
TFAM	78.8 ± 19.3	125.4 (↑) ± 20.4
CI	51.4 ± 26.3	177.2 ↑* ± 25.2
COX5A	65.1 ± 16.0	95.4 ± 9.6
ATP5D	80.1 ± 17.7	58.8 ± 24.0
GPx1	65.8 ± 18.6	163.0 ↑** ± 19.7
CAT	54.1 ↓* ± 19.9	66.6 ↓* ± 15.2
SOD2	62.3 ↓* ± 13.6	50.2 ↓*** ± 11.3

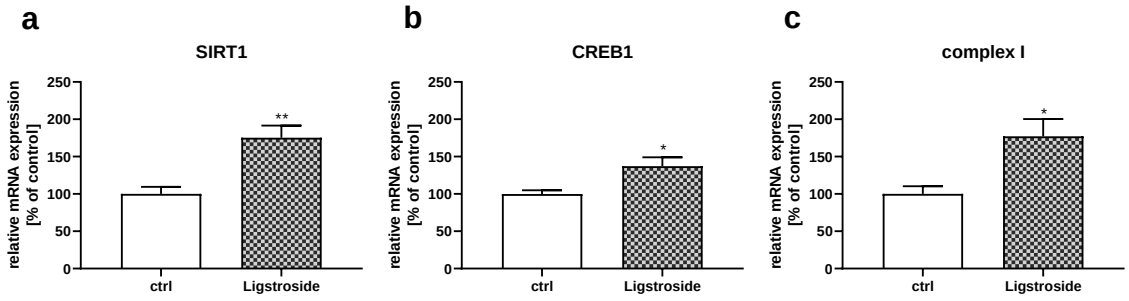

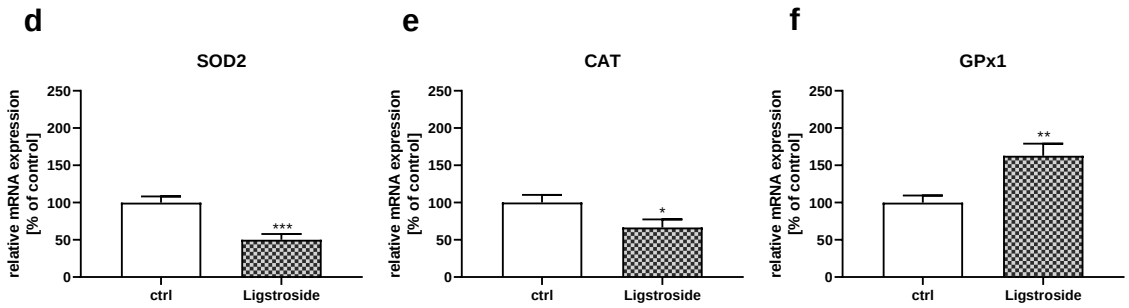

Figure 4.17 Realtive mRNA level of ligstroside treated SH-SY5Y-APP$_{695}$ cells. Relative mRNA expression after 24 h incubation with 0.05 µM ligstroside in SH-SY5Y-APP$_{695}$ cells. (a) SIRT1, (b) CREB1, (c) complex I and (f) GPx1 are significantly upregulated after ligstroside treatment. (d) SOD2 and (e) CAT show a significant decrease through ligstroside incubation. Data are represented as mean ± SEM; student´s unpaired *t*-test (∗p < 0.05, ∗∗p < 0.01, ∗∗∗p < 0.001); n = 7.

4.2.5 Influence of ligstroside on protein levels in SH-SY5Y-MOCK cells

To assess the effects of ligstroside on protein levels, western blot analyses were performed. We analysed the expression of proteins involved in mitochondrial biogenesis (CREB1, pCREB, PGC-1α). Furthermore, we determined protein levels of CS and a core component of the outer mitochondrial membrane protein translocation pore TOM22 as well as proteins of the respiratory system (complex I – complex V).

The levels of all tested proteins did not lead to any significant changes (Table 4.8) in SH-SY5Y-MOCK cells. TOM22 protein levels showed a tendency to lower protein syntheses, whereas PGC-1α and complex II tended to increase. Interestingly, protein expression of CREB from EtOH treated (solvent control) SH-SY5Y-MOCK cells lead to a significant increase compared to medium control.

Table 4.8 Protein levels of ligstroside treated SH-SY5Y-MOCK cells. Protein levels in SH-SY5Y-MOCK cells after 24 h treatment with EtOH as solvent control or ligstroside, normalized to loading control tubulin or GAPDH. Cell culture medium served as control for normalization (100%); mean ± SEM with one-way ANOVA with Tukey´s multiple comparison post-hoc test; n = 6.

Protein	Ctrl	Ligstroside
CREB	141.2 ± 12.79	103.5 ± 8.162
pCREB	94.27 ± 6.496	106. ± 16.51

PGC-1α	120.2 ± 16.19	129.2 ± 1.982
TOM22	99.77 ± 10.09	86.84 (↓) ± 7.448
CS	92.01 ± 6.780	99.72 ± 8.484
CI	94.29 ± 12.14	77.72 (↓) ± 8.325
CII	124.2 ± 10.64	136 (↑) ± 17.62
CIII	83.48 ± 5.053	95.68 ± 4.22
CIV	92.44 ± 11.31	105.9 ± 13.02
CV	96.2 ± 13.07	100.5 ± 4.968

4.2.6 Influence of ligstroside on protein levels in SH-SY5Y-APP$_{695}$ cells

To verify if ligstroside is able to influence the protein expression in impaired cells, western blot analysis were performed in SH-SY5Y-APP$_{695}$ cells after 24 h incubation with ligstroside (0.05 µM).

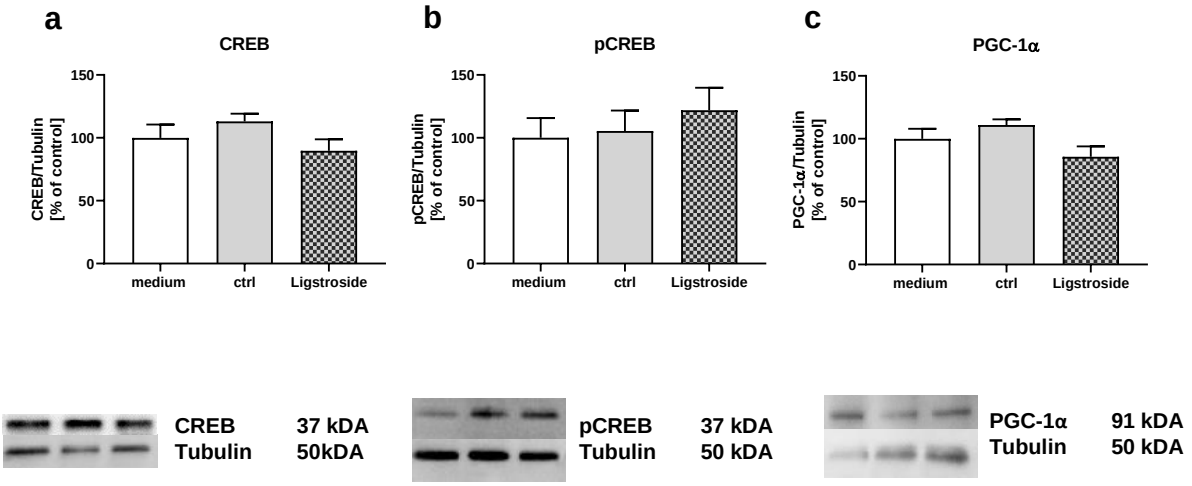

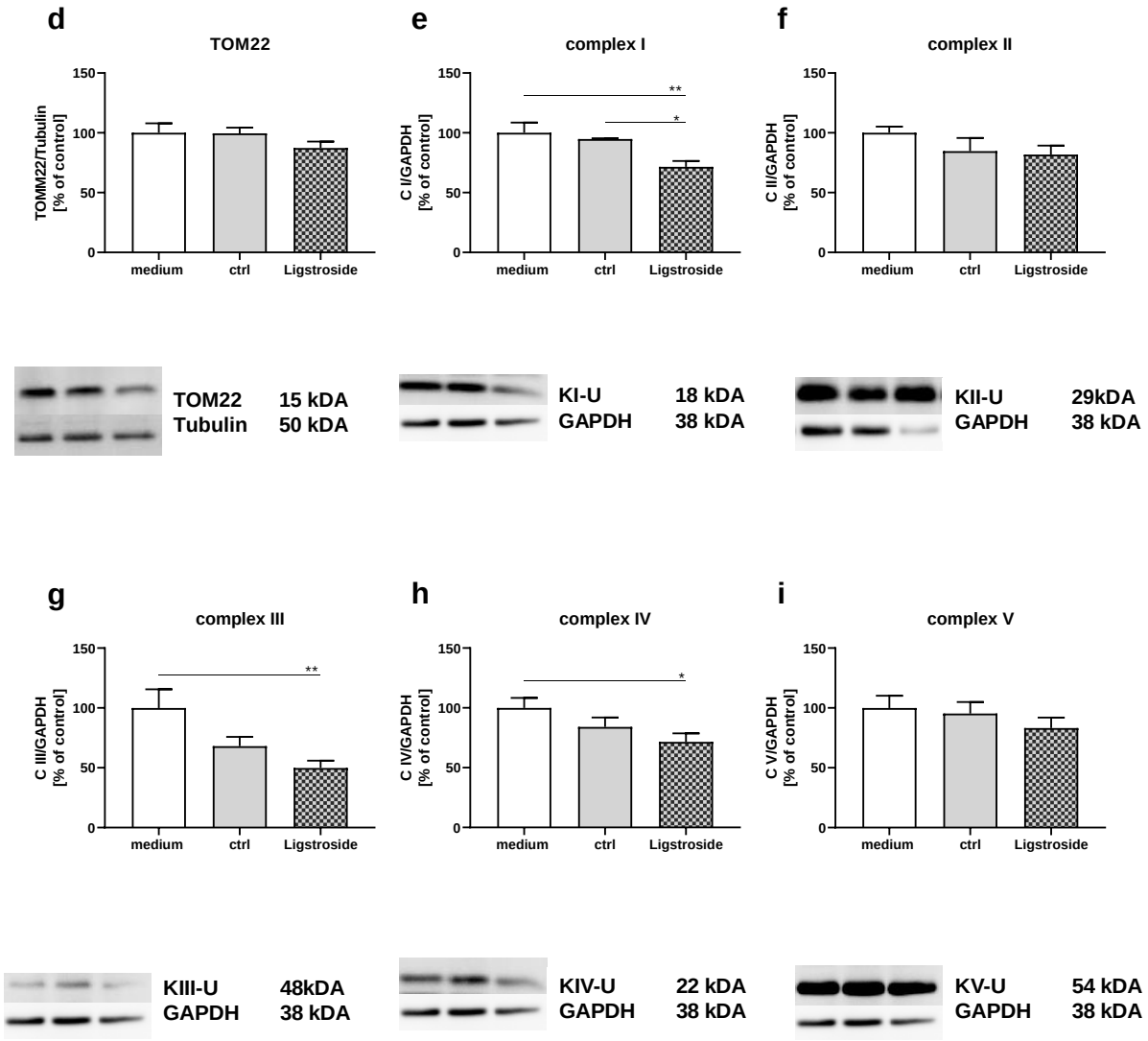

Figure 4.18 Protein levels of ligstroside incubated SH-SY5Y-APP$_{695}$ cells. Protein levels of (a) CREB (b) pCREB (c) PGC-1α (d) TOM22 (e) complex I (f) complex II (g) complex III (h) complex IV (i) complex V after 24 h incubation with 0.05 µM ligstroside in SH-SY5Y-APP$_{695}$ cells; pictures of representative western blots are depicted in the lower part of each figure; first band: SH-SY5Y-APP $_{695}$ cells incubated with cell culture medium, band 2: SH-SY5Y-APP $_{695}$ cells incubated with EtOH control, band 3: SH-SY5Y-APP $_{695}$ cells incubated with ligstroside. Data are represented as mean ± SEM; one-way ANOVA with Tukey´s multiple comparison post-hoc test (∗p < 0.05, ∗∗p < 0.01); n = 7.

Table 4.9 Protein levels of ligstroside treated SH-SY5Y-APP$_{695}$ cells. Protein levels in SH-SY5Y-APP$_{695}$ after 24 h treatment with EtOH as solvent control or ligstroside normalized to loading control tubulin or GAPDH. Cell culture medium served as control for normalization (100%); mean ± SEM with one-way ANOVA with Tukey´s multiple comparison post-hoc test; (∗p < 0.05); n = 6.

Protein	Ctrl	Ligstroside
CREB	113.1 ± 6.073	89.65 ± 9.10
pCREB	105.4 ± 16.33	122.0 ± 17.83
PGC-1α	111.0 ± 4.519	85.63 ± 8.322
TOM22	99.56 ± 4.745	87.36 ± 5.361
CS	90.12 ± 6.649	91.88 ± 5.066
CI	94.78 ± 0.692	71.54 ↓* ± 4.857
CII	84.71 ± 11.00	81.83 ± 7.509
CIII	68.05 ± 7.698	49.78 ± 6118
CIV	84.12 ± 7.766	71.58 ± 7.088
CV	95.27 ± 9.68	83.20 ± 8.854

4.2.7 Influence of oleocanthal and ligstroside on $A\beta_{1-40}$ levels in SH-SY5Y- APP_{695} cells

Understanding the mechanisms by which ligstroside and oleocanthal protect against mitochondrial dysfunction, $A\beta_{1-40}$ levels were measured. SH-SY5Y-APP_{695} cells were incubated for 24 h with 0.05 µM ligstroside or oleocanthal. The effects of both substances on Aβ production was assessed by ELISA.

Oleocanthal treatment significantly enhanced $A\beta_{1-40}$ clearance compared to solvent control. Incubation with ligstroside did not show any effect on $A\beta_{1-40}$ levels (Figure 4.19).

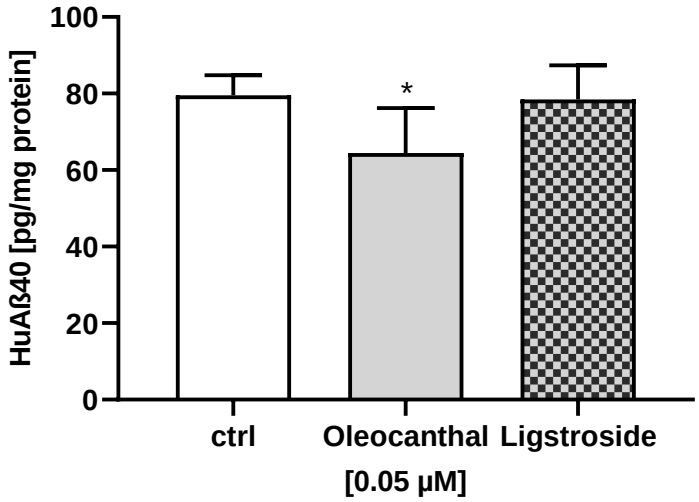

Figure 4.19 $A\beta_{1-40}$ level of oleocanthal and ligstroside treated SH-SY5Y-APP_{695} cells. Human $A\beta_{1-40}$ level in SH-SY5Y-APP_{695} cells after 24 h incubation with EtOH as control, oleocanthal or ligstroside. Cells were lysed and Aβ levels were determined by ELISA, and normalized to protein content. Data are represented as mean ± SEM with one-way ANOVA with Tukey´s multiple comparison post-hoc test; ($*p < 0.05$); n = 8.

5 Discussion

5.1 SH-SY5Y cell line as a model for late-onset AD

Since 2003, there have been no new drugs approved for AD and all phase III clinical trials failed, until today. One reason for the failure is thought to be that drugs being administered too late in the progression of the disease and therefore no reverse of the damage can occur. That is why ongoing trials have expanded to include people with preclinical and prodromal AD. Additionally, preclinical testing should also be performed in models of sporadic AD. Common *in vitro* AD models induce Aβ mostly externally, resulting in extremely high Aβ levels and therefore represent the familial form of AD (Leuner et al., 2012; Schmitt et al., 2012). Models for the far more common form, sporadic or late-onset AD, should display a low Aβ accumulation.

When choosing cell culture models, attention should be paid to the tissue of the cell line and the organism from which it originates, as both factors have an influence on the genotype and phenotype. Since AD, involves the degeneration of neurons, SH-SY5Y cells were chosen which are not only of neuronal origin, but also represent a human cell line. To represent the sporadic form of AD, SH-SY5Y cells were transfected with the human APP_{695} gene, generating very low Aβ levels (Stockburger et al., 2014b). Such a model is well suited for the collection of a large amount of data, as they continuously divide and provide the required quantity of cells for different experiments without showing variability. However, the deficits associated with an immortalised cell line must be considered. For example, most of tumour cells reveal changes in their energy metabolism. It is well accepted that tumour cells have an increased glycolytic activity due to an impaired OXPHOS, the so called Warburg effect (Warburg, 1956; Diaz-Ruiz et al., 2011). On the other hand, it has been demonstrated that some cancer cell lines have functional mitochondria and obtain their energy in form of ATP mainly from OXPHOS (Guppy et al., 2002). Nevertheless, it needs to be kept in mind that tumour cells differ in their growth performance or rather doubling time, metabolic pathways, and genetic properties (Xicoy et al., 2017). Despite the limitations, post-mitotic cells have the advantage to be cultured for a long period of time as they continuously divide and thus provide an unlimited supply of material. As they grow quickly and continuously, it is possible to extract large amounts of protein or RNA for the use of biochemical assays. Especially for the testing of several compounds to understand molecular pathways in fighting against incurable disease, post mitotic cells have the greater potential and are more easy to use (Kaur and Dufour, 2012; Maqsood et al., 2013; Slanzi et al.,

2020). Additionally, it is possible to create cell lines that stably express a gene of interest, such as a mutant version of a protein and in our case the transfection with the human form of APP. Another advantage of immortalized SH-SY5Y cells is their well characterization and the possibility to differentiate the cells into a more mature neuron-like phenotype. To investigate basic functions of the cell, such as mitochondrial functions the use of undifferentiated cells is sufficient. Additionally, undifferentiated cells do not have the disadvantage to not undergo cell division, as mature neurons do once they are differentiated (Gordon et al., 2013). A high throughput is therefore guaranteed.

As discussed in chapter 1.2.2, mitochondrial dysfunction, associated with reduced energy metabolism and enhanced oxidative stress due to ageing and slightly elevated Aβ levels, is an early event in the pathogenesis of AD. In our study, SH-SY5Y-APP$_{695}$ cells exhibit around 80 pg/mg protein Aβ$_{1-40}$. This is a very moderate concentration compared to other *in vitro* cell models, where Aβ is induced exogenous in micromolar concentrations (Kornelius et al., 2017). As plaque formation is also found in the brains of cognitively healthy older people, the biological processes underlying AD are present decades before clinical symptoms begin (Bennett et al., 2006). Furthermore, low Aβ levels seem to be highly important in the initiation of mitochondrial dysfunction (Müller et al., 2010; Swerdlow, 2018). Because late-onset AD occurs on a background of ageing accompanied with slightly elevated Aβ levels (Jansen et al., 2015), cells transfected with human APP mutants expressing Aβ in very low concentrations, are more relevant for late-onset AD, rather than for early-onset AD.

To investigate the effects of the expression of low Aβ levels, we compared mitochondrial function between vector transfected SH-SY5Y-MOCK control cells and SH-SY5Y-APP$_{695}$ cells. Mitochondrial dysfunction is associated with a decline of cellular ATP levels and has been reported to be one of the characteristics of an early stage of AD (Beck et al., 2016). In this study, we detected a decrease in the respiratory capacity of the respiration chain and a subsequent decline of ATP levels in SH-SY5Y-APP$_{695}$ cells compared to control cells which is in line with earlier published data (Stockburger et al., 2014a). OXPHOS was not only affected by reduced complex activities, but also by significantly impaired mitochondrial coupling in SH-SY5Y-APP$_{695}$ cells, marked by a significantly decrease of respiratory control ratio (RCR). RCR is calculated as ratio between uncoupled complex I and II respiration and leak respiration. Therefore, small RCR values indicate that either uncoupled complex I and II is small or leak respiration is high. The decreased RCR indicates that protons leak through the inner

mitochondrial membrane without contributing to ATP production (Gnaiger, 2001). Additionally, rhodamine-123 fluorescence proportional to MMP, was significantly reduced in SH-SY5Y- APP_{695} cells. These results are similar to those previously reported of our and other groups, in which it has been repeatedly shown that Aβ adversely affects different parameters of mitochondrial function (Rhein et al., 2009b; Pagani and Eckert, 2011; Hagl et al., 2015b; Grewal et al., 2020). It is remarkable that already low Aβ expression (picomolar range) in SH-SY5Y-APP_{695} cells leads to an overall impairment of mitochondrial function.

Underlying molecular mechanisms were investigated by determination of mRNA expression in both cell lines. Gene expression of complex I was significantly reduced in SH-SY5Y-APP_{695} cells compared to control cells. Complex I is the largest enzyme of the respiratory chain, building the entry for most of the reducing agents generated during metabolism (Hirst, 2013). Dysfunction of complex I is associated with AD (Holper et al., 2019). Furthermore it is well known, that complex I abundance and activity decrease during ageing. According to our data, decreased gene expression of complex I was shown in Aβ treated SH-SY5Y cells (Cieślik et al., 2020). Furthermore, this was also confirmed in a study with patients with early AD and definite AD. Downregulation of complex I mRNA was seen in both, early and definite AD brain specimens (Reddy and Beal, 2008). Whereas several other studies reported an additional decrease in complex IV, our data reveals no changes in complex IV as well as in complex V. Interestingly, Manczak et al. observed similar effects for these complexes. Complex I was downregulated, while complexes III and IV showed increased mRNA expression in early and definite AD brain specimens (Manczak et al., 2004). As we measured an overall reduction in the activity of the respiratory chain complexes and a depletion of ATP production, the unaltered gene expression of complex IV and V might be due to a compensatory mechanism. In other words, the mitochondrial encoded genes may be activated to compensate for the loss of energy.

Moreover, complex I is a major contributor to ROS production (Murphy, 2009). The downregulation of complex I might lead to an acceleration of ROS, which can be explained by a higher ratio of $NADH/NAD^+$ (Kussmaul and Hirst, 2006). The rise in this ratio can lead to oxidative damage of lipids, proteins and DNA, but also of complex I, which further increases the release of ROS, resulting in a vicious cycle.

Regarding the antioxidative defence system, SH-SY5Y-APP_{695} cells exhibit a significant lower GPx1 expression compared to control cells. GPx1 reduces free hydrogen peroxide to water, what makes it play a crucial role of inhibiting lipid peroxidation (Ighodaro and Akinloye, 2018).

The reduced expression of GPx1 provides a preliminary indication of a limited antioxidative capacity. To obtain a precise conclusion about the antioxidative system, the measurement of enzyme activities is also necessary. Wan et al. have already been able to show a significant reduced activity of CAT in APP_{695} transfected SH-SY5Y cells (Wan et al., 2012).

The impairment of complex I together with the reduced GPx1 is quite severe, as neural cells are considered to be more sensitive to oxidative damage compared to other body tissues (Uttara et al., 2009).

On the other hand, protein levels of complex I were only numerically, but not significantly down regulated. However, the decrease in complex I respiratory capacity is likely due to the decreased gene expression and reduced protein synthesis of complex I. Notably, mRNA analysis and determination of protein syntheses were measured each of two different subunits of complex I. However, protein levels of complex II and III were significantly reduced compared to control cells. According to our results, Lopez Sanchez et al. measured a significant decrease of protein synthesis of complexes I, II and III in SH-SY5Y-APP_{695} cells (Lopez Sanchez et al., 2017). In addition, Pedrós et al. found significant reduced protein levels of complex II and III in brain homogenates of the hippocampus of APPswe/PS1 mice (Pedrós et al., 2014).

Although complex V revealed no alterations in mRNA expression and protein synthesis, the impairment of the other complexes and the overall reduction of respiratory capacity emerges a significant lower ATP production in SH-SY5Y-APP_{695} cells.

The impaired energy metabolism seen in APP transfected cells may also suggest impaired mitochondrial biogenesis. PGC1-α is considered to be the master regulator of mitochondrial biogenesis and additionally regulates a wide variety of genes involved in energy metabolism by interactions with different transcription factors (NRFs and TFAM) (Ventura-Clapier et al., 2008). Through the interaction of PGC1-α with NRFs and TFAM, proteins such as subunits of complexes of the respiratory system and protein import are activated. A reduced expression of the transcription factor is therefore associated with an impaired functionality of the mitochondrion. The present data shows a numerically reduced gene expression of the entire PGC1-α signalling pathway, indicating a reduced mitochondrial biogenesis in SH-SY5Y-APP_{695} cells. This was also shown in AD hippocampal tissues and APPsw transfected cells (Sheng et al., 2012). In particular, CREB, SIRT1 and TFAM were numerically decreased, whereas NRF1 revealed no changes in mRNA expression compared to control cells.

As discussed in chapter 1.2.1, SIRT1 responds when cellular energy is low. Regarding the impaired respiratory capacity and decrease of ATP production, one would expect an activation of SIRT1. The instead measured down regulation of SIRT1 may arise from a lower activity of AMPK, which plays a key role in energy homeostasis. On the other hand, Julien et al. have shown a significant reduction of SIRT1 (mRNA and protein) in the cortex of AD patients, but not in patients with mild cognitive impairment (Julien et al., 2009). As far as one can compare both with each other these results match to our findings - as we have only seen a numerical and not significant reduction of SIRT1 mRNA level in SH-SY5Y-APP$_{695}$ cells, which represent a model of late-onset AD. Another study found reduced levels of SIRT1 expression in neuronal primary cells after insult with rotenone (Pallàs et al., 2008). As earlier described, rotenone inhibits complex I of the respiratory chain. The reduced SIRT1 expression can therefore occur because of the significant down regulation and decreased capacity of complex I.

CREB has a critical role in the formation of memory and therefore in the pathology of AD (Kandel, 2012). We observed reduced CREB1 mRNA expression, significant decreased protein level and decreased pCREB1 protein level in SH-SY5Y-APP$_{695}$ cells compared to SH-SY5Y-MOCK control cells. It has been shown from several groups, that CREB signalling is dysfunctional in brains of mouse models of AD (Gong et al., 2004; Bartolotti et al., 2016b). Moreover, CREB and its activated form pCREB were reduced in the prefrontal cortex and in blood cells of AD patients (Bartolotti et al., 2016a). Total and activated CREB were also reduced in post-mortem hippocampus of individuals with AD (Pugazhenthi et al., 2011). Same findings were as well observed in cultured neurons insulted with Aβ (Tong et al., 2004). Another study found in differentiated SH-SY5Y cells treated with oligomeric Aβ significantly reduced CREB mRNA expression as well as a decrease in the total, and activated form of CREB1 proteins. Furthermore, there was no alteration between pCREB relatively to total CREB1 levels (Rosa and Fahnestock, 2015). These findings are in accordance with our data, as we observed an unaltered ratio between pCREB and CREB1. That is why a reduced phosphorylation via the activation of protein kinase A (PKA) can thus be excluded. It has been shown that an inactivation of CREB1 in isolated neurons of mice results in a significant decrease in SIRT1 gene expression and protein synthesis, which underlines our results (Fusco et al., 2012). Besides (Larsen et al., 2012) the direct influence of CREB1 on SIRT1, CREB1 is also a transcriptional regulator of brain-derived neurotrophic factor (BDNF). BDNF, which plays an important role in learning and memory processes, is well known to be down regulated in AD (Allen et al., 2011; Budni et al., 2015; Ng et al., 2019). Rosa et al. propose a downregulation of BDNF

mediated by Aβ induced down regulation of CREB1 together with unchanged protein level of activated pCREB (Rosa and Fahnestock, 2015). Same findings were observed by Sheng et al. APP transfected M17 cells had unchanged CREB levels, whereas the active phosphorylated form of CREB was significantly reduced (Sheng et al., 2012). On the other hand, Oguchi et al. showed a reduced ratio of pCREB/CREB1 in Aβ treated SH-SY5Y cells (Oguchi et al., 2017). It needs to be noted, that there seems to be a difference between the use and preparation of oligomeric or fibrillary amyloid peptide exposure to cells as well as in the method of differentiation. This could be an explanation for the controversial results.

Examining gene expression of CS in SH-SY5Y-APP_{695} cells and SH-SY5Y-MOCK cells reveals no changes, neither on protein level. Rhein et al. measured CS activity in SH-SY5Y cells. In line with our results, there was no difference between APP transfected and control cells. CS activity is known to be a marker very closely correlated to mitochondrial content (Larsen et al., 2012). Thus, the detected reduced expression of genes involved in mitochondrial biogenesis does not appear to have an initial effect on mitochondrial mass in SH-SY5Y-APP_{695} cells. Another suitable marker for the determination of mitochondrial content is Mitotracker Green (MTG) fluorescence. Hauptmann et al. measured MTG in mitochondria from dissociated brain cells derived from Thy-1 APP mice resulting in unaltered mitochondrial mass, which supports our assumption (Hauptmann et al., 2009). On the other hand, we found significantly reduced protein synthesis of PGC-1α levels in SH-SY5Y-APP_{695} cells. Additionally, protein level of complexes II and III were significantly downregulated and complex I was numerically decreased. This reflects the overall impaired detected respiratory capacity in APP transfected cells.

The main entry side for precursor proteins is the TOM complex. It has been shown, that excess of oxidative stress leads to an inhibition of the import machinery in mitochondria (Wright et al., 2001a). Surprisingly, protein synthesis of the central receptor TOM22 was slightly elevated in SH-SY5Y-APP_{695} cells compared to control cells, which indicates a proper functioning of the import of proteins. Chai et al. reported also a tendency for increased synthesis of TOM22 in brain homogenates of AD patients (Chai et al., 2018). Additionally, it has been shown that APP forms stable complexes with TOM40 and TIM23 in AD brains, which led to an inhibition of the entry of nuclear-encoded proteins (Devi et al., 2006). Accordingly, the increased protein synthesis of TOM20 in SH-SY5Y-APP_{695} cells can be seen as a compensatory mechanism of the possibly restricted protein import mediated by APP. Furthermore, an increase of TOM22

can be accompanied by an higher import of Aβ, as this was shown by Hu et al. in isolated mitochondria from yeast (Hu et al., 2018). The increased import of Aβ may also be the cause of our results regarding the highly impaired mitochondrial function seen in SH-SY5Y-APP$_{695}$ cells.

Complex I-inhibition as a model for simulating ageing in SH-SY5Y cells

As described before, complex I is the largest of the five enzyme super complexes and performs the major first step of the OXPHOS pathway in the respiratory chain. The mitochondrial theory of ageing hypothesises a decreased functionality of the ETC (Sun et al., 2016). Many studies support the decreased functionality of the respiratory system, in particular an impairment of complex I (Ventura et al., 2002; Sandhu and Kaur, 2003; Petrosillo et al., 2009; Rygiel et al., 2014). The impairment of complex I is thought to be most severely affected since mitochondrial DNA encodes for its subunits rather than nuclear DNA. Mitochondrial DNA is more susceptible to oxidative stress as it is near the origin of ROS and is not protected by histones or other chromatin proteins. Additionally, mtDNA is independent of cellular division and thereby the replication rate is higher than for nuclear DNA, which leads to a more severe effect of mutations (Wang et al., 2019). Therefore, complex I is highly involved and associated with brain ageing.

To simulate this scenario *in vitro*, we insulted SH-SY5Y-MOCK and SH-SY5Y-APP$_{695}$ cells with rotenone. Besides its use as pesticide and insecticide, rotenone is a well-known inhibitor of complex I. To assess mitochondrial changes during simulated ageing *in vitro*, we measured MMP and ATP level in SH-SY5Y cells after insult with rotenone. Both parameters were significantly decreased in a dose dependent manner. Similar results were previously obtained in SH-SY5Y cells and HEK cells (Leuner et al., 2012; Stockburger et al., 2014b). Regarding ATP levels, APP transfected SH-SY5Y cells seem to need a higher rotenone concentration to reach a significant decrease in ATP production. Since the whole respiratory chain of SH-SY5Y-APP$_{695}$ cells is already affected, a specifically inhibition of complex I needs higher doses. Presumably, already impaired mitochondria try to compensate a further insult, whereas impaired mitochondria can no longer counteract an exposure of high or rather more toxic concentrations of rotenone, leading to the measured significant depletion of ATP.

In summary, SH-SY5Y-APP$_{695}$ cells seem to be a well suited model for the early stages of late-onset AD. Thus, in the following, it will be discussed to what extend highly purified olive polyphenols are able to counteract the Aβ-induced mitochondrial changes.

5.2 Secoiridoid derivatives and their effects on ATP synthesis

General improvement in lifestyle and medication has increased life expectancy in the past decades. However, the demographic change has led to an increased prevalence of AD. Upon now, the treatment of AD has remained symptomatic and no drug or treatment strategy has been approved (Polanco et al., 2018). Since the disease develops years before clinical symptoms occur, prevention is still the best strategy to fight the pathological conditions of AD (Grodzicki and Dziendzikowska, 2020). Therefore, food natural compounds have arisen as molecules with high preventive or therapeutic potential for AD (Amini et al., 2020). Populations along the Mediterranean Sea have a remarkable low prevalence of AD among others. The health promoting attributes rely in the daily consumption of EVOO, being the main dietary lipid source. Mainly, secoiridoids are the promising compounds present in EVOO or olives (Castejón et al., 2020). Therefore, we tested the effect of ten different highly purified olive phenolic secoiridoids and two plant metabolites in very low doses on their influence on ATP synthesis, firstly in SH-SY5Y-MOCK control cells and secondly in SH-SY5Y-APP_{695} cells, since mitochondria are one important target of Aβ toxicity. Additionally, we simulated artificial ageing by complex I inhibition.

5.2.1 Secoiridoid derivatives and their effects in SH-SY5Y-MOCK cells on ATP synthesis

To determine the most effective concentration on ATP production, we incubated SH-SY5Y-MOCK cells with the most simple olive phenolics hydroxytyrosol and tyrosol in different concentrations (0.5 to 50 µM). Between concentrations from 0.5 to 10 µM both, hydroxytyrosol and tyrosol elevated ATP levels significantly. Elevating the concentration to 50 µM, showed no effect for tyrosol, whereas the treatment with 50 µM hydroxytyrosol lead to a significant decrease of ATP level. Adverse effects of different polyphenols in high doses and protective effects in low doses have been previously reported. It has been shown, that flavonoids induce cytotoxicity, DNA strand breaks, DNA fragmentation and caspase activation at concentrations from 50 µM in rat hepatoma cells, whereas low concentrations were protective (Wätjen et al., 2005). Additionally, several *in vitro* and *in vivo* studies have demonstrated anticancer effects of hydroxytyrosol and other olive polyphenols (Fabiani et al., 2012; Parkinson and Cicerale, 2016; Rigacci and Stefani, 2016). Oleuropein for example lead to cell cycle arrest and induced

apoptosis in SH-SY5Y cells at a concentration of 350 µM (Seçme et al., 2016). Most likely tyrosol does not react cytotoxic because of its high stability. Hydroxytyrosol is easily oxidised to *o*-quinone. The electrophilic quinone is rather unstable and undergoes several reactions, which might lead to the seen impairment of energy production when using high concentrations of hydroxytyrosol. Tyrosol in contrast is not oxidised, even not under forcing conditions (Napolitano et al., 2010). However, the nature of the possible products formed during physiological conditions or in cell culture has been very poorly investigated.

The remaining substances were tested in a concentration range between 0.05 up to 10 µM. Apart from ligstroside aglycone and oleuroside aglycone, all substances showed with the exception of oleuroside already in the smallest concentration of 0.05 µM a significant elevation of ATP level. The highest effect, with an increase of 15% compared to solvent control was achieved when SH-SY5Y-MOCK cells were treated with ligstroside at a concentration of 1 µM. It has been shown that polyphenols like resveratrol, quercetin, curcumin, rice bran and many others induce similar effects on ATP level (Eckert et al., 2013; Hagl et al., 2015a; Sharma et al., 2015; Douiev et al., 2016). Notably, the seen positive effects were observed in very low *in vitro* concentrations. This is very unusual compared to common used concentrations in the literature. Nevertheless, there is no data available for ligstroside or rather purified secoiridoid derivatives and their influence on ATP level.

Complex I inhibition with rotenone lead to an approximately drop of ATP level to 65%. Protective effects in the smallest concentration were only detected for ligstroside, ligustaloside B, oleocanthal, oleuropein and oleuroside. The remaining substances were able to significantly elevate insulted ATP level at 0.1 µM. Generally, polyphenols are known to act as antioxidants. For the scavenging potential of polyphenols towards ROS are two main antioxidation mechanisms proposed (Wright et al., 2001b), which will be discussed in the next chapter.

5.2.2 Secoiridoid derivatives and their effects in SH-SY5Y-APP$_{695}$ cells on ATP synthesis

All investigated olive secoiridoids, except the two tested aglycones, ligstroside aglycone and oleuroside aglycone, significantly increased cellular ATP levels in SH-SY5Y-APP$_{695}$ cells. The lowest tested concentration of 0.05 µM elevated ATP levels approximately between 7 to 11%,

whereas tyrosol and ligustaloside B had the smallest effect, below 7% increase of ATP level. Since a decline of the mitochondrial bioenergetics system is a hallmark of both, AD and brain ageing these findings may reveal a positive influence of olive secoiridoids on the cellular energy metabolism and probably in the prevention of mitochondrial dysfunction. Complex I inhibition with 25 µM rotenone lead to an approximately decrease of 50% of ATP levels. Ligstroside, ligustaloside B, oleuropein, oleuroside, tyrosol and homovanillic acid could significantly elevate insulted ATP level. Hydroxytyrosol had by far the highest protective effect and significantly increased ATP level even in the low concentration of 0.05 µM. Interestingly, there was no protective effect after incubation with elenolic acid, oleacein or oleocanthal. The incubation with 10 µM oleacein or oleocanthal led even to a further significant decrease of ATP level after rotenone insult. The high antioxidative capacity of hydroxytyrosol is well known. Omar et al. investigated the effects from different commercial olive extracts containing mainly oleuropein and hydroxytyrosol, on their potential to scavenge superoxide radicals and hydrogen peroxide in SH-SY5Y cells. The highest protection regarding the olive phenolic compounds was as well observed by hydroxytyrosol (Omar et al., 2017). The mechanism of free radical scavenging by hydroxytyrosol is attributed to the presence of the *o*-dihydroxyphenyl moiety. Through the hydrogen-atom transfer, the phenol functional group donates a hydrogen atom to a free radical. In this way, the phenolic antioxidant itself becomes a free radical. The resulting free phenoxy radical does not react any further, because of its stability due to the intramolecular hydrogen bond. Overall, catecholic species like hydroxytyrosol act very well as H-atom donors, mainly because they are extra stabilized through hydrogen-bonding with the adjacent hydroxy group (Leopoldini et al., 2004). Furthermore, Leopoldini et al. performed density functional theory calculations to evaluate the antioxidant activity for different phenolic compounds present in the Mediterranean diet. Hydroxytyrosol was one of the most active systems to be able to transfer H-atoms (Leopoldini et al., 2004).

Compounds which are not able to stabilize radicals by intramolecular hydrogen-bonding, but exhibit instead an enhanced electronic delocalization are considered to act as antioxidants by transferring an electron to free radicals. Considering oleacein and oleocanthal that differ in the number of their hydroxy moiety show no protective or rather antioxidant property. Both secoiridoids harbour in contrast to the remaining compounds, two aldehydic groups (see Figure 1.9). The aldehyde moiety is a conjugated electron-withdrawing group and additionally, there is no possibility of allowing resonance effects. This might explain the lack of antioxidative capability. This applies also to elenolic acid.

A comparison between both cell lines reveals similar effects of the tested substances on ATP production, even though the ATP increase in SH-SY5Y-MOCK cells was slightly higher. The more effective antioxidant capacity seen in SH-SY5Y-MOCK cells compared to SH-SY5Y-APP_{695} cells might be due to the intact antioxidative defence system in healthy control cells. As discussed in chapter 5.1, SH-SY5Y-APP_{695} cells show an impaired activity of respiratory chain complexes, decreased mRNA expression of complex I and of the antioxidative enzyme GPx1. These impairments lead, most probably to an excess of ROS formation. In this case, an overproduction of ROS accompanied by a deficiency of enzymatic antioxidants seems to be too high to be counteracted by the substances.

However, regarding the basal effects on ATP level in SH-SY5Y-APP_{695} cells, oleacein, oleocanthal, oleuroside and ligstroside had a slightly higher effect on elevating basal ATP levels. For this reason, following determination of respiratory capacity was performed exclusively for these four hit substances.

5.3 Influence of oleacein, oleocanthal, oleuroside and ligstroside on mitochondrial respiratory capacity

To evaluate if the identified four hit substances are able to compensate the global defect of the mitochondrial respiratory capacity in SH-SY5Y-APP_{695} cells, we measured the activities of the respiratory system complexes after 24 h incubation with the respective four compounds. In accordance with the results of ATP production in SH-$SY5Y_{695}$ cells, ligstroside and oleocanthal incubation led to a significant improvement of mitochondrial respiration, whereas oleuroside and oleacein showed no changes in oxygen consumption, despite measuring an increase in ATP levels. This finding may indicate a shift of metabolism towards upregulated glycolytic ATP production to compensate for declining mitochondrial respiration and OXPHOS energy production. The conversion of energy production from OXPHOS to glycolysis was previously reported in late-onset AD fibroblasts and hippocampal neurons from 3xTg-AD mice (Sonntag et al.; Yao et al., 2009). However, hydroxytyrosol, a well-studied olive polyphenol, improved complex I, II, III and IV activity in adipocytes (Hao et al., 2010). Furthermore, Martins et al. determined oxygen consumption of a mitochondrial suspension with olive mill waste water, which led to an increase of complex IV respiration (Martins et al., 2008) and increase of the mitochondrial membrane potential in dissociated brain cells (Schaffer et al., 2007). In a

previous study, we assessed mitochondrial respiratory activity in isolated brain mitochondria from aged NMRI mice, long-term treated with a purified secoiridoid-rich extract. The mixture contained oleuropein aglycone, hydroxytyrosol, oleacein, elenolic acid, oleuropein and oleuroside. The activity of respiratory chain complexes was unaffected (Reutzel et al., 2018), which matches our observed results in SH-SY5Y-APP$_{695}$ cells treated with oleuroside or oleacein.

Based on the observed positive results on OXPHOS after oleocanthal and ligstroside incubation, it is reasonable to assume that an enhanced mitochondrial mass is the cause of the obtained results. This thesis was confirmed, since oleocanthal and ligstroside significantly increased citrate synthase activity which is a well described marker for mitochondrial content (Larsen et al., 2012), whereas oleuroside and oleacein had no effect on this Krebs cycle enzyme. There are hardly no data available regarding the effects of olive polyphenols on citrate synthase activity in neuronal cells. However, olive oil fed rats did not show any effects on mitochondrial mass in muscle homogenates (Bronnikov et al., 2015), which is consistent with our results of oleacein and oleuroside. Nevertheless, incubation with ligstroside and oleocanthal led to a significant increase of CS in SH-SY5Y-APP$_{695}$ cells. This could be an indication of a beneficial effect on mitochondrial biogenesis, which is known to be impaired in both, ageing and AD (Sheng et al., 2012; Golpich et al., 2017; Srivastava, 2017).

Respiration normalized for CS gives an indication of the respiratory capacity for a single mitochondrion. As expected, there was no alteration in complex activities by oleuroside or oleacein incubation. Normalization for CS activity in oleocanthal treated cells revealed an increased endogenous respiration, whereas ligstroside treatment had the highest influence on respiratory chain complexes. Endogenous, complex I, uncoupled complex I+II respiration and ETS capacity were significantly increased. The state of endogenous respiration reflects the physiological state of the cell as the cells are not yet permeabilized and respire using their own endogenous substrates (Gnaiger, 2012). It seems that the functionality of the single mitochondrion increased, following oleocanthal and especially ligstroside incubation, indicating that each mitochondrion has higher activities of respiratory system complexes leading to elevated ATP production.

Regarding mitochondrial function in the impaired system of SH-SY5Y-APP$_{695}$ cells, oleocanthal and ligstroside are the most promising secoiridoid derivatives. Taken together both substances elevated ATP levels, elevated cell-count normalized mitochondrial respiration,

elevated CS activity and elevated CS normalized respiration, which assumes an increase of functionality of a single mitochondrion. Therefore, we determined underlying molecular mechanisms for these two lead substances, which will be discussed in the following chapters.

5.4 Influence of oleocanthal and ligstroside on mRNA expression in SH-SY5Y-MOCK cells

PGC-1α is an important key transcription factor of mitochondrial biogenesis that is activated by deacetylation by SIRT1 or phosphorylation via AMPK. PGC-1α itself activates NRF1 and TFAM which induces mitochondrial biogenesis (Cantó and Auwerx, 2009; Fernandez-Marcos and Auwerx, 2011). Oleocanthal significantly increased the expression of the PGC-1α activator SIRT1. Furthermore, NRF1 was significantly elevated by oleocanthal. Ligstroside also positively intervened in the PGC-1α pathway. SIRT1 was significantly enhanced by incubation with ligstroside. Moreover, the mRNA expression of CREB1, PGC-1α, NRF1 and TFAM were all significantly increased by ligstroside compared to solvent control. Additionally, protein level of CREB1, pCREB, PGC-1α and TFAM tended to be upregulated by ligstroside treatment. The obtained positive influences suggest an increase of mitochondrial biogenesis in healthy cells. Generally, several polyphenols activate SIRT1, as reported in many studies and summarized by Ayissi et al. (Ayissi et al., 2014). Menendez et al. demonstrated an upregulation of SIRT1, AMPK and NRF2 protein synthesis by EVOO enriched with secoiridoids in immortalised breast cancer cells (Menendez et al., 2013). Additionally, hydroxytyrosol increased the expression of SIRT1 in human chondrocytes (D'Adamo et al., 2017). Another study from Kikusato et al. underlined our results. Hereby, the study has shown an induction of mitochondrial biogenesis by oleuropein in avian muscle cells. According to our study, SIRT1, PGC-1α, NRF1 and TFAM were significantly increased (Kikusato et al., 2016a). Another study has shown the positive influence of tyrosol and oleuropein on oxidative damage in HepG2 cells, by upregulating the gene expression of SIRT1 (Stiuso et al., 2016). However, there are no data available regarding ligstroside and its influence on mitochondrial parameters. Our data suggests that the ester and sugar moiety are important for interfering in the mitochondrial biogenesis pathway, as ligstroside has shown a much higher influence than oleocanthal with its two aldehydic groups.

We further considered the gene expression of selected complexes of the respiratory system. Both secoiridoids, oleocanthal and ligstroside showed significant positive effects on the gene expression of complex I. On the other hand, ligstroside treatment led to a significant reduction of complex V expression. We speculate that the impairment of complex V may be attributed to a compensatory mechanism, as complex I was significantly increased and complex I is the main entry point for electrons and is therefore suggested to be a rate-limiting step in the whole respiratory system (Sharma et al., 2009). However, ligstroside was able to significantly increase mRNA expression of complex IV compared to solvent control. As previously described, a reduced activity of complex I and IV in particular is associated with mitochondrial dysfunction. Additionally, ROS is considered to be mainly generated by complex I and complex III. Therefore, maintaining the functionality of these two complexes plays an important role in the prevention and therapy of AD. Hao et al. have shown an increase in activity and protein expression of respiratory complexes I, II, III and V after hydroxytyrosol treatment in adipocytes (Hao et al., 2010). Additionally, hydroxytyrosol administration led to elevated expression levels of complexes I, II and IV in the brain of db/db mice (Zheng et al., 2015).

Interestingly, ligstroside treatment revealed a downregulation of CS gene expression. Anyhow, protein level of CS did not show any alterations. This disparity is not surprising as gene expression level in a cell is determined by the stability of mRNA and by post-translational events (Macdonald, 2001).

Regarding the antioxidative system, oleocanthal and ligstroside increased the gene expression of SOD2, whereas the expression of GPx1 was only significantly elevated by ligstroside. However, oleocanthal and ligstroside seem to increase the antioxidative capacity in SH-SY5Y-MOCK cells. This is supported by a study of tyrosol by Dewapriya et al. Briefly, the treatment with tyrosol in murine neuronal brain cells lead to an upregulation of SOD1 and SOD2 (Dewapriya et al., 2013). Additionally, Kouka et al. investigated the influence of an olive oil rich in polyphenols in rats. The detected mRNA and protein levels of SOD1 were significantly increased in the brain, whereas CAT levels revealed no changes (Kouka et al., 2020). This is also in accordance with our results, as we did not detect any changes in CAT levels after treatment with ligstroside. A study by Rosignoli et al. examined if hydroxytyrosol has an influence on CAT. Human monocytes from healthy donors were exposed to hydroxytyrosol with and without CAT. Neither in the presence nor in the absence of CAT, the amount of H_2O_2 changed, suggesting that hydroxytyrosol has no influence on the H_2O_2 scavenging enzyme CAT

(Rosignoli et al., 2013), which is again in accordance with our results. Independent of the structure of the different olive polyphenol derivatives it seems, that they have a positive effect on antioxidant mechanisms, briefly on the expression of the enzymes SOD2 and GPx1. SOD, a first line defence antioxidants and the most powerful antioxidant in the cell, catalyses the dismutation of O_2^- and generates H_2O_2 (Fridovich, 1995). CAT catalyses the degradation or reduction of H_2O_2 to water and molecular oxygen. GPx also breaks down H_2O_2 to water. Our results indicate that ligstroside and oleocanthal have each a different effect on GPx1 and CAT. CAT reacts efficiently with hydrogen donors (Ighodaro and Akinloye, 2018), what might explain the observed results for the two structural different substances ligstroside and oleocanthal.

5.5 Influence of oleocanthal and ligstroside on mRNA expression in SH-SY5Y-APP$_{695}$ cells

In SH-SY5Y-APP$_{695}$ cells, genes of the mitochondrial biogenesis pathway tend to be downregulated compared to control cells. In order to determine the molecular mechanism of the two lead substances, mRNA expression was also determined in SH-SY5Y-APP$_{695}$ cells after 24 h incubation with oleocanthal and ligstroside. Concerning the influence on genes of mitochondrial biogenesis, only ligstroside could be considered as a potential candidate to induce mitochondrial replication via the PGC-1α cascade, due to the significant upregulation of SIRT1, CREB1 and numerical increase of TFAM and NRF1. Previously, our group reported no influence on mRNA expression in mice, which received a mixture of purified olive polyphenols (oleuropein aglycone, hydroxytyrosol, oleacein, elenolic acid derivatives, oleuropein and oleuroside) for 6 months (Reutzel et al., 2018). On the other hand, it has been shown, that mice receiving hydroxytyrosol (10 or 50 mg/kg per day) for 8 weeks, led to an improvement of protein expression of SIRT1 and PGC-1α in brain tissue (Zheng et al., 2015). Other polyphenols like resveratrol, quercetin and curcumin have been reported as potential activators of mitochondrial biogenesis (Diaz-Gerevini et al., 2016; Calabriso et al., 2018; Qiu et al., 2018). In muscle cells, oleuropein showed a significant increase of mRNA levels of TFAM and NRF1 (Kikusato et al., 2016b). Nevertheless, the influence of olive polyphenols on mitochondrial mRNA expression is barely investigated.

Previous studies have already shown direct and indirect mechanisms of antioxidative properties of olive polyphenols. Visioli et al. presented the direct binding and elimination of ROS by hydroxytyrosol and oleuropein in human neutrophils (Visioli et al., 1998). Omar et al. showed an increase in H_2O_2 treated SH-SY5Y cells for the imitation of oxidative stress (Omar et al., 2017). Oleuropein and hydroxytyrosol were able to increase the cell viability compared to non-incubated cells. Our experiments showed an elevation of GPx1 mRNA expression after ligstroside incubation, whereas the antioxidative enzymes CAT and SOD2 were downregulated by ligstroside and oleocanthal. The influence of olive polyphenols on the antioxidant system was also observed *in vivo*. Brain tissue of 6 weeks oleocanthal-rich EVOO treated SAMP8 mice showed a significant increase of GSH as well as a significantly increased SOD activity (Farr et al., 2012). Therefore, further investigations regarding the influence of purified secoiridoids on the antioxidative defence system should include the measurement of enzyme activities.

5.6 Influence of ligstroside on protein levels in SH-SY5Y-APP$_{695}$ cells

Regarding the protein amount of CREB1, we measured no changes after treatment with ligstroside. Even though there was a tendency for increased phosphorylation, which was observed by an increased amount of pCREB. The increased pCREB/CREB1 ratio suggests an increased activation of CREB1 by PKA. Impellizzeri et al. have shown the positive influence of oleuropein aglycone on the activity and synthesis of PKA. Therefore, the quantification of protein levels of PKA after ligstroside treatment will be useful in the future.

Despite the significantly increased complex I mRNA expression, the corresponding protein was synthesized significantly less after the treatment with ligstroside. However, it should be noted that the gene expression was considered to subunit NDUFV1, whereas the protein synthesis of subunit NDUFB8 was quantified. This might explain the ambivalent effects of ligstroside on gene and protein level. Complex I is composed of 45 subunits, including NDUFV1 as a core subunit and NDUFB8 on the other hand represents a secondary subunit (Stroud et al., 2016). Since ligstroside could significantly increase the gene expression of the main subunit, the analysis of protein synthesis of NDUFV1 is also of interest. Additionally, protein synthesis of complexes II, III and IV tend to be downregulated.

Furthermore, the different influences of ligstroside on gene expression and protein synthesis can be explained by the fact that only about 40% of the variance in protein content is expressed by altered gene expression (Schwanhäusser et al., 2011). Thus, an increased transcription does not automatically indicate an equally increased translation. Since ligstroside, with the exception of pCREB protein levels, had no or negative effect on the synthesis of the investigated proteins in SH-SY5Y-APP$_{695}$ cells, it is assumed that ligstroside is involved in posttranscriptional or posttranslational modifications. A large part of the variance in protein content can be attributed to post-transcriptional modifications of mRNA, translational regulation and protein degradation (Vogel and Marcotte, 2012).

However, there is also the consideration of a protective effect of ligstroside by downregulating the respiratory chain complexes. A reduced activity of ETS simultaneously reduces the production of ROS, which are mainly produced by complexes I and III. Lopez Sanchez et al. already established this thesis for untreated SY5Y-APP cells (Lopez Sanchez et al., 2017).

5.7 Influence of oleocanthal and ligstroside on Aβ$_{1-40}$ levels in SH-SY5Y-APP$_{695}$ cells

Previous studies described oleocanthal as a potential candidate to clear Aβ levels in mice brain and reduce Aβ levels in SH-SY5Y-APP cells (Abuznait et al., 2013; Qosa et al., 2015; Batarseh et al., 2017). According to the literature, we also found significantly enhanced Aβ$_{1-40}$ clearance compared to solvent control. Furthermore, there are additional previous studies, which have shown the ability of oleocanthal to attenuate Aβ *in vitro* and enhance Aβ clearance in the brains of mice. Pang and Chin et al. and Bartaseh et al. have shown that oleocanthal reduced Aβ in neurons and decreased the inflammation of astrocytes (Batarseh et al., 2017; Pang and Chin, 2018). In another study, oleocanthal enhanced Aβ clearance in mouse brain via upregulation of two major Aβ transport proteins, P-glycoprotein and LDL lipoprotein receptor related protein-1 (LRP1) at the blood brain barrier (BBB) (Abuznait et al., 2013). Same results and mechanisms were obtained in a study from Qosa et al., where oleocanthal significantly reduced Aβ load in a mouse model of AD and *in vitro* in a BBB model (Qosa et al., 2015). Another study investigated the effect of the acetylcholine esterase inhibitor, donepezil together with EVOO rich in oleocanthal in a mouse model of AD. The results showed that the combination led to significantly reduced Aβ levels (Batarseh and Kaddoumi, 2018). Grossi et al. observed as well a reduction of Aβ deposition in N2a neuroblastoma cells and transgenic AD mice by suggesting

the positive obtained data results from an induction of autophagy activation by oleuropein aglycone proceeded through mTOR inhibition (Grossi et al., 2013). Another pathway of olive polyphenols to interfere in Aβ aggregation was shown by Kostomoiri et al. The treatment of APP_{695} transfected HEK293 cells with oleuropein led to elevated levels of soluble sAPPα and to a significant reduction of Aβ oligomers. The underlying mechanism was proposed to be associated with oleuropein promoting the non-amyloidogenic pathway, by favouring α-secretase cleavage of APP (Kostomoiri et al., 2013). Regarding the mechanism of the clearance of Aβ by oleuropein, NMR analyses have shown an interaction between oleuropein and $Aβ_{40}$, modifying its aggregation. The study suggests a noncovalent interaction between $Aβ_{40}$ and oleuropein with interactions of the protons of the methyl group, protons of the ester group and protons of the aromatic ring playing the major role of chemical shift alterations (Galanakis et al., 2011). Oleuropein and ligstroside differ only in their number of the hydroxy moieties. Therefore, the suggested mechanism is in contradiction to our findings, since ligstroside did not affect $Aβ_{1-40}$ levels. The beneficial effect of ligstroside on mitochondrial function might be independent of the Aβ-pathway. These findings additionally flaw the Aβ-hypothesis and focus on new mechanisms (Kuehn, 2020).

6 Conclusion

In the present study, a cell model for the sporadic form of AD was established. Therefore, we determined mitochondrial parameters and underlying molecular mechanisms in the neuroblastoma cell line SH-SY5Y cells. We found that APP transfected SH-SY5Y cells exhibit very low levels of $A\beta_{1-40}$, briefly $A\beta_{1-40}$ concentrations came out in the picomolar range. A comparison between control SH-SY5Y-MOCK and SH-SY5Y-APP_{695} cells revealed differences in their mitochondrial function. In particular, ATP levels and MMP were severely impaired in APP transfected cells. Additionally, respiratory capacity was distinctly impaired showing a reduction throughout all respiratory complexes and an additional impaired mitochondrial coupling in SH-SY5Y-APP_{695} cells. Gene expression analyses and quantification of protein levels underlined the observed results. Especially, genes and proteins of mitochondrial biogenesis and antioxidative capacity revealed significant deficits. The overall detected reduced functionality of mitochondrial parameters together with slightly elevated Aβ production suggest SH-SY5Y-APP_{695} cells as an appropriate model for the late-onset form of AD.

Furthermore, we investigated the influence of ten different purified olive secoiridoids and two metabolites on mitochondrial function in the established neuronal cell model of late-onset AD. The screening of these compounds led to the identification of four hit substances, in particular, oleuroside, oleacein, oleocanthal and ligstroside showing the highest increase of ATP production. Determination of mitochondrial respiration and citrate synthase activity was carried out after incubation with these four compounds. Only oleocanthal and ligstroside enhanced the capacity of respiratory chain complexes. To elaborate the underlying molecular mechanisms, we determined the expression of genes associated with mitochondrial biogenesis, respiration and antioxidative capacity after oleocanthal and ligstroside treatment. Exclusively ligstroside improved mRNA expression in APP transfected SH-SY5Y cells. Additionally, quantification of protein levels were determined after ligstroside treatment. Determination of $A\beta_{1-40}$ levels revealed that oleocanthal, but not ligstroside decreased $A\beta_{1-40}$ production in SH-SY5Y-APP_{695} cells.

Although our study does not provide a causative mechanism on how secoiridoid derivatives interact in detail, the current results identified different effects on mitochondrial dysfunction and energy metabolism of the individual compounds present in EVOO. Specifically, ligstroside

showed the highest potential to combat mitochondrial dysfunction in a cellular model of late-onset AD by mechanisms that may not interfere with Aβ production.

7 Summary

In the past decades life expectancy has increased substantially which is accompanied with an increase in diseases such as the neurodegenerative disorder Alzheimer disease (AD). AD is a multifactorial disease with a complex pathobiology marked by declines in memory and thinking which is associated with a high social and economic burden. Today, over 47 million people suffer from the most common form of dementia. The prevalence of AD is expected to triple by 2050. Although the disease has been described over a century ago, there is no cure yet. Since 2003, there have been no new drugs approved and a high rate of failure in AD drug development is present until today. Over 25 years, amyloid-beta is the primary target in most clinical trials. The lack of success in AD drug development is amongst others explained by intervening at a state where the disease progression is too advanced. Additionally, many cell and animal models mimic the familial form of AD. This form of AD represents only a small number of patients, whereas the late-onset AD, with over 90% is more common. Therefore, we established a cell model for the late-onset AD, using SH-SY5Y-APP_{695} neuronal cells stably expressing the human APP_{695} isoform. We observed $A\beta_{1\text{-}40}$ expression in a picomolar range, which is representative for the sporadic form of AD. Since mitochondrial dysfunction is involved in both, brain ageing and early states of AD, we investigated mitochondrial parameters in APP_{695} transfected cells. Mitochondrial membrane potential (MMP), adenosine triphosphate (ATP) levels as well as the capacity of mitochondrial respiration were significantly decreased. Furthermore, genes of mitochondrial biogenesis and genes of the antioxidative defence system were significant lower expressed. Quantitative analyses of mitochondrial proteins were additionally impaired.

As components of the Mediterranean diet (MedDiet), olive polyphenols may play a crucial role for the prevention of AD. Therefore, we investigated in the second part of the present work, effects of 10 different highly purified phenolic secoiridoids (hydroxytyrosol, tyrosol, oleacein, oleuroside, oleuroside aglycone, oleuropein, oleocanthal, ligstroside, ligstroside aglycone and ligustaloside B) and two metabolites (the plant metabolite elenolic acid and the mammalian metabolite homovanillic acid) in very low doses on mitochondrial function in SH-SY5Y-APP_{695} cells. All tested secoiridoids significantly increased basal ATP levels in the present cell model. Oleacein, oleuroside, oleocanthal and ligstroside showed the highest effect on ATP levels and were additionally tested on mitochondrial respiration. Only oleocanthal and ligstroside were

able to significantly enhance the capacity of respiratory chain complexes. To investigate their underlying molecular mechanisms, the expression of genes associated with mitochondrial biogenesis, respiration and antioxidative capacity (PGC-1α, SIRT1, CREB1, NRF1, TFAM, complex I, IV and V, GPx1, SOD2, CAT) were determined using qRT-PCR. Exclusively ligstroside increased mRNA expression of SIRT1, CREB1, complex I, and GPx1 in SH-SY5Y-APP_{695} cells. Furthermore, oleocanthal but not ligstroside decreased $A\beta_{1–40}$ levels in SH-SY5Y-APP_{695} cells. Our findings indicate that purified ligstroside has outstanding performance on mitochondrial bioenergetics in a cell model of late-onset AD by mechanisms that may not interfere with Aβ production.

8 Bibliography

Abuznait, A.H., Qosa, H., Busnena, B.A., El Sayed, K.A., and Kaddoumi, A. (2013). Olive-oil-derived oleocanthal enhances β-amyloid clearance as a potential neuroprotective mechanism against Alzheimer's disease: in vitro and in vivo studies. ACS chemical neuroscience *4*, 973-982.

Allen, D.D., Caviedes, R., Cárdenas, A.M., Shimahara, T., Segura-Aguilar, J., and Caviedes, P.A. (2005). Cell lines as in vitro models for drug screening and toxicity studies. Drug development and industrial pharmacy *31*, 757-768.

Allen, S.J., Watson, J.J., and Dawbarn, D. (2011). The neurotrophins and their role in Alzheimer's disease. Current neuropharmacology *9*, 559-573.

Alois Alzheimer (1906). Alzheimer A. Über einen eigenartigen schweren Erkrankungsprozeßder Hirnrinde.;:1129–3. Neurologisches Centralblatt, 1129–3.

Alonso-Salces, R.M., Héberger, K., Holland, M.V., Moreno-Rojas, J.M., Mariani, C., Bellan, G., Reniero, F., and Guillou, C. (2010). Multivariate analysis of NMR fingerprint of the unsaponifiable fraction of virgin olive oils for authentication purposes. Food chemistry *118*, 956-965.

Alzheimer´s Association (2020). 2020 Alzheimer's disease facts and figures. Alzheimer's & dementia : the journal of the Alzheimer's Association.

Amini, Y., Saif, N., Greer, C., Hristov, H., and Isaacson, R. (2020). The Role of Nutrition in Individualized Alzheimer's Risk Reduction. Current nutrition reports *9*, 55-63.

Andjelkovic, M., VANCAMP, J., DEMEULENAER, B., DEPAEMELAERE, G., SOCACIU, C., VERLOO, M., and VERHE, R. (2006). Iron-chelation properties of phenolic acids bearing catechol and galloyl groups. Food chemistry *98*, 23-31.

Andrieu, S., Guyonnet, S., Coley, N., Cantet, C., Bonnefoy, M., Bordes, S., Bories, L., Cufi, M.-N., Dantoine, T., and Dartigues, J.-F., et al. (2017). Effect of long-term omega 3 polyunsaturated fatty acid supplementation with or without multidomain intervention

on cognitive function in elderly adults with memory complaints (MAPT): a randomised, placebo-controlled trial. The Lancet Neurology *16*, 377-389.

Anoop, A., Singh, P.K., Jacob, R.S., and Maji, S.K. (2010). CSF Biomarkers for Alzheimer's Disease Diagnosis. International journal of Alzheimer's disease *2010*.

Ansari, M.A., and Scheff, S.W. (2010). Oxidative stress in the progression of Alzheimer disease in the frontal cortex. J Neuropathol Exp Neurol *69*, 155-167.

Aridi, Y.S., Walker, J.L., and Wright, O.R.L. (2017). The Association between the Mediterranean Dietary Pattern and Cognitive Health. A Systematic Review. Nutrients *9*.

Ayissi, V.B.O., Ebrahimi, A., and Schluesenner, H. (2014). Epigenetic effects of natural polyphenols: a focus on SIRT1-mediated mechanisms. Molecular nutrition & food research *58*, 22-32.

B. Alberts (2015). B. Alberts, A. Johnson, J. Lewis, P. Walter, M. Raff, and Molecular Biology of the Cell. International Student Edition (Routledge: Taylor & Francis).

Baloyannis, S.J., Costa, V., and Michmizos, D. (2004). Mitochondrial alterations in Alzheimer's disease. American journal of Alzheimer's disease and other dementias *19*, 89-93.

Banik, A., Brown, R.E., Bamburg, J., Lahiri, D.K., Khurana, D., Friedland, R.P., Chen, W., Ding, Y., Mudher, A., and Padjen, A.L., et al. (2015). Translation of Pre-Clinical Studies into Successful Clinical Trials for Alzheimer's Disease: What are the Roadblocks and How Can They Be Overcome? JAD *47*, 815-843.

Barnes, D.E., and Yaffe, K. (2011). The projected effect of risk factor reduction on Alzheimer's disease prevalence. The Lancet Neurology *10*, 819-828.

Bartolotti, N., Bennett, D.A., and Lazarov, O. (2016a). Reduced pCREB in Alzheimer's disease prefrontal cortex is reflected in peripheral blood mononuclear cells. Molecular psychiatry *21*, 1158-1166.

Bartolotti, N., Segura, L., and Lazarov, O. (2016b). Diminished CRE-Induced Plasticity is Linked to Memory Deficits in Familial Alzheimer's Disease Mice. JAD *50*, 477-489.

Batarseh, Y.S., and Kaddoumi, A. (2018). Oleocanthal-rich extra-virgin olive oil enhances donepezil effect by reducing amyloid-β load and related toxicity in a mouse model of Alzheimer's disease. The Journal of nutritional biochemistry *55*, 113-123.

Batarseh, Y.S., Mohamed, L.A., Al Rihani, S.B., Mousa, Y.M., Siddique, A.B., El Sayed, K.A., and Kaddoumi, A. (2017). Oleocanthal ameliorates amyloid-β oligomers' toxicity on astrocytes and neuronal cells: In vitro studies. Neuroscience *352*, 204-215.

Baumgart, M., Snyder, H.M., Carrillo, M.C., Fazio, S., Kim, H., and Johns, H. (2015). Summary of the evidence on modifiable risk factors for cognitive decline and dementia. A population-based perspective. Alzheimer's & dementia : the journal of the Alzheimer's Association *11*, 718-726.

Beck, S.J., Guo, L., Phensy, A., Tian, J., Wang, L., Tandon, N., Gauba, E., Lu, L., Pascual, J.M., and Kroener, S., et al. (2016). Deregulation of mitochondrial F1FO-ATP synthase via OSCP in Alzheimer's disease. Nature communications *7*, 11483.

Bennett, D.A., Schneider, J.A., Arvanitakis, Z., Kelly, J.F., Aggarwal, N.T., Shah, R.C., and Wilson, R.S. (2006). Neuropathology of older persons without cognitive impairment from two community-based studies. Neurology *66*, 1837-1844.

Berendsen, A.A.M., Kang, J.H., van de Rest, O., Feskens, E.J.M., Groot, L.C.P.G.M. de, and Grodstein, F. (2017). The Dietary Approaches to Stop Hypertension Diet, Cognitive Function, and Cognitive Decline in American Older Women. Journal of the American Medical Directors Association *18*, 427-432.

Bertram, L., and Tanzi, R.E. (2008). Thirty years of Alzheimer's disease genetics: the implications of systematic meta-analyses. Nature reviews. Neuroscience *9*, 768-778.

Bhatti, J.S., Bhatti, G.K., and Reddy, P.H. (2017). Mitochondrial dysfunction and oxidative stress in metabolic disorders - A step towards mitochondria based therapeutic strategies. Biochimica et biophysica acta. Molecular basis of disease *1863*, 1066-1077.

Biedler, J.L., Roffler-Tarlov, S., Schachner, M., and Freedman, L.S. (1978). Multiple neurotransmitter synthesis by human neuroblastoma cell lines and clones. Cancer research *38*, 3751-3757.

Bousquet, J., and Meunier, J.M. (1962). Organotypic culture, on natural and artificial media, of fragments of the adult rat hypophysis. Comptes rendus des seances de la Societe de biologie et de ses filiales *156*, 65-67.

Bronnikov, G.E., Kulagina, T.P., Aripovskii, A.V., and Kramarova, L.I. (2015). Correction of Mitochondrial Enzyme Activities in the Skeletal Muscles of Old Rats in Response to Addition of Olive Oil to the Ration. Bulletin of experimental biology and medicine *159*, 266-268.

Brooks, W.M., Lynch, P.J., Ingle, C.C., Hatton, A., Emson, P.C., Faull, R.L.M., and Starkey, M.P. (2007). Gene expression profiles of metabolic enzyme transcripts in Alzheimer's disease. Brain research *1127*, 127-135.

Bubber, P., Haroutunian, V., Fisch, G., Blass, J.P., and Gibson, G.E. (2005). Mitochondrial abnormalities in Alzheimer brain. Mechanistic implications. Annals of neurology *57*, 695-703.

Budni, J., Bellettini-Santos, T., Mina, F., Garcez, M.L., and Zugno, A.I. (2015). The involvement of BDNF, NGF and GDNF in aging and Alzheimer's disease. Aging and disease *6*, 331-341.

Calabriso, N., Gnoni, A., Stanca, E., Cavallo, A., Damiano, F., Siculella, L., and Carluccio, M.A. (2018). Hydroxytyrosol Ameliorates Endothelial Function under Inflammatory Conditions by Preventing Mitochondrial Dysfunction. Oxidative medicine and cellular longevity *2018*, 9086947.

Cantó, C., and Auwerx, J. (2009). PGC-1alpha, SIRT1 and AMPK, an energy sensing network that controls energy expenditure. Current opinion in lipidology *20*, 98-105.

Cao, L., Tan, L., Wang, H.-F., Jiang, T., Zhu, X.-C., Lu, H., Tan, M.-S., and Yu, J.-T. (2016). Dietary Patterns and Risk of Dementia: a Systematic Review and Meta-Analysis of Cohort Studies. Molecular neurobiology *53*, 6144-6154.

Carrillo, M.C., Dean, R.A., Nicolas, F., Miller, D.S., Berman, R., Khachaturian, Z., Bain, L.J., Schindler, R., and Knopman, D. (2013). Revisiting the framework of the National

Institute on Aging-Alzheimer's Association diagnostic criteria. Alzheimer's & dementia : the journal of the Alzheimer's Association *9*, 594-601.

Castejón, M.L., Montoya, T., Alarcón-de-la-Lastra, C., and Sánchez-Hidalgo, M. (2020). Potential Protective Role Exerted by Secoiridoids from Olea europaea L. in Cancer, Cardiovascular, Neurodegenerative, Aging-Related, and Immunoinflammatory Diseases. Antioxidants (Basel, Switzerland) *9*.

Cenini, G., and Voos, W. (2019). Mitochondria as Potential Targets in Alzheimer Disease Therapy: An Update. Frontiers in pharmacology *10*, 902.

Chai, Y.L., Xing, H., Chong, J.R., Francis, P.T., Ballard, C.G., Chen, C.P., and Lai, M.K.P. (2018). Mitochondrial Translocase of the Outer Membrane Alterations May Underlie Dysfunctional Oxidative Phosphorylation in Alzheimer's Disease. JAD *61*, 793-801.

Chakravorty, A., Jetto, C.T., and Manjithaya, R. (2019). Dysfunctional Mitochondria and Mitophagy as Drivers of Alzheimer's Disease Pathogenesis. Frontiers in aging neuroscience *11*, 311.

Chen, G.-f., Xu, T.-h., Yan, Y., Zhou, Y.-r., Jiang, Y., Melcher, K., and Xu, H.E. (2017). Amyloid beta. Structure, biology and structure-based therapeutic development. Acta Pharmacol Sin *38*, 1205-1235.

Cieślik, M., Czapski, G.A., Wójtowicz, S., Wieczorek, I., Wencel, P.L., Strosznajder, R.P., Jaber, V., Lukiw, W.J., and Strosznajder, J.B. (2020). Alterations of Transcription of Genes Coding Anti-oxidative and Mitochondria-Related Proteins in Amyloid β Toxicity: Relevance to Alzheimer's Disease. Molecular neurobiology *57*, 1374-1388.

Citron, M., Oltersdorf, T., Haass, C., McConlogue, L., Hung, A.Y., Seubert, P., Vigo-Pelfrey, C., Lieberburg, I., and Selkoe, D.J. (1992). Mutation of the beta-amyloid precursor protein in familial Alzheimer's disease increases beta-protein production. Nature *360*, 672-674.

Clayden, J. (2009). Organic chemistry (Oxford: Oxford Univ. Press).

Corona, G., Tzounis, X., Assunta Dessì, M., Deiana, M., Debnam, E.S., Visioli, F., and Spencer, J.P.E. (2006). The fate of olive oil polyphenols in the gastrointestinal tract: implications

of gastric and colonic microflora-dependent biotransformation. Free radical research *40*, 647-658.

Crane, P.K., Walker, R., Hubbard, R.A., Li, G., Nathan, D.M., Zheng, H., Haneuse, S., Craft, S., Montine, T.J., and Kahn, S.E., et al. (2013). Glucose levels and risk of dementia. The New England journal of medicine *369*, 540-548.

Croteau, E., Castellano, C.A., Fortier, M., Bocti, C., Fulop, T., Paquet, N., and Cunnane, S.C. (2018). A cross-sectional comparison of brain glucose and ketone metabolism in cognitively healthy older adults, mild cognitive impairment and early Alzheimer's disease. Experimental gerontology *107*, 18-26.

Cummings, J., Lee, G., Ritter, A., Sabbagh, M., and Zhong, K. (2019). Alzheimer's disease drug development pipeline. 2019. Alzheimer's & dementia (New York, N. Y.) *5*, 272-293.

Daayf, F. and Lattanzio, V. (2009). Recent advances in polyphenol research ; Bd 1 (Oxford: Wiley-Blackwell).

D'Adamo, S., Cetrullo, S., Guidotti, S., Borzì, R.M., and Flamigni, F. (2017). Hydroxytyrosol modulates the levels of microRNA-9 and its target sirtuin-1 thereby counteracting oxidative stress-induced chondrocyte death. Osteoarthritis and Cartilage *25*, 600-610.

Deiana, P., Santona, M., Dettori, S., Culeddu, N., Dore, A., and Molinu, M.G. (2019). Multivariate approach to assess the chemical composition of Italian virgin olive oils as a function of variety and harvest period. Food chemistry *300*, 125243.

D'Ercole, A.J., Ye, P., Calikoglu, A.S., and Gutierrez-Ospina, G. (1996). The role of the insulin-like growth factors in the central nervous system. Molecular neurobiology *13*, 227-255.

Deutschl, G. and Maier, W. (2016). S3-Leitlinie Demenzen. Leitlinien für Diagnostik und Therapie in der Neurologie.

Devi, L., Prabhu, B.M., Galati, D.F., Avadhani, N.G., and Anandatheerthavarada, H.K. (2006). Accumulation of amyloid precursor protein in the mitochondrial import channels of human Alzheimer's disease brain is associated with mitochondrial dysfunction. The Journal of neuroscience : the official journal of the Society for Neuroscience *26*, 9057-9068.

Dewapriya, P., Himaya, S.W.A., Li, Y.-X., and Kim, S.-K. (2013). Tyrosol exerts a protective effect against dopaminergic neuronal cell death in in vitro model of Parkinson's disease. Food chemistry *141*, 1147-1157.

Di Meo, S., Reed, T.T., Venditti, P., and Victor, V.M. (2016). Role of ROS and RNS Sources in Physiological and Pathological Conditions. Oxidative medicine and cellular longevity *2016*, 1245049.

Diaz-Gerevini, G.T., Repossi, G., Dain, A., Tarres, M.C., Das, U.N., and Eynard, A.R. (2016). Beneficial action of resveratrol. How and why? Nutrition (Burbank, Los Angeles County, Calif.) *32*, 174-178.

Diaz-Ruiz, R., Rigoulet, M., and Devin, A. (2011). The Warburg and Crabtree effects: On the origin of cancer cell energy metabolism and of yeast glucose repression. Biochimica et biophysica acta *1807*, 568-576.

Dilberger, B., Passon, M., Asseburg, H., Silaidos, C.V., Schmitt, F., Schmiedl, T., Schieber, A., and Eckert, G.P. (2019). Polyphenols and Metabolites Enhance Survival in Rodents and Nematodes-Impact of Mitochondria. Nutrients *11*.

Douiev, L., Soiferman, D., Alban, C., and Saada, A. (2016). The Effects of Ascorbate, N-Acetylcysteine, and Resveratrol on Fibroblasts from Patients with Mitochondrial Disorders. Journal of clinical medicine *6*.

Dubey, S.K., Ram, M.S., Krishna, K.V., Saha, R.N., Singhvi, G., Agrawal, M., Ajazuddin, Saraf, S., Saraf, S., and Alexander, A. (2019). Recent Expansions on Cellular Models to Uncover the Scientific Barriers Towards Drug Development for Alzheimer's Disease. Cellular and molecular neurobiology *39*, 181-209.

Eckert, G.P., Schiborr, C., Hagl, S., Abdel-Kader, R., Müller, W.E., Rimbach, G., and Frank, J. (2013). Curcumin prevents mitochondrial dysfunction in the brain of the senescence-accelerated mouse-prone 8. Neurochemistry international *62*, 595-602.

Fabiani, R., Sepporta, M.V., Rosignoli, P., Bartolomeo, A. de, Crescimanno, M., and Morozzi, G. (2012). Anti-proliferative and pro-apoptotic activities of hydroxytyrosol on different

tumour cells: the role of extracellular production of hydrogen peroxide. European journal of nutrition *51*, 455-464.

Fang, E.F., Hou, Y., Palikaras, K., Adriaanse, B.A., Kerr, J.S., Yang, B., Lautrup, S., Hasan-Olive, M.M., Caponio, D., and Dan, X., et al. (2019). Mitophagy inhibits amyloid-β and tau pathology and reverses cognitive deficits in models of Alzheimer's disease. Nature neuroscience *22*, 401-412.

Farr, S.A., Price, T.O., Dominguez, L.J., Motisi, A., Saiano, F., Niehoff, M.L., Morley, J.E., Banks, W.A., Ercal, N., and Barbagallo, M. (2012). Extra virgin olive oil improves learning and memory in SAMP8 mice. Journal of Alzheimer's disease : JAD *28*, 81-92.

Fernandez-Marcos, P.J., and Auwerx, J. (2011). Regulation of PGC-1α, a nodal regulator of mitochondrial biogenesis. The American journal of clinical nutrition *93*, 884S-90.

Finck, B.N., and Kelly, D.P. (2006). PGC-1 coactivators. Inducible regulators of energy metabolism in health and disease. The Journal of clinical investigation *116*, 615-622.

Freudenberg-Hua, Y., Li, W., and Davies, P. (2018). The Role of Genetics in Advancing Precision Medicine for Alzheimer's Disease—A Narrative Review. Front. Med. *5*, 203.

Fridovich, I. (1995). Superoxide radical and superoxide dismutases. Annual review of biochemistry *64*, 97-112.

Friedman, J.R., and Nunnari, J. (2014). Mitochondrial form and function. Nature *505*, 335-343.

Fusco, S., Ripoli, C., Podda, M.V., Ranieri, S.C., Leone, L., Toietta, G., McBurney, M.W., Schütz, G., Riccio, A., and Grassi, C., et al. (2012). A role for neuronal cAMP responsive-element binding (CREB)-1 in brain responses to calorie restriction. Proceedings of the National Academy of Sciences of the United States of America *109*, 621-626.

Galanakis, P.A., Bazoti, F.N., Bergquist, J., Markides, K., Spyroulias, G.A., and Tsarbopoulos, A. (2011). Study of the interaction between the amyloid beta peptide (1-40) and antioxidant compounds by nuclear magnetic resonance spectroscopy. Biopolymers *96*, 316-327.

Gaudreault, R., and Mousseau, N. (2019). Mitigating Alzheimer's Disease with Natural Polyphenols. A Review. CAR *16*, 529-543.

Gavahian, M., Mousavi Khaneghah, A., Lorenzo, J.M., Munekata, P.E.S., Garcia-Mantrana, I., Collado, M.C., Meléndez-Martínez, A.J., and Barba, F.J. (2019). Health benefits of olive oil and its components. Impacts on gut microbiota antioxidant activities, and prevention of noncommunicable diseases. Trends in Food Science & Technology *88*, 220-227.

Glenner, G.G., and Wong, C.W. (1984). Alzheimer's disease. Initial report of the purification and characterization of a novel cerebrovascular amyloid protein. Biochemical and Biophysical Research Communications *120*, 885-890.

Gnaiger, E. (2001). Bioenergetics at low oxygen: dependence of respiration and phosphorylation on oxygen and adenosine diphosphate supply. Respiration Physiology *128*, 277-297.

Gnaiger, E. (2012). Mitochondrial pathways and respiratory control. An introduction to OXPHOS analysis ; mitochondr physiol network 17.18.

Golpich, M., Amini, E., Mohamed, Z., Azman Ali, R., Mohamed Ibrahim, N., and Ahmadiani, A. (2017). Mitochondrial Dysfunction and Biogenesis in Neurodegenerative diseases. Pathogenesis and Treatment. CNS neuroscience & therapeutics *23*, 5-22.

Gong, B., Vitolo, O.V., Trinchese, F., Liu, S., Shelanski, M., and Arancio, O. (2004). Persistent improvement in synaptic and cognitive functions in an Alzheimer mouse model after rolipram treatment. The Journal of clinical investigation *114*, 1624-1634.

Gordon, B.A., Blazey, T.M., Su, Y., Hari-Raj, A., Dincer, A., Flores, S., Christensen, J., McDade, E., Wang, G., and Xiong, C., et al. (2018). Spatial patterns of neuroimaging biomarker change in individuals from families with autosomal dominant Alzheimer's disease: a longitudinal study. The Lancet Neurology *17*, 241-250.

Gordon, J., Amini, S., and White, M.K. (2013). General overview of neuronal cell culture. Methods in molecular biology (Clifton, N.J.) *1078*, 1-8.

Gordon, K., Clouaire, T., Bao, X.X., Kemp, S.E., Xenophontos, M., Las Heras, J.I. de, and Stancheva, I. (2014). Immortality, but not oncogenic transformation, of primary human

cells leads to epigenetic reprogramming of DNA methylation and gene expression. Nucleic acids research *42*, 3529-3541.

Gray, M.W. (2012). Mitochondrial Evolution. Cold Spring Harbor Perspectives in Biology *4*, a011403-a011403.

Greene, L.A., and Tischler, A.S. (1976). Establishment of a noradrenergic clonal line of rat adrenal pheochromocytoma cells which respond to nerve growth factor. Proc Natl Acad Sci USA *73*, 2424-2428.

Grewal, R., Reutzel, M., Dilberger, B., Hein, H., Zotzel, J., Marx, S., Tretzel, J., Sarafeddinov, A., Fuchs, C., and Eckert, G.P. (2020). Purified oleocanthal and ligstroside protect against mitochondrial dysfunction in models of early Alzheimer's disease and brain ageing. Experimental neurology *328*, 113248.

Grimm, A., Friedland, K., and Eckert, A. (2016). Mitochondrial dysfunction. The missing link between aging and sporadic Alzheimer’s disease. Biogerontology *17*, 281-296.

Grodzicki, W., and Dziendzikowska, K. (2020). The Role of Selected Bioactive Compounds in the Prevention of Alzheimer's Disease. Antioxidants (Basel, Switzerland) *9*.

Grossi, C., Rigacci, S., Ambrosini, S., Ed Dami, T., Luccarini, I., Traini, C., Failli, P., Berti, A., Casamenti, F., and Stefani, M. (2013). The polyphenol oleuropein aglycone protects TgCRND8 mice against Aß plaque pathology. PloS one *8*, e71702.

Guppy, M., Leedman, P., Zu, X., and Russell, V. (2002). Contribution by different fuels and metabolic pathways to the total ATP turnover of proliferating MCF-7 breast cancer cells. Biochemical Journal *364*, 309-315.

Haas, R.H. (2019). Mitochondrial Dysfunction in Aging and Diseases of Aging. Biology *8*.

Hagl, S., Asseburg, H., Heinrich, M., Sus, N., Blumrich, E.-M., Dringen, R., Frank, J., and Eckert, G.P. (2016a). Effects of Long-Term Rice Bran Extract Supplementation on Survival, Cognition and Brain Mitochondrial Function in Aged NMRI Mice. Neuromolecular medicine *18*, 347-363.

Hagl, S., Berressem, D., Bruns, B., Sus, N., Frank, J., and Eckert, G.P. (2015a). Beneficial Effects of Ethanolic and Hexanic Rice Bran Extract on Mitochondrial Function in PC12 Cells and the Search for Bioactive Components. Molecules (Basel, Switzerland) *20*, 16524-16539.

Hagl, S., Berressem, D., Grewal, R., Sus, N., Frank, J., and Eckert, G.P. (2016b). Rice bran extract improves mitochondrial dysfunction in brains of aged NMRI mice. Nutritional neuroscience *19*, 1-10.

Hagl, S., Grewal, R., Ciobanu, I., Helal, A., Khayyal, M.T., Muller, W.E., and Eckert, G.P. (2015b). Rice bran extract compensates mitochondrial dysfunction in a cellular model of early Alzheimer's disease. Journal of Alzheimer's disease : JAD *43*, 927-938.

Hales, K.G. (2004). The machinery of mitochondrial fusion, division, and distribution, and emerging connections to apoptosis. Mitochondrion *4*, 285-308.

Hampel, H., O'Bryant, S.E., Molinuevo, J.L., Zetterberg, H., Masters, C.L., Lista, S., Kiddle, S.J., Batrla, R., and Blennow, K. (2018). Blood-based biomarkers for Alzheimer disease: mapping the road to the clinic. Nature reviews. Neurology *14*, 639-652.

Hao, J., Shen, W., Yu, G., Jia, H., Li, X., Feng, Z., Wang, Y., Weber, P., Wertz, K., and Sharman, E., et al. (2010). Hydroxytyrosol promotes mitochondrial biogenesis and mitochondrial function in 3T3-L1 adipocytes. The Journal of nutritional biochemistry *21*, 634-644.

Hardy, J., and Higgins, G. (1992). Alzheimer's disease. The amyloid cascade hypothesis. Science *256*, 184-185.

Hauptmann, S., Scherping, I., Dröse, S., Brandt, U., Schulz, K.L., Jendrach, M., Leuner, K., Eckert, A., and Müller, W.E. (2009). Mitochondrial dysfunction: an early event in Alzheimer pathology accumulates with age in AD transgenic mice. Neurobiology of aging *30*, 1574-1586.

Herzig, S., Long, F., Jhala, U.S., Hedrick, S., Quinn, R., Bauer, A., Rudolph, D., Schutz, G., Yoon, C., and Puigserver, P., et al. (2001). CREB regulates hepatic gluconeogenesis through the coactivator PGC-1. Nature *413*, 179-183.

Hill, E., Goodwill, A.M., Gorelik, A., and Szoeke, C. (2019). Diet and biomarkers of Alzheimer's disease. A systematic review and meta-analysis. Neurobiology of aging *76*, 45-52.

Hirst, J. (2013). Mitochondrial complex I. Annual review of biochemistry *82*, 551-575.

Holper, L., Ben-Shachar, D., and Mann, J.J. (2019). Multivariate meta-analyses of mitochondrial complex I and IV in major depressive disorder, bipolar disorder, schizophrenia, Alzheimer disease, and Parkinson disease. Neuropsychopharmacology : official publication of the American College of Neuropsychopharmacology *44*, 837-849.

Hu, W., Wang, Z., and Zheng, H. (2018). Mitochondrial accumulation of amyloid β (Aβ) peptides requires TOMM22 as a main Aβ receptor in yeast. The Journal of biological chemistry *293*, 12681-12689.

Iadanza, M.G., Jackson, M.P., Hewitt, E.W., Ranson, N.A., and Radford, S.E. (2018). A new era for understanding amyloid structures and disease. Nature reviews. Molecular cell biology *19*, 755-773.

Ighodaro, O.M., and Akinloye, O.A. (2018). First line defence antioxidants-superoxide dismutase (SOD), catalase (CAT) and glutathione peroxidase (GPX): Their fundamental role in the entire antioxidant defence grid. Alexandria Journal of Medicine *54*, 287-293.

Impellizzeri, J., and Lin, J. (2006). A simple high-performance liquid chromatography method for the determination of throat-burning oleocanthal with probated antiinflammatory activity in extra virgin olive oils. Journal of agricultural and food chemistry *54*, 3204-3208.

Iqbal, K., Liu, F., Gong, C.-X., and Grundke-Iqbal, I. (2010). Tau in Alzheimer disease and related tauopathies. Current Alzheimer research *7*, 656-664.

Israel, M.A., Yuan, S.H., Bardy, C., Reyna, S.M., Mu, Y., Herrera, C., Hefferan, M.P., van Gorp, S., Nazor, K.L., and Boscolo, F.S., et al. (2012). Probing sporadic and familial Alzheimer's disease using induced pluripotent stem cells. Nature *482*, 216-220.

Ivanov, S.M., Atanasova, M., Dimitrov, I., and Doytchinova, I.A. (2020). Cellular polyamines condense hyperphosphorylated Tau, triggering Alzheimer's disease. Scientific reports *10*, 10098.

Jagust, W.J., and Landau, S.M. (2012). Apolipoprotein E, not fibrillar β-amyloid, reduces cerebral glucose metabolism in normal aging. The Journal of neuroscience : the official journal of the Society for Neuroscience *32*, 18227-18233.

Jansen, W.J., Ossenkoppele, R., Knol, D.L., Tijms, B.M., Scheltens, P., Verhey, F.R.J., Visser, P.J., Aalten, P., Aarsland, D., and Alcolea, D., et al. (2015). Prevalence of cerebral amyloid pathology in persons without dementia: a meta-analysis. JAMA *313*, 1924-1938.

Julien, C., Tremblay, C., Emond, V., Lebbadi, M., Salem, N., Bennett, D.A., and Calon, F. (2009). Sirtuin 1 reduction parallels the accumulation of tau in Alzheimer disease. J Neuropathol Exp Neurol *68*, 48-58.

Kandel, E.R. (2012). The molecular biology of memory: cAMP, PKA, CRE, CREB-1, CREB-2, and CPEB. Molecular brain *5*, 14.

Kapogiannis, D., and Mattson, M.P. (2011). Disrupted energy metabolism and neuronal circuit dysfunction in cognitive impairment and Alzheimer's disease. The Lancet Neurology *10*, 187-198.

Karkoula, E., Skantzari, A., Melliou, E., and Magiatis, P. (2012). Direct measurement of oleocanthal and oleacein levels in olive oil by quantitative (1)H NMR. Establishment of a new index for the characterization of extra virgin olive oils. Journal of agricultural and food chemistry *60*, 11696-11703.

Karkoula, E., Skantzari, A., Melliou, E., and Magiatis, P. (2014). Quantitative measurement of major secoiridoid derivatives in olive oil using qNMR. Proof of the artificial formation of aldehydic oleuropein and ligstroside aglycon isomers. Journal of agricultural and food chemistry *62*, 600-607.

Kaur, G., and Dufour, J.M. (2012). Cell lines: Valuable tools or useless artifacts. Spermatogenesis *2*, 1-5.

Kikusato, M., Muroi, H., Uwabe, Y., Furukawa, K., and Toyomizu, M. (2016a). Oleuropein induces mitochondrial biogenesis and decreases reactive oxygen species generation in cultured avian muscle cells, possibly via an up-regulation of peroxisome proliferator-activated receptor γ coactivator-1α. Animal science journal = Nihon chikusan Gakkaiho *87*, 1371-1378.

Kikusato, M., Muroi, H., Uwabe, Y., Furukawa, K., and Toyomizu, M. (2016b). Oleuropein induces mitochondrial biogenesis and decreases reactive oxygen species generation in cultured avian muscle cells, possibly via an up-regulation of peroxisome proliferator-activated receptor γ coactivator-1α. Animal Science Journal *87*, 1371-1378.

Kim, J.-A., Wei, Y., and Sowers, J.R. (2008). Role of mitochondrial dysfunction in insulin resistance. Circulation research *102*, 401-414.

Kondo, T., Asai, M., Tsukita, K., Kutoku, Y., Ohsawa, Y., Sunada, Y., Imamura, K., Egawa, N., Yahata, N., and Okita, K., et al. (2013). Modeling Alzheimer's disease with iPSCs reveals stress phenotypes associated with intracellular Aβ and differential drug responsiveness. Cell stem cell *12*, 487-496.

Kornelius, E., Li, H.-H., Peng, C.-H., Hsiao, H.-W., Yang, Y.-S., Huang, C.-N., and Lin, C.-L. (2017). Mevastatin promotes neuronal survival against Aβ-induced neurotoxicity through AMPK activation. Metabolic brain disease *32*, 1999-2007.

Kostomoiri, M., Fragkouli, A., Sagnou, M., Skaltsounis, L.A., Pelecanou, M., Tsilibary, E.C., and Tzinia, A.K. (2013). Oleuropein, an Anti-oxidant Polyphenol Constituent of Olive Promotes α-Secretase Cleavage of the Amyloid Precursor Protein (AβPP). Cellular and molecular neurobiology *33*, 147-154.

Kouka, P., Tekos, F., Papoutsaki, Z., Stathopoulos, P., Halabalaki, M., Tsantarliotou, M., Zervos, I., Nepka, C., Liesivuori, J., and Rakitskii, V.N., et al. (2020). Olive oil with high polyphenolic content induces both beneficial and harmful alterations on rat redox status depending on the tissue. Toxicology reports *7*, 421-432.

Kovalevich, J., and Langford, D. (2013). Considerations for the use of SH-SY5Y neuroblastoma cells in neurobiology. Methods in molecular biology (Clifton, N.J.) *1078*, 9-21.

Krishnan, K.J., Ratnaike, T.E., Gruyter, H.L.M. de, Jaros, E., and Turnbull, D.M. (2012). Mitochondrial DNA deletions cause the biochemical defect observed in Alzheimer's disease. Neurobiology of aging *33*, 2210-2214.

Ksiezak-Reding, H., Liu, W.-K., and Yen, S.-H. (1992). Phosphate analysis and dephosphorylation of modified tau associated with paired helical filaments. Brain research *597*, 209-219.

Kuehn, B.M. (2020). In Alzheimer Research, Glucose Metabolism Moves to Center Stage. JAMA.

Kussmaul, L., and Hirst, J. (2006). The mechanism of superoxide production by NADH:ubiquinone oxidoreductase (complex I) from bovine heart mitochondria. Proc Natl Acad Sci USA *103*, 7607-7612.

Lakatos, A., Derbeneva, O., Younes, D., Keator, D., Bakken, T., Lvova, M., Brandon, M., Guffanti, G., Reglodi, D., and Saykin, A., et al. (2010). Association between mitochondrial DNA variations and Alzheimer's disease in the ADNI cohort. Neurobiology of aging *31*, 1355-1363.

Larsen, S., Nielsen, J., Hansen, C.N., Nielsen, L.B., Wibrand, F., Stride, N., Schroder, H.D., Boushel, R., Helge, J.W., and Dela, F., et al. (2012). Biomarkers of mitochondrial content in skeletal muscle of healthy young human subjects. The Journal of physiology *590*, 3349-3360.

Lasser, M., Tiber, J., and Lowery, L.A. (2018). The Role of the Microtubule Cytoskeleton in Neurodevelopmental Disorders. Frontiers in cellular neuroscience *12*, 165.

LaVail, J.H., and Wolf, M.K. (1973). Postnatal development of the mouse dentate gyrus in organotypic cultures of the hippocampal formation. The American journal of anatomy *137*, 47-65.

Leopoldini, M., Marino, T., Russo, N., and Toscano, M. (2004). Antioxidant Properties of Phenolic Compounds: H-Atom versus Electron Transfer Mechanism. J. Phys. Chem. A *108*, 4916-4922.

Leuner, K., Müller, W.E., and Reichert, A.S. (2012). From mitochondrial dysfunction to amyloid beta formation: novel insights into the pathogenesis of Alzheimer's disease. Molecular neurobiology *46*, 186-193.

Löffler, T., Flunkert, S., Taub, N., Schofield, E.L., Ward, M.A., Windisch, M., and Hutter-Paier, B. (2012). Stable mutated tau441 transfected SH-SY5Y cells as screening tool for Alzheimer's disease drug candidates. Journal of molecular neuroscience : MN *47*, 192-203.

Long, J.M., and Holtzman, D.M. (2019). Alzheimer Disease. An Update on Pathobiology and Treatment Strategies. Cell *179*, 312-339.

Lopez Sanchez, M.I.G., Waugh, H.S., Tsatsanis, A., Wong, B.X., Crowston, J.G., Duce, J.A., and Trounce, I.A. (2017). Amyloid precursor protein drives down-regulation of mitochondrial oxidative phosphorylation independent of amyloid beta. Scientific reports *7*, 9835.

Macdonald, P. (2001). Diversity in translational regulation. Current Opinion in Cell Biology *13*, 326-331.

Mahley, R. (1988). Apolipoprotein E. Cholesterol transport protein with expanding role in cell biology. Science *240*, 622-630.

Maliszewska-Cyna, E., Lynch, M., Oore, J.J., Nagy, P.M., and Aubert, I. (2017). The Benefits of Exercise and Metabolic Interventions for the Prevention and Early Treatment of Alzheimer's Disease. Current Alzheimer research *14*, 47-60.

Manczak, M., Calkins, M.J., and Reddy, P.H. (2011). Impaired mitochondrial dynamics and abnormal interaction of amyloid beta with mitochondrial protein Drp1 in neurons from patients with Alzheimer's disease: implications for neuronal damage. Human molecular genetics *20*, 2495-2509.

Manczak, M., Park, B.S., Jung, Y., and Reddy, P.H. (2004). Differential Expression of Oxidative Phosphorylation Genes in Patients With Alzheimer's Disease: Implications for Early Mitochondrial Dysfunction and Oxidative Damage. NMM *5*, 147-162.

Maqsood, M.I., Matin, M.M., Bahrami, A.R., and Ghasroldasht, M.M. (2013). Immortality of cell lines: challenges and advantages of establishment. Cell biology international *37*, 1038-1045.

Martínez-Lapiscina, E.H., Clavero, P., Toledo, E., Estruch, R., Salas-Salvadó, J., San Julián, B., Sanchez-Tainta, A., Ros, E., Valls-Pedret, C., and Martinez-Gonzalez, M.Á. (2013). Mediterranean diet improves cognition: the PREDIMED-NAVARRA randomised trial. Journal of neurology, neurosurgery, and psychiatry *84*, 1318-1325.

Martins, F., Gomes-Laranjo, J., Amaral, C., Almeida, J., and Peixoto, F. (2008). Evaluation of olive oil mill wastewaters acute toxicity. A study on the mitochondrial bioenergetics. Ecotoxicology and environmental safety *69*, 480-487.

Masters, C.L., Bateman, R., Blennow, K., Rowe, C.C., Sperling, R.A., and Cummings, J.L. (2015). Alzheimer's disease. Nature reviews. Disease primers *1*, 15056.

Matsumoto, K., Akao, Y., Yi, H., Shamoto-Nagai, M., Maruyama, W., and Naoi, M. (2006). Overexpression of amyloid precursor protein induces susceptibility to oxidative stress in human neuroblastoma SH-SY5Y cells. Journal of neural transmission (Vienna, Austria : 1996) *113*, 125-135.

McDade, E., Wang, G., Gordon, B.A., Hassenstab, J., Benzinger, T.L.S., Buckles, V., Fagan, A.M., Holtzman, D.M., Cairns, N.J., and Goate, A.M., et al. (2018). Longitudinal cognitive and biomarker changes in dominantly inherited Alzheimer disease. Neurology *91*, e1295-e1306.

Menendez, J.A., Joven, J., Aragonès, G., Barrajón-Catalán, E., Beltrán-Debón, R., Borrás-Linares, I., Camps, J., Corominas-Faja, B., Cufí, S., and Fernández-Arroyo, S., et al. (2013). Xenohormetic and anti-aging activity of secoiridoid polyphenols present in extra virgin olive oil: a new family of gerosuppressant agents. Cell cycle (Georgetown, Tex.) *12*, 555-578.

Miro-Casas, E., Covas, M.-I., Farre, M., Fito, M., Ortuño, J., Weinbrenner, T., Roset, P., and La Torre, R. de (2003). Hydroxytyrosol disposition in humans. Clinical chemistry *49*, 945-952.

Miró-Casas, E., Covas, M.-I., Fitó, M., Farré-Albadalejo, M., Marrugat, J., and La Torre, R. de (2003). Tyrosol and hydroxytyrosol are absorbed from moderate and sustained doses of virgin olive oil in humans. European journal of clinical nutrition *57*, 186-190.

Mishra, P., and Chan, D.C. (2014). Mitochondrial dynamics and inheritance during cell division, development and disease. Nature reviews. Molecular cell biology *15*, 634-646.

Miyazono, Y., Hirashima, S., Ishihara, N., Kusukawa, J., Nakamura, K.-I., and Ohta, K. (2018). Uncoupled mitochondria quickly shorten along their long axis to form indented spheroids, instead of rings, in a fission-independent manner. Scientific reports *8*, 350.

Morris, M.C., Tangney, C.C., Wang, Y., Sacks, F.M., Barnes, L.L., Bennett, D.A., and Aggarwal, N.T. (2015a). MIND diet slows cognitive decline with aging. Alzheimer's & dementia : the journal of the Alzheimer's Association *11*, 1015-1022.

Morris, M.C., Tangney, C.C., Wang, Y., Sacks, F.M., Bennett, D.A., and Aggarwal, N.T. (2015b). MIND diet associated with reduced incidence of Alzheimer's disease. Alzheimer's & dementia : the journal of the Alzheimer's Association *11*, 1007-1014.

Müller, W.E., Eckert, A., Kurz, C., Eckert, G.P., and Leuner, K. (2010). Mitochondrial dysfunction: common final pathway in brain aging and Alzheimer's disease--therapeutic aspects. Molecular neurobiology *41*, 159-171.

Muratore, C.R., Rice, H.C., Srikanth, P., Callahan, D.G., Shin, T., Benjamin, L.N.P., Walsh, D.M., Selkoe, D.J., and Young-Pearse, T.L. (2014). The familial Alzheimer's disease APPV717I mutation alters APP processing and Tau expression in iPSC-derived neurons. Human molecular genetics *23*, 3523-3536.

Murphy, M.P. (2009). How mitochondria produce reactive oxygen species. The Biochemical journal *417*, 1-13.

Murphy, M.P., and LeVine, H. (2010). Alzheimer's disease and the amyloid-beta peptide. Journal of Alzheimer's disease : JAD *19*, 311-323.

Mutisya, E.M., Bowling, A.C., and Beal, M.F. (1994). Cortical cytochrome oxidase activity is reduced in Alzheimer's disease. J. Neurochem. *63*, 2179-2184.

Nalivaeva, N.N., and Turner, A.J. (2013). The amyloid precursor protein. A biochemical enigma in brain development, function and disease. FEBS Letters *587*, 2046-2054.

Napolitano, A., Lucia, M. de, Panzella, L., and d'Ischia, M. (2010). The Chemistry of Tyrosol and Hydroxytyrosol. In Olives and Olive Oil in Health and Disease Prevention (Elsevier), pp. 1225–1232.

Nelson, P.T., Alafuzoff, I., Bigio, E.H., Bouras, C., Braak, H., Cairns, N.J., Castellani, R.J., Crain, B.J., Davies, P., and Tredici, K.D., et al. (2012). Correlation of Alzheimer Disease Neuropathologic Changes With Cognitive Status. A Review of the Literature. J Neuropathol Exp Neurol *71*, 362-381.

Ng, T.K.S., Ho, C.S.H., Tam, W.W.S., Kua, E.H., and Ho, R.C.-M. (2019). Decreased Serum Brain-Derived Neurotrophic Factor (BDNF) Levels in Patients with Alzheimer's Disease (AD): A Systematic Review and Meta-Analysis. International journal of molecular sciences *20*.

Ngandu, T., Lehtisalo, J., Solomon, A., Levälahti, E., Ahtiluoto, S., Antikainen, R., Bäckman, L., Hänninen, T., Jula, A., and Laatikainen, T., et al. (2015). A 2 year multidomain intervention of diet, exercise, cognitive training, and vascular risk monitoring versus control to prevent cognitive decline in at-risk elderly people (FINGER): a randomised controlled trial. The Lancet *385*, 2255-2263.

Nicolson, G.L. (2014). Mitochondrial Dysfunction and Chronic Disease. Treatment With Natural Supplements. Integrative medicine (Encinitas, Calif.) *13*, 35-43.

Norton, S., Matthews, F.E., Barnes, D.E., Yaffe, K., and Brayne, C. (2014). Potential for primary prevention of Alzheimer's disease: an analysis of population-based data. The Lancet Neurology *13*, 788-794.

Nunnari, J., and Suomalainen, A. (2012). Mitochondria. In sickness and in health. Cell *148*, 1145-1159.

Oguchi, T., Ono, R., Tsuji, M., Shozawa, H., Somei, M., Inagaki, M., Mori, Y., Yasumoto, T., Ono, K., and Kiuchi, Y. (2017). Cilostazol Suppresses Aβ-induced Neurotoxicity in SH-

SY5Y Cells through Inhibition of Oxidative Stress and MAPK Signaling Pathway. Frontiers in aging neuroscience *9*, 337.

Olsson, F., Schmidt, S., Althoff, V., Munter, L.M., Jin, S., Rosqvist, S., Lendahl, U., Multhaup, G., and Lundkvist, J. (2014). Characterization of intermediate steps in amyloid beta (Aβ) production under near-native conditions. The Journal of biological chemistry *289*, 1540-1550.

Omar, S.H., Kerr, P.G., Scott, C.J., Hamlin, A.S., and Obied, H.K. (2017). Olive (Olea europaea L.) Biophenols: A Nutriceutical against Oxidative Stress in SH-SY5Y Cells. Molecules (Basel, Switzerland) *22*.

Ouni, Y., Taamalli, A., Gómez-Caravaca, A.M., Segura-Carretero, A., Fernández-Gutiérrez, A., and Zarrouk, M. (2011). Characterisation and quantification of phenolic compounds of extra-virgin olive oils according to their geographical origin by a rapid and resolutive LC-ESI-TOF MS method. Food chemistry *127*, 1263-1267.

Pagani, L., and Eckert, A. (2011). Amyloid-Beta interaction with mitochondria. International journal of Alzheimer's disease *2011*, 925050.

Påhlman, S., Ruusala, A.-I., Abrahamsson, L., Mattsson, M.E.K., and Esscher, T. (1984). Retinoic acid-induced differentiation of cultured human neuroblastoma cells: a comparison with phorbolester-induced differentiation. Cell Differentiation *14*, 135-144.

Pallàs, M., Pizarro, J.G., Gutierrez-Cuesta, J., Crespo-Biel, N., Alvira, D., Tajes, M., Yeste-Velasco, M., Folch, J., Canudas, A.M., and Sureda, F.X., et al. (2008). Modulation of SIRT1 expression in different neurodegenerative models and human pathologies. Neuroscience *154*, 1388-1397.

Pang, K.-L., and Chin, K.-Y. (2018). The Biological Activities of Oleocanthal from a Molecular Perspective. Nutrients *10*.

Panza, F., Solfrizzi, V., Am Colacicco, D'Introno, A., Capurso, C., Torres, F., Del Parigi, A., Capurso, S., and Capurso, A. (2004). Mediterranean diet and cognitive decline. Public Health Nutr. *7*, 959-963.

Parker, W.D., Filley, C.M., and Parks, J.K. (1990). Cytochrome oxidase deficiency in Alzheimer's disease. Neurology *40*, 1302-1303.

Parkinson, L., and Cicerale, S. (2016). The Health Benefiting Mechanisms of Virgin Olive Oil Phenolic Compounds. Molecules (Basel, Switzerland) *21*.

Pedrós, I., Petrov, D., Allgaier, M., Sureda, F., Barroso, E., Beas-Zarate, C., Auladell, C., Pallàs, M., Vázquez-Carrera, M., and Casadesús, G., et al. (2014). Early alterations in energy metabolism in the hippocampus of APPswe/PS1dE9 mouse model of Alzheimer's disease. Biochimica et biophysica acta *1842*, 1556-1566.

Petrosillo, G., Matera, M., Moro, N., Ruggiero, F.M., and Paradies, G. (2009). Mitochondrial complex I dysfunction in rat heart with aging: critical role of reactive oxygen species and cardiolipin. Free radical biology & medicine *46*, 88-94.

Pfanner, N., and Meijer, M. (1997). Mitochondrial biogenesis. The Tom and Tim machine. Current Biology *7*, R100-R103.

Pfanner, N., and Wiedemann, N. (2002). Mitochondrial protein import. Two membranes, three translocases. Current Opinion in Cell Biology *14*, 400-411.

Pohland, M., Pellowska, M., Asseburg, H., Hagl, S., Reutzel, M., Joppe, A., Berressem, D., Eckert, S.H., Wurglics, M., and Schubert-Zsilavecz, M., et al. (2018). MH84 improves mitochondrial dysfunction in a mouse model of early Alzheimer's disease. Alzheimers Res Ther *10*, 18.

Polanco, J.C., Li, C., Bodea, L.-G., Martinez-Marmol, R., Meunier, F.A., and Götz, J. (2018). Amyloid-β and tau complexity - towards improved biomarkers and targeted therapies. Nature reviews. Neurology *14*, 22-39.

Price, J.L. (1994). Tangles and plaques in healthy aging and Alzheimer's disease. Independence or interaction? Seminars in Neuroscience *6*, 395-402.

Pugazhenthi, S., Wang, M., Pham, S., Sze, C.-I., and Eckman, C.B. (2011). Downregulation of CREB expression in Alzheimer's brain and in Aβ-treated rat hippocampal neurons. Molecular neurodegeneration *6*, 60.

Qiu, L., Luo, Y., and Chen, X. (2018). Quercetin attenuates mitochondrial dysfunction and biogenesis via upregulated AMPK/SIRT1 signaling pathway in OA rats. Biomedicine & pharmacotherapy = Biomedecine & pharmacotherapie *103*, 1585-1591.

Qosa, H., Batarseh, Y.S., Mohyeldin, M.M., El Sayed, K.A., Keller, J.N., and Kaddoumi, A. (2015). Oleocanthal enhances amyloid-β clearance from the brains of TgSwDI mice and in vitro across a human blood-brain barrier model. ACS chemical neuroscience *6*, 1849-1859.

Quideau, S., Deffieux, D., Douat-Casassus, C., and Pouységu, L. (2011). Pflanzliche Polyphenole: chemische Eigenschaften, biologische Aktivität und Synthese. Angew. Chem. *123*, 610-646.

Raja, W.K., Mungenast, A.E., Lin, Y.-T., Ko, T., Abdurrob, F., Seo, J., and Tsai, L.-H. (2016). Self-Organizing 3D Human Neural Tissue Derived from Induced Pluripotent Stem Cells Recapitulate Alzheimer's Disease Phenotypes. PloS one *11*, e0161969.

Rapoport, S.I. (1991). Positron emission tomography in Alzheimer's disease in relation to disease pathogenesis. A critical review. Cerebrovascular and brain metabolism reviews *3*, 297-335.

Reddy, P.H., and Beal, M.F. (2008). Amyloid beta, mitochondrial dysfunction and synaptic damage: implications for cognitive decline in aging and Alzheimer's disease. Trends in molecular medicine *14*, 45-53.

Reddy, P.H., and Oliver, D.M. (2019). Amyloid Beta and Phosphorylated Tau-Induced Defective Autophagy and Mitophagy in Alzheimer's Disease. Cells *8*.

Rees, K., Hartley, L., Clarke, A., Thorogood, M., and Stranges, S. (2012). 'Mediterranean' dietary pattern for the primary prevention of cardiovascular disease. The Cochrane database of systematic reviews *2012*.

Reiman, E.M., Arboleda-Velasquez, J.F., Quiroz, Y.T., Huentelman, M.J., Beach, T.G., Caselli, R.J., Chen, Y., Su, Y., Myers, A.J., and Hardy, J., et al. (2020). Exceptionally low likelihood of Alzheimer's dementia in APOE2 homozygotes from a 5,000-person neuropathological study. Nature communications *11*, 667.

Reutzel, M., Grewal, R., Silaidos, C., Zotzel, J., Marx, S., Tretzel, J., and Eckert, G.P. (2018). Effects of Long-Term Treatment with a Blend of Highly Purified Olive Secoiridoids on Cognition and Brain ATP Levels in Aged NMRI Mice. Oxidative medicine and cellular longevity *2018*, 4070935.

Rhein, V., Baysang, G., Rao, S., Meier, F., Bonert, A., Müller-Spahn, F., and Eckert, A. (2009a). Amyloid-beta leads to impaired cellular respiration, energy production and mitochondrial electron chain complex activities in human neuroblastoma cells. Cellular and molecular neurobiology *29*, 1063-1071.

Rhein, V., Song, X., Wiesner, A., Ittner, L.M., Baysang, G., Meier, F., Ozmen, L., Bluethmann, H., Dröse, S., and Brandt, U., et al. (2009b). Amyloid-beta and tau synergistically impair the oxidative phosphorylation system in triple transgenic Alzheimer's disease mice. Proceedings of the National Academy of Sciences of the United States of America *106*, 20057-20062.

Rigacci, S., and Stefani, M. (2016). Nutraceutical Properties of Olive Oil Polyphenols. An Itinerary from Cultured Cells through Animal Models to Humans. International journal of molecular sciences *17*.

Robertson, R.T., Baratta, J., Kageyama, G.H., Ha, D.H., and Yu, J. (1997). Specificity of attachment and neurite outgrowth of dissociated basal forebrain cholinergic neurons seeded on to organotypic slice cultures of forebrain. Neuroscience *80*, 741-752.

Román, G.C., Jackson, R.E., Reis, J., Román, A.N., Toledo, J.B., and Toledo, E. (2019). Extra-virgin olive oil for potential prevention of Alzheimer disease. Revue neurologique.

Rosa, E., and Fahnestock, M. (2015). CREB expression mediates amyloid β-induced basal BDNF downregulation. Neurobiology of aging *36*, 2406-2413.

Rosignoli, P., Fuccelli, R., Fabiani, R., Servili, M., and Morozzi, G. (2013). Effect of olive oil phenols on the production of inflammatory mediators in freshly isolated human monocytes. The Journal of nutritional biochemistry *24*, 1513-1519.

Rubió, L., Macià, A., Valls, R.M., Pedret, A., Romero, M.-P., Solà, R., and Motilva, M.-J. (2012). A new hydroxytyrosol metabolite identified in human plasma: hydroxytyrosol acetate sulphate. Food chemistry *134*, 1132-1136.

Rygiel, K.A., Grady, J.P., and Turnbull, D.M. (2014). Respiratory chain deficiency in aged spinal motor neurons. Neurobiology of aging *35*, 2230-2238.

Sandhu, S.K., and Kaur, G. (2003). Mitochondrial electron transport chain complexes in aging rat brain and lymphocytes. Biogerontology *4*, 19-29.

Scarmeas, N., Luchsinger, J.A., Schupf, N., Brickman, A.M., Cosentino, S., Tang, M.X., and Stern, Y. (2009a). Physical activity, diet, and risk of Alzheimer disease. JAMA *302*, 627-637.

Scarmeas, N., Stern, Y., Mayeux, R., and Luchsinger, J.A. (2006a). Mediterranean diet, Alzheimer disease, and vascular mediation. Archives of neurology *63*, 1709-1717.

Scarmeas, N., Stern, Y., Mayeux, R., Manly, J.J., Schupf, N., and Luchsinger, J.A. (2009b). Mediterranean diet and mild cognitive impairment. Archives of neurology *66*, 216-225.

Scarmeas, N., Stern, Y., Tang, M.-X., Mayeux, R., and Luchsinger, J.A. (2006b). Mediterranean diet and risk for Alzheimer's disease. Annals of neurology *59*, 912-921.

Schaffer, S., Asseburg, H., Kuntz, S., Muller, W.E., and Eckert, G.P. (2012). Effects of polyphenols on brain ageing and Alzheimer's disease. Focus on mitochondria. Molecular neurobiology *46*, 161-178.

Schaffer, S., Eckert, G.P., Schmitt-Schillig, S., and Müller, W.E. (2006). Plant foods and brain aging. A critical appraisal. Forum of nutrition *59*, 86-115.

Schaffer, S., Podstawa, M., Visioli, F., Bogani, P., Müller, W.E., and Eckert, G.P. (2007). Hydroxytyrosol-rich olive mill wastewater extract protects brain cells in vitro and ex vivo. Journal of agricultural and food chemistry *55*, 5043-5049.

Schindler, S.E., Bollinger, J.G., Ovod, V., Mawuenyega, K.G., Li, Y., Gordon, B.A., Holtzman, D.M., Morris, J.C., Benzinger, T.L.S., and Xiong, C., et al. (2019). High-precision

plasma β-amyloid 42/40 predicts current and future brain amyloidosis. Neurology *93*, e1647-e1659.

Schmitt, K., Grimm, A., Kazmierczak, A., Strosznajder, J.B., Götz, J., and Eckert, A. (2012). Insights into mitochondrial dysfunction: aging, amyloid-β, and tau-A deleterious trio. Antioxidants & Redox Signaling *16*, 1456-1466.

Schneider, L.S., Mangialasche, F., Andreasen, N., Feldman, H., Giacobini, E., Jones, R., Mantua, V., Mecocci, P., Pani, L., and Winblad, B., et al. (2014). Clinical trials and late-stage drug development for Alzheimer's disease: an appraisal from 1984 to 2014. Journal of internal medicine *275*, 251-283.

Schwanhäusser, B., Busse, D., Li, N., Dittmar, G., Schuchhardt, J., Wolf, J., Chen, W., and Selbach, M. (2011). Global quantification of mammalian gene expression control. Nature *473*, 337-342.

Schwingshackl, L., Morze, J., and Hoffmann, G. (2019). Mediterranean diet and health status. Active ingredients and pharmacological mechanisms. British journal of pharmacology.

Seçme, M., Eroğlu, C., Dodurga, Y., and Bağcı, G. (2016). Investigation of anticancer mechanism of oleuropein via cell cycle and apoptotic pathways in SH-SY5Y neuroblastoma cells. Gene *585*, 93-99.

Serreli, G., and Deiana, M. (2018). Biological Relevance of Extra Virgin Olive Oil Polyphenols Metabolites. Antioxidants (Basel, Switzerland) *7*.

Sharma, D.R., Sunkaria, A., Wani, W.Y., Sharma, R.K., Verma, D., Priyanka, K., Bal, A., and Gill, K.D. (2015). Quercetin protects against aluminium induced oxidative stress and promotes mitochondrial biogenesis via activation of the PGC-1α signaling pathway. Neurotoxicology *51*, 116-137.

Sharma, L.K., Lu, J., and Bai, Y. (2009). Mitochondrial respiratory complex I: structure, function and implication in human diseases. Current medicinal chemistry *16*, 1266-1277.

Sheng, B., Wang, X., Su, B., Lee, H.-g., Casadesus, G., Perry, G., and Zhu, X. (2012). Impaired mitochondrial biogenesis contributes to mitochondrial dysfunction in Alzheimer's disease. Journal of neurochemistry *120*, 419-429.

Shi, Y., Dierckx, A., Wanrooij, P.H., Wanrooij, S., Larsson, N.-G., Wilhelmsson, L.M., Falkenberg, M., and Gustafsson, C.M. (2012). Mammalian transcription factor A is a core component of the mitochondrial transcription machinery. Proceedings of the National Academy of Sciences of the United States of America *109*, 16510-16515.

Singh, B., Parsaik, A.K., Mielke, M.M., Erwin, P.J., Knopman, D.S., Petersen, R.C., and Roberts, R.O. (2014). Association of mediterranean diet with mild cognitive impairment and Alzheimer's disease. A systematic review and meta-analysis. Journal of Alzheimer's disease : JAD *39*, 271-282.

Slanzi, A., Iannoto, G., Rossi, B., Zenaro, E., and Constantin, G. (2020). In vitro Models of Neurodegenerative Diseases. Frontiers in cell and developmental biology *8*, 328.

Smith, P.J., Blumenthal, J.A., Babyak, M.A., Craighead, L., Welsh-Bohmer, K.A., Browndyke, J.N., Strauman, T.A., and Sherwood, A. (2010). Effects of the dietary approaches to stop hypertension diet, exercise, and caloric restriction on neurocognition in overweight adults with high blood pressure. Hypertension (Dallas, Tex. : 1979) *55*, 1331-1338.

Solfrizzi, V., Panza, F., and Capurso, A. (2003). The role of diet in cognitive decline. Journal of neural transmission (Vienna, Austria : 1996) *110*, 95-110.

Sonntag, K.-C., Ryu, W.-I., Amirault, K.M., Healy, R.A., Siegel, A.J., McPhie, D.L., Forester, B., and Cohen, B.M. Late-onset Alzheimer’s disease is associated with inherent changes in bioenergetics profiles. Sci Rep *7*, 1-13.

Spinelli, J.B., and Haigis, M.C. (2018). The multifaceted contributions of mitochondria to cellular metabolism. Nature cell biology *20*, 745-754.

Srivastava, S. (2017). The Mitochondrial Basis of Aging and Age-Related Disorders. Genes *8*.

Stewart, V.C., Sharpe, M.A., Clark, J.B., and Heales, S.J. (2000). Astrocyte-derived nitric oxide causes both reversible and irreversible damage to the neuronal mitochondrial respiratory chain. J. Neurochem. *75*, 694-700.

Stiuso, P., Bagarolo, M.L., Ilisso, C.P., Vanacore, D., Martino, E., Caraglia, M., Porcelli, M., and Cacciapuoti, G. (2016). Protective Effect of Tyrosol and S-Adenosylmethionine against Ethanol-Induced Oxidative Stress of Hepg2 Cells Involves Sirtuin 1, P53 and Erk1/2 Signaling. International journal of molecular sciences *17*.

Stockburger, C., Gold, V.A.M., Pallas, T., Kolesova, N., Miano, D., Leuner, K., and Müller, W.E. (2014a). A cell model for the initial phase of sporadic Alzheimer's disease. Journal of Alzheimer's disease : JAD *42*, 395-411.

Stockburger, C., Gold, V.A.M., Pallas, T., Kolesova, N., Miano, D., Leuner, K., and Müller, W.E. (2014b). A Cell Model for the Initial Phase of Sporadic Alzheimer's Disease. JAD *42*, 395-411.

Strauss, M., Hofhaus, G., Schröder, R.R., and Kühlbrandt, W. (2008). Dimer ribbons of ATP synthase shape the inner mitochondrial membrane. EMBO J *27*, 1154-1160.

Stroud, D.A., Surgenor, E.E., Formosa, L.E., Reljic, B., Frazier, A.E., Dibley, M.G., Osellame, L.D., Stait, T., Beilharz, T.H., and Thorburn, D.R., et al. (2016). Accessory subunits are integral for assembly and function of human mitochondrial complex I. Nature *538*, 123-126.

Suárez, M., Valls, R.M., Romero, M.-P., Macià, A., Fernández, S., Giralt, M., Solà, R., and Motilva, M.-J. (2011). Bioavailability of phenols from a phenol-enriched olive oil. The British journal of nutrition *106*, 1691-1701.

Sun, L., Zhou, R., Yang, G., and Shi, Y. (2017). Analysis of 138 pathogenic mutations in presenilin-1 on the in vitro production of Aβ42 and Aβ40 peptides by γ-secretase. Proc Natl Acad Sci USA *114*, E476-E485.

Sun, N., Youle, R.J., and Finkel, T. (2016). The Mitochondrial Basis of Aging. Molecular cell *61*, 654-666.

Swerdlow, R.H. (2018). Mitochondria and Mitochondrial Cascades in Alzheimer's Disease. Journal of Alzheimer's disease : JAD *62*, 1403-1416.

Swerdlow, R.H., Burns, J.M., and Khan, S.M. (2010). The Alzheimer's disease mitochondrial cascade hypothesis. Journal of Alzheimer's disease : JAD *20 Suppl 2*, S265-79.

Swerdlow, R.H., Burns, J.M., and Khan, S.M. (2014). The Alzheimer's disease mitochondrial cascade hypothesis. Progress and perspectives. Biochimica et biophysica acta *1842*, 1219-1231.

Swerdlow, R.H., and Khan, S.M. (2004). A "mitochondrial cascade hypothesis" for sporadic Alzheimer's disease. Medical hypotheses *63*, 8-20.

Takagi-Niidome, S., Sasaki, T., Osawa, S., Sato, T., Morishima, K., Cai, T., Iwatsubo, T., and Tomita, T. (2015). Cooperative Roles of Hydrophilic Loop 1 and the C-Terminus of Presenilin 1 in the Substrate-Gating Mechanism of -Secretase. Journal of Neuroscience *35*, 2646-2656.

Talbot, K., Wang, H.-Y., Kazi, H., Han, L.-Y., Bakshi, K.P., Stucky, A., Fuino, R.L., Kawaguchi, K.R., Samoyedny, A.J., and Wilson, R.S., et al. (2012). Demonstrated brain insulin resistance in Alzheimer's disease patients is associated with IGF-1 resistance, IRS-1 dysregulation, and cognitive decline. The Journal of clinical investigation *122*, 1316-1338.

Tangney, C.C., Li, H., Wang, Y., Barnes, L., Schneider, J.A., Bennett, D.A., and Morris, M.C. (2014). Relation of DASH- and Mediterranean-like dietary patterns to cognitive decline in older persons. Neurology *83*, 1410-1416.

Tilokani, L., Nagashima, S., Paupe, V., and Prudent, J. (2018). Mitochondrial dynamics. Overview of molecular mechanisms. Essays in biochemistry *62*, 341-360.

Tong, L., Balazs, R., Thornton, P.L., and Cotman, C.W. (2004). Beta-amyloid peptide at sublethal concentrations downregulates brain-derived neurotrophic factor functions in cultured cortical neurons. The Journal of neuroscience : the official journal of the Society for Neuroscience *24*, 6799-6809.

Tuomilehto, J., Lindström, J., Eriksson, J.G., Valle, T.T., Hämäläinen, H., Ilanne-Parikka, P., Keinänen-Kiukaanniemi, S., Laakso, M., Louheranta, A., and Rastas, M., et al. (2001). Prevention of type 2 diabetes mellitus by changes in lifestyle among subjects with impaired glucose tolerance. The New England journal of medicine *344*, 1343-1350.

Turner, N., and Heilbronn, L.K. (2008). Is mitochondrial dysfunction a cause of insulin resistance? Trends in endocrinology and metabolism: TEM *19*, 324-330.

Uttara, B., Singh, A.V., Zamboni, P., and Mahajan, R.T. (2009). Oxidative stress and neurodegenerative diseases: a review of upstream and downstream antioxidant therapeutic options. Current neuropharmacology *7*, 65-74.

Valls-Pedret, C., Sala-Vila, A., Serra-Mir, M., Corella, D., La Torre, R. de, Martínez-González, M.Á., Martínez-Lapiscina, E.H., Fitó, M., Pérez-Heras, A., and Salas-Salvadó, J., et al. (2015). Mediterranean Diet and Age-Related Cognitive Decline. A Randomized Clinical Trial. JAMA internal medicine *175*, 1094-1103.

Ventura, B., Genova, M.L., Bovina, C., Formiggini, G., and Lenaz, G. (2002). Control of oxidative phosphorylation by Complex I in rat liver mitochondria: implications for aging. Biochimica et Biophysica Acta (BBA) - Bioenergetics *1553*, 249-260.

Ventura-Clapier, R., Garnier, A., and Veksler, V. (2008). Transcriptional control of mitochondrial biogenesis: the central role of PGC-1alpha. Cardiovascular research *79*, 208-217.

Vermunt, L., Sikkes, S.A.M., van den Hout, A., Handels, R., Bos, I., van der Flier, W.M., Kern, S., Ousset, P.-J., Maruff, P., and Skoog, I., et al. (2019). Duration of preclinical, prodromal, and dementia stages of Alzheimer's disease in relation to age, sex, and APOE genotype. Alzheimer's & dementia : the journal of the Alzheimer's Association *15*, 888-898.

Visioli, F., Bellomo, G., and Galli, C. (1998). Free radical-scavenging properties of olive oil polyphenols. Biochemical and Biophysical Research Communications *247*, 60-64.

Visioli, F., Franco, M., Toledo, E., Luchsinger, J., Willett, W.C., Hu, F.B., and Martinez-Gonzalez, M.A. (2018). Olive oil and prevention of chronic diseases. Summary of an International conference. Nutrition, metabolism, and cardiovascular diseases : NMCD *28*, 649-656.

Visioli, F., and Galli, C. (1995). Natural antioxidants and prevention of coronary heart disease: the potential role of olive oil and its minor constituents. Nutrition, metabolism, and cardiovascular diseases : NMCD, 306-314.

Visioli, F., Galli, C., Bornet, F., Mattei, A., Patelli, R., Galli, G., and Caruso, D. (2000). Olive oil phenolics are dose-dependently absorbed in humans. FEBS Letters *468*, 159-160.

Vissers, M.N., Zock, P.L., Roodenburg, A.J.C., Leenen, R., and Katan, M.B. (2002). Olive oil phenols are absorbed in humans. The Journal of nutrition *132*, 409-417.

Vogel, C., and Marcotte, E.M. (2012). Insights into the regulation of protein abundance from proteomic and transcriptomic analyses. Nature reviews. Genetics *13*, 227-232.

Wai, T., and Langer, T. (2016). Mitochondrial Dynamics and Metabolic Regulation. Trends in endocrinology and metabolism: TEM *27*, 105-117.

Walsh, K., Megyesi, J., and Hammond, R. (2005). Human central nervous system tissue culture: a historical review and examination of recent advances. Neurobiology of disease *18*, 2-18.

Wan, L., Nie, G., Zhang, J., and Zhao, B. (2012). Overexpression of human wild-type amyloid-β protein precursor decreases the iron content and increases the oxidative stress of neuroblastoma SH-SY5Y cells. JAD *30*, 523-530.

Wang, Y., Xu, E., Musich, P.R., and Lin, F. (2019). Mitochondrial dysfunction in neurodegenerative diseases and the potential countermeasure. CNS neuroscience & therapeutics *25*, 816-824.

WARBURG, O. (1956). On the origin of cancer cells. Science *123*, 309-314.

Wätjen, W., Michels, G., Steffan, B., Niering, P., Chovolou, Y., Kampkötter, A., Tran-Thi, Q.-H., Proksch, P., and Kahl, R. (2005). Low concentrations of flavonoids are protective in rat H4IIE cells whereas high concentrations cause DNA damage and apoptosis. The Journal of nutrition *135*, 525-531.

Weggen, S., and Beher, D. (2012). Molecular consequences of amyloid precursor protein and presenilin mutations causing autosomal-dominant Alzheimer's disease. Alzheimers Res Ther *4*, 9.

Weidling, I., and Swerdlow, R.H. (2019). Mitochondrial Dysfunction and Stress Responses in Alzheimer's Disease. Biology *8*.

Wengreen, H., Munger, R.G., Cutler, A., Quach, A., Bowles, A., Corcoran, C., Tschanz, J.T., Norton, M.C., and Welsh-Bohmer, K.A. (2013). Prospective study of Dietary Approaches to Stop Hypertension- and Mediterranean-style dietary patterns and age-related cognitive change: the Cache County Study on Memory, Health and Aging. The American journal of clinical nutrition *98*, 1263-1271.

Whetsell, W.O., and Schwarcz, R. (1983). The organotypic tissue culture model of corticostriatal system used for examining amino acid neurotoxicity and its antagonism: studies on kainic acid, quinolinic acid and (-) 2-amino-7-phosphonoheptanoic acid. Journal of neural transmission. Supplementum *19*, 53-63.

Wood Dos Santos, T., Cristina Pereira, Q., Teixeira, L., Gambero, A., A Villena, J., and Lima Ribeiro, M. (2018). Effects of Polyphenols on Thermogenesis and Mitochondrial Biogenesis. International journal of molecular sciences *19*.

Wright, G., Terada, K., Yano, M., Sergeev, I., and Mori, M. (2001a). Oxidative stress inhibits the mitochondrial import of preproteins and leads to their degradation. Experimental cell research *263*, 107-117.

Wright, J.S., Johnson, E.R., and DiLabio, G.A. (2001b). Predicting the activity of phenolic antioxidants. Theoretical method, analysis of substituent effects, and application to major families of antioxidants. Journal of the American Chemical Society *123*, 1173-1183.

Xicoy, H., Wieringa, B., and Martens, G.J.M. (2017). The SH-SY5Y cell line in Parkinson's disease research: a systematic review. Molecular neurodegeneration *12*, 10.

Yagi, T., Ito, D., Okada, Y., Akamatsu, W., Nihei, Y., Yoshizaki, T., Yamanaka, S., Okano, H., and Suzuki, N. (2011). Modeling familial Alzheimer's disease with induced pluripotent stem cells. Human molecular genetics *20*, 4530-4539.

Yamazaki, Y., Zhao, N., Caulfield, T.R., Liu, C.-C., and Bu, G. (2019). Apolipoprotein E and Alzheimer disease. Pathobiology and targeting strategies. Nat Rev Neurol *15*, 501-518.

Yao, J., Irwin, R.W., Zhao, L., Nilsen, J., Hamilton, R.T., and Brinton, R.D. (2009). Mitochondrial bioenergetic deficit precedes Alzheimer's pathology in female mouse model of Alzheimer's disease. Proceedings of the National Academy of Sciences of the United States of America *106*, 14670-14675.

Yassine, H.N., Croteau, E., Rawat, V., Hibbeln, J.R., Rapoport, S.I., Cunnane, S.C., and Umhau, J.C. (2017). DHA brain uptake and APOE4 status: a PET study with 1-11C-DHA. Alzheimers Res Ther *9*, 23.

Youle, R.J., and Narendra, D.P. (2011). Mechanisms of mitophagy. Nature reviews. Molecular cell biology *12*, 9-14.

Youle, R.J., and van der Bliek, A.M. (2012). Mitochondrial fission, fusion, and stress. Science *337*, 1062-1065.

Zheng, A., Li, H., Xu, J., Cao, K., Li, H., Pu, W., Yang, Z., Peng, Y., Long, J., and Liu, J., et al. (2015). Hydroxytyrosol improves mitochondrial function and reduces oxidative stress in the brain of db/db mice: role of AMP-activated protein kinase activation. The British journal of nutrition *113*, 1667-1676.

Published Work

1. Babylon, Lukas; Grewal, Rekha; Eckert, Ralph W.; Keck, Cornelia; Eckert, Gunter P.: Hesperetin nanocrystals improve mitochondrial function in a cell model of early Alzheimer´s disease. In: Antioxidants (2020); under Review.

2. Fuchs, Christine; Bakuradze, Tamara; Steinke, Regina; Grewal, Rekha; Eckert, Gunter P.; Richling, Elke: Polyphenolic composition of extracts from winery by-products and effects on cellular cytotoxicity and mitochondrial functions in HepG2 cells. In: Journal Function Food (2020), 103988. DOI: 10.1016/j.jff.2020.103988.

3. Reutzel, Martina; Grewal, Rekha; Dilberger, Benjamin; Silaidos, Carmina; Joppe, Aljoscha; Eckert, Gunter P.: Cerebral Mitochondrial Function and Cognitive Performance during Aging: A Longitudinal Study in NMRI Mice. In: Oxidative Medicine and Cellular Longevity (2020), 4060769. DOI: 10.1155/2020/4060769.

4. Grewal, Rekha; Reutzel, Martina; Dilberger, Benjamin; Hein, Hannah; Zotzel, Jens; Marx Stefan; Tretzel Joachim; Sarafeddinov, Alla; Fuchs Christopher; Eckert, G. P.: Purified Oleocanthal and Ligstroside protect against mitochondrial dysfunction in models of early Alzheimer´s Disease and brain ageing. In: Experimental Neurology (2020), 113248. DOI: 10.1016/j.expneurol.2020.

5. Esselun, Carsten; Bruns, Bastian; Hagl, Stephanie; Grewal, Rekha; Eckert, Gunter P.: Differential Effects of Silibinin A on Mitochondrial Function in Neuronal PC12 and HepG2 Liver Cells. In: Oxidative medicine and cellular longevity (2019), S. 1652609. DOI: 10.1155/2019/1652609.

6. Reutzel, Martina; Grewal, Rekha; Silaidos, Carmina; Zotzel, Jens; Marx, Stefan; Tretzel, Joachim; Eckert, Gunter P.: Effects of Long-Term Treatment with a Blend of Highly Purified Olive Secoiridoids on Cognition and Brain ATP Levels in Aged NMRI Mice. In: Oxidative medicine and cellular longevity (2018), S. 4070935. DOI: 10.1155/2018/4070935.

7. Silaidos, C.; Pilatus, U.; Grewal, R.; Matura, S.; Lienerth, B.; Pantel, J.; Eckert, G. P.: Sex-associated differences in mitochondrial function in human peripheral blood mononuclear

cells (PBMCs) and brain. In: Biology of sex differences 9 (1) (2018), S. 34. DOI: 10.1186/s13293-018-0193-7.

8. Stark, Tina; Lieblein, Tobias; Pohland, Maximilian; Kalden, Elisabeth; Freund, Petra; Zangl, René; Grewal, Rekha; Heilemann, Mike; Eckert, Gunter P.; Morgner, Nina; Göbel, Michael W.: Peptidomimetics That Inhibit and Partially Reverse the Aggregation of Aβ1-42. In: Biochemistry 56 (36) (2017) S. 4840–4849. DOI: 10.1021/acs.biochem.7b00223.

9. Hagl, Stephanie; Berressem, Dirk; Grewal, Rekha; Sus, Nadine; Frank, Jan; Eckert, Gunter P. Rice bran extract improves mitochondrial dysfunction in brains of aged NMRI mice. In: Nutritional Neuroscience (19) (2016) S. 1-10. DOI: 10.1179/1476830515Y.0000000040

10. Hagl, Stephanie; Grewal, Rekha; Ciobanu, Ion; Helal, Amr; Khayyal, Mohamed T.; Muller, Walter E.; Eckert, Gunter P.: Rice bran extract compensates mitochondrial dysfunction in a cellular model of early Alzheimer's disease. In: Journal of Alzheimer's disease JAD 43 (3) (2015), S. 927–938. DOI: 10.3233/JAD-132084.

11. Januszewski, Estera; Lorbach, Andreas; Grewal, Rekha; Bolte, Michael; Bats, Jan W.; Lerner, Hans-Wolfram; Wagner, Matthias (2011): Unsymmetrically substituted 9,10-dihydro-9,10-diboraanthracenes as versatile building blocks for boron-doped π-conjugated systems. In: Chemistry 17 (45) (2011), S. 12696–12705. DOI: 10.1002/chem.201101701.

Danksagung

Auf dem Weg meiner Promotion haben mich viele Menschen begleitet und unterstützt, bei denen ich mich an dieser Stelle von Herzen bedanken möchte.

Besonderer Dank gilt meinem Doktorvater Prof. Dr. Gunter Eckert für den unkomplizierten und hilfsbereiten Umgang, das mir entgegengebrachte Vertrauen, die angenehme Arbeitsatmosphäre, die erlebnisreichen gemeinsamen Aktivitäten und vor allem für seine Unterstützung in allen Belangen.

Weiterhin möchte ich mich für die Übernahme des Zweitgutachtens bei Herrn Prof. Thomas Linn bedanken.

Vielen Dank an die Mitarbeiter und Arbeitsgruppe vom Institut Ernährung in Prävention und Therapie. Danke Petze und Dani für Euren herzlichen Empfang nach unserem Umzug aus Frankfurt, die Hilfe bei administrativen Belangen und die schönen Momente auf der Terrasse.

Ein ganz besonderer Dank geht an das ehemalige Team am pharmakologischen Institut für Naturwissenschaftler in Frankfurt. Danke Stephanie Hagl, Maximilian Pohland, Heike Asseburg, Martina Heinrich und Carmina Silaidos für die sehr schöne gemeinsame Zeit im Labor, Eure Unterstützung in jeglicher Hinsicht und Eure Hilfsbereitschaft.

Ich danke meinen Kooperationspartnern der TU-Darmstadt, Prof. Dr. Warzecha, Dr. Jascha Volk und dem Team von N-Zyme BioTec, Dr. Joachim Tretzl, Stefan Marx, Jens Zotzel, Ala Sarafeddinov und Christopher Fuchs. Es war eine tolle und produktive Zusammenarbeit in den letzten Jahren.

Für die Unterstützung im Labor möchte ich mich bei Božana Knežić, Mareike Dörr, Melanie Janßen, Vanessa Luciano und Hannah Hein bedanken, die mir im Rahmen ihrer Praktika bzw. Bachelor- oder Masterarbeiten im Labor geholfen und Daten für die vorliegende Arbeit erstellt haben.

Ein großer Dank gilt meinen Freunden, die mich immer motiviert und unterstützt haben.

Ein besonderer Dank gilt meiner Mutter, die mich seelisch, beratend und motivierend während der gesamten Studien- und Promotionszeit unterstützt hat. Danke für die tollen Gespräche und das große Verständnis und das Ertragen meiner Launen.

Erklärung

Ich erkläre: Ich habe die vorgelegte Dissertation selbständig und ohne unerlaubte fremde Hilfe und nur mit den Hilfen angefertigt, die ich in der Dissertation angegeben habe. Alle Textstellen, die wörtlich oder sinngemäß aus veröffentlichten Schriften entnommen sind, und alle Angaben, die auf mündlichen Auskünften beruhen, sind als solche kenntlich gemacht. Bei den von mir durchgeführten und in der Dissertation erwähnten Untersuchungen habe ich die Grundsätze guter wissenschaftlicher Praxis, wie sie in der „Satzung der Justus-Liebig-Universität Gießen zur Sicherung guter wissenschaftlicher Praxis“ niedergelegt sind, eingehalten.

_____ _____

Datum Unterschrift